

BJZ

Belgian Journal of Zoology

Published by the

KONINKLIJKE BELGISCHE VERENIGING VOOR DIERKUNDE
KONINKLIJK BELGISCH INSTITUUT VOOR NATUURWETENSCHAPPEN

—
SOCIÉTÉ ROYALE ZOOLOGIQUE DE BELGIQUE
INSTITUT ROYAL DES SCIENCES NATURELLES DE BELGIQUE

Volume 144 (1)
(January, 2014)

Managing Editor of the Journal

Isa Schön
Royal Belgian Institute of Natural Sciences
Freshwater Biology
Vautierstraat 29
B - 1000 Brussels (Belgium)

CONTENTS

Volume 144 (1)

- 5** | **Giuseppe DODARO & Corrado BATTISTI**
Rose -ringed parakeet (Psittacula krameri) and starling (Sturnus vulgaris) syntopics in a Mediterranean urban park: evidence for competition in nest-site selection?
- 15** | **Laith A. JAWAD**
A case of partial albinism in the yellow-belly flounder, Rhombosolea leporina Günther, 1862 (Pleuronectiformes: Pleuronectidae) collected from Manukau Harbor, Auckland, New Zealand
- 20** | **Emilie DESCAMPS, Alicja SOCHACKA, Barbara DE KEGEL, Denis VAN LOO, Luc VAN HOOREBEKE & Dominique ADRIAENS**
Soft tissue discrimination with contrast agents using micro-CT scanning
- 41** | **Eduardo DE LA PEÑA, Viki VANDOMME & Enric FRAGO**
Facultative endosymbionts of aphid populations from coastal dunes of the North Sea
- 51** | **Gilles LEPOINT, Olivier MOUCHETTE, Corine PELAPRAT & Sylvie GOBERT**
An ecological study of Electra posidoniae Gautier, 1954 (Cheilostomata, Anasca), a bryozoan epiphyte found solely on the seagrass Posidonia oceanica (L.) Delile, 1813
- 64** | **ERRATUM to: Naureen Aziz QURESHI & Noor Us SAHER**
Burrow morphology of three species of fiddler crab (Uca) along the coast of Pakistan – Belgian Journal of Zoology 142 (2): 114-126

ISSN 0777-6276

Cover photograph: Using contrast agents allows the visualisation of soft tissue details, as shown in these zebrafish (top), *Xenopus* tadpole (middle) and mouse (bottom). Images represent volume rendering of specimens stained with phosphomolybdic (zebrafish and mouse) and phosphotungstic acid (tadpole), see paper by E. DESCAMPS et al.

Zoology Congress 2014
University of Liège
12 and 13 December 2014

Zoology 2014, the 21st Benelux Congress of Zoology co-organized by the Royal Belgian and Dutch Zoological Societies, will take place in Liège (Belgium) on 12 & 13 December 2014 at the Institute of Zoology (University of Liège).

Four general topics will be illustrated by four keynote speakers: open access in science publishing, ecological interactions, animal evolution and conservation biology.

Two special sessions will be devoted to widely used techniques: one about state-of-the-art genetic research methods in zoology, and one about the use of biomarkers to study trophic links and food web structure.

While keynote speakers will give presentations related to the general topics of the congress, Zoology 2014 will welcome oral presentations and posters from researchers at all stages of their scientific career (master students, PhD students, post-docs or confirmed scientists) and from all fields of animal science, from molecules to biosphere. The conference is also open to the general public interested in advances in animal science.

Zoology 2014 will be an excellent opportunity for zoology students and young scientists to meet colleagues and to present and discuss the results of their research. Moreover, the conference will give an overview of the current scientific work from many European universities and zoological institutions, and thus provide ample opportunity to establish contacts for collaboration.



Rose -ringed parakeet (*Psittacula krameri*) and starling (*Sturnus vulgaris*) syntopics in a Mediterranean urban park: evidence for competition in nest-site selection?

Giuseppe Dodaro ¹ & Corrado Battisti ^{2,*}

¹ Ambiente Italia s.r.l., via Vicenza 5a, 00185 Rome (Italy); e-mail: giuseppe.dodaro@ambienteitalia.it

² "Torre Flavia" LTER (Long Term Environmental Research) Station, Servizio Ambiente, Provincia di Roma, via Tiburtina, 691, 00159 Rome (Italy); e-mail: c.battisti@provincia.roma.it

* Corresponding author: c.battisti@provincia.roma.it

ABSTRACT. Introduced species may compete with indigenous ones, e.g. for space resources, but evidence for syntopic cavity-nester birds is limited, at least for Mediterranean urban parks. In this work we report data on nest-site habitat use, availability and selection in two species: the introduced rose-ringed parakeet (*Psittacula krameri*) and the autochthonous starling (*Sturnus vulgaris*) nesting in ornamental tree (*Cedrus libanotica*) patches occurring in an historical urban park (Rome, central Italy). In particular, in our study we hypothesize that parakeets negatively affect starling nest-site selection. On 55 trees, we detected 73 available holes for nesting (38.4 % of which hosted nests: 9 of rose-ringed parakeet, 16 of starling, 3 of house sparrow). Birds utilized for nesting only a limited number (< 20%) of the ornamental trees (all larger than 80 cm in diameter). Compared to the total number of available trees, nesting trees had a significantly larger diameter at breast height. We observed a shift in the frequency distribution of nest hole height classes between starlings and parakeets suggesting competition for nesting sites between these two species. Starlings located their nests significantly lower than did rose-ringed parakeets, resulting in a higher specialization for starlings (as measured by the Feinsinger index) than for rose-ringed parakeets. The analysis of co-occurrence highlights a spatial segregation in nest holes. We argue that these differences in preferred nest height are indicative of parakeet dominance over starlings in cavity selection for nesting.

KEY WORDS: height habitat selection, niche overlap, competition, introduced species, central Italy.

INTRODUCTION

Introduced species may compete for resources with indigenous ones (e.g. nest-holes, food for juvenile recruitment; DAVIS, 2003). Particularly in communities where strong interspecific competition between native species is lacking, exotic and native species often exhibit intense competition resulting in the decline of native populations (EDELMAN *et al.*, 2009). However, evidence of similarly negative competition effects in syntopic birds is limited, at least for some species (BAUER & WOOG, 2008, 2011). This situation is even more striking in a group of vertebrates such as the birds, where data quality with respect to occurrence, numbers and population trends is usually very high

(EBENHARD, 1988, BLACKBURN *et al.*, 2009; KESTENHOLZ *et al.*, 2005).

Urban parks embedded in anthropized landscapes host peculiar ecosystems, biological communities and species (REBELE, 1994; CLERGEAU, 2006). In urban areas wooded patches are often composed of ornamental vegetation characterized by a high density of large, mature trees that have not been subjected to intensive coppice management. As a consequence there is often high availability of cavities, invertebrates and plant food (FALK, 1976; DORNEY *et al.*, 1984; MCKINNEY, 2002), and urban parks may therefore host a specific guild of specialized species, such as the cavity nesting birds (BEISSINGER & OSBORNE, 1982, BLAIR, 2001).

Cavity nesting birds, also named “hole-nesting birds”, represent a guild of species (such as woodpeckers, nuthatches, tits, treecreepers, starlings and sparrows) highly dependent on old trees or dead wood for nesting, and secondarily, for roosting and feeding. This guild can be divided into (i) excavators (e.g., woodpeckers), species that excavate cavities secondarily used by insects, reptiles, birds and mammals, and (ii) non-excavators, a large number of species that use natural or previously excavated tree holes for nesting (MARTIN & LI, 1992; MARTIN & EADIE, 1999; BLANC & WALTERS, 2008). The occurrence, abundance and richness of cavity-nesting birds largely depend on the availability of suitable nesting cavities and food resources linked to mature trees (CRAMP & PERRINS, 1993).

Cavity-nesting bird guilds include rare and specialized species but also generalist and synanthropic ones (both urban adapters and exploiters). The latter are linked to human-transformed habitats and often exhibit more flexibility in nest site choice (e.g. nesting also in buildings; BLAIR, 2001). Synanthropic species may be secondarily adapted to human-transformed ecosystems (termed ‘adapters’) or actively select these environments (termed ‘exploiters’; see BLAIR, 2001). Moreover, many synanthropic species are not native (e.g. some species of parakeets, order Psittaciformes).

In this study, we focused on two synanthropic species that are commonly found in forest patches of South-European urban parks. Our first study species, the starling (*Sturnus vulgaris*) (Linnaeus, 1758), is a species that, over the last decades, has become more and more abundant in anthropized landscapes across the Southern Mediterranean region (BIRDLIFE INTERNATIONAL, 2004). This contrasts strongly with its status in Northern Europe, where it is declining and disappearing from urban areas (ROBINSON *et al.*, 2005; MENNECHEZ & CLERGEAU, 2006). Secondly, we assessed the rose-ringed parakeet (*Psittacula krameri*) (Scopoli, 1769), an introduced species (JUNIPER and PARR, 1998) that has established

self-sustaining (i. e. naturalized) populations in many European cities (CASSEY *et al.*, 2004; CZAJKA *et al.*, 2011, NEWSON *et al.*, 2011). Previous studies have suggested that because of a strong overlap in preferred nesting cavities, starlings and rose-ringed parakeets are likely to compete for tree cavities in the areas where they co-occur, although empirical evidence for competition between these species is currently lacking (STRUBBE & MATTHYSEN, 2007, STRUBBE & MATTHYSEN, 2009a, 2010, CZAJKA *et al.*, 2011, NEWSON *et al.*, 2011). However, these studies have been carried out in Northern and Central Europe, and information on habitat and nesting preferences of these species in the Mediterranean area remains rare.

In this work, we focused on ecological traits related to the selection of nest holes of the two locally most abundant species: rose-ringed parakeet, an introduced species, and starling. We tested whether there are differences in the height of the cavities that are selected for breeding by both species. In particular, since we observed localized syntopy (i.e. an occurrence of individuals in the same wood patches) between these two species, we tested the hypothesis that locally, rose-ringed parakeets may negatively affect starling nest-site selection.

MATERIALS AND METHODS

Study area

The study was carried out inside the Villa Doria Pamphili (Rome, central Italy), a large urban park (about 120 hectares, about 50 m a.s.l.) designed as a Site of Nature Conservation Interest (SNCI) (‘Habitat’ Directive 92/43/EEC; 41° 53’ N, 12° 27’ E). This historical urban park, embedded in a continuous urbanized matrix, was created in the 17th century and represents a heterogeneous patchy landscape with wood fragments where oaks are dominant tree species (*Quercus ilex*, *Q. pubescens*, *Q. petrae*). Wooded patches with ornamental tree species (*Cedrus libanotica*, *Cupressus* sp. and others), open areas,

and artificial lakes also occur (BATTISTI, 1986; CELESTI-GRAPPOW, 1995). Inside the study area, we focused the sampling protocol on a small wooded patch composed of ornamental trees (size area: 0.5 ha; 57 trees: 55 *Cedrus libanotica*, 1 *Cupressus* sp., 1 *Platanus orientalis*).

Field Methodology

Inside the forest patch, we analysed only data of *Cedrus libanotica* trees (n = 55). For each tree, we measured the diameter at breast height (DBH, in cm) and the tree height (TH) in size classes (0-2 m, >2-4, >4-6, >6-8, >8-10, >10-12, >12-14, >14-16) obtaining a mean value of these two parameters (MEAN DBH and MEAN TH). Each tree was surveyed for cavities potentially suitable for cavity-nesting birds (hole nests; see BIBBY *et al.*, 2000). Each tree hole discovered was assigned to a height class (see above), and during the breeding season, we determined whether a cavity-nesting bird occupied it or not. From March to June 2012, we carried out six visits to the study area in the first hours of the morning (about 07.00 a.m.), when these species are more easily detectable near the hole nests, to the late morning (about 11.00 a.m.), when foraging activities are more intense (e.g. for juvenile recruitment) so allowing the detection of hole nests (total research effort: about 24 hours).

Data Analysis

First, to test whether rose-ringed parakeet and starling nest site choice was neutral with respect to the height at which cavities were located or not, we calculated the Feinsinger index (FEINSINGER *et al.*, 1981). We first calculated the frequency of available occupied holes for each height class, allowing us to obtain the Feinsinger index through the following formula (FEINSINGER *et al.*, 1981):

$$PS = 1 - 0,5 \sum |p_i - q_i|$$

In this index, p_i is the proportion of the utilized resource (i.e., the frequency of nest holes in

each tree height class) and q_i the proportion of the available resource (i.e., the frequency of available holes in each tree height class). The index varies from 0 (extreme specialist for that specific resource) to 1 (extreme generalist).

Second, in order to assess the degree to which rose-ringed parakeet and starling nest site choice overlaps, we applied a niche overlap index. Nesting site niche overlap was obtained through the following formula (KREBS 1989):

$$O_i = \sum (p_{j1}p_{j2}/a_j),$$

where p_{j1} and p_{j2} are the relative frequencies, respectively, of the species 1 and 2 recorded among the habitat type j , and a_j is the relative frequency of the available habitat type j . The index varies from 0 (absence of overlapping) to 1 (total overlap).

To assess whether rose-ringed parakeets and starlings significantly differ in nest site choice, we compared the frequency distribution of nesting cavity heights for the two species using a Kolmogorov-Smirnov test. To test whether parakeets and starlings prefer trees with different average values in DBH, we performed the non parametric U Mann-Whitney test for unpaired data (DYTHAM, 2011).

We performed all statistical non parametric analyses using SPSS version 13.0 (SPSS Inc., 2003). We assumed an alpha level of 5% as level of significance.

Moreover, we performed a null model analysis of species co-occurrence pattern in order to test whether the two study birds avoided colonizing a tree already occupied by the other species (GOTELLI, 2000). As the co-occurrence measure, we used the STONE and ROBERTS' (1990) C-score. The C-score measures the average number of "checkerboard units" between all possible pairs of species. The number of checkerboard units (CU) for each species pair is calculated as: $CU = (r_i - S)(r_j - S)$, where S is the number of shared sites (sites containing both species) and r_i and r_j are the row totals for species i and j . The C-score is the average of

TABLE 1

Mean diameter (and standard deviation, s.d.) at breast height (MEAN DBH, in cm) and mean tree height (MEAN TH; and standard deviation, s.d.) both for all *Cedrus libanotica* trees and for trees occupied by the two cavity nesters studied: rose-ringed parakeet (*Psittacula krameri*) and starling (*Sturnus vulgaris*).

Categories	N	MEAN DBH (s.d.)	MEAN TH (s.d.)
All trees	55	65.05 (25.06)	11.87 (2.90)
With available holes	10	97.79 (11.89)	14.50 (1.51)
With nest holes	9	94.78 (8.34)	14.33 (1.73)
With rose-ringed parakeet holes	4	94.5 (7.93)	14.50 (1.00)
With starling holes	7	94.36 (8.14)	14.43 (1.90)

all possible checkerboard pairs, calculated for species that occur at least once in the matrix. The C-Score measures the tendency for species to not occur together. The larger the C-score, the less the average co-occurrence among species pairs. If a community was structured by competition, we would expect the C-score to be large relative to a randomly assembled community (GOTELLI 2000; GOTELLI & ENTSIMNGER 2001). As randomization algorithm we used (i) “fixed sum” as row constraint and (ii) “equiprobable” for column constraint, that is: (i) the observed row totals are maintained in the simulation (the number of occurrences of each species in the null communities is the same as in the original data set), and (ii) each column (site) is equally likely to be represented (we supposed that all trees are equivalent to one another, that is from the species perspective, all the trees with holes are equally likely to be successfully colonized). With this randomization algorithm, in the simulation, the occurrences for each species (row sums) are distributed randomly among the different columns (GOTELLI & ENTSIMNGER 2001). For each occurrence, a column is chosen randomly and equiprobably, although if a cell already has a 1 placed in it, another column is randomly chosen until an empty site is found. This procedure is repeated until all of the occurrences of each species are randomly distributed among the columns. The analyses of co-occurrence were performed by using Ecosim software (GOTELLI & ENTSIMNGER 2001).

RESULTS

In the wooded patch, the mean diameter at breast height of the *Cedrus libanotica* trunks was 65.05 cm (\pm 25.06) and the mean tree height was 11.87 m (\pm 2.89). Among the trees, 17 (30.91 %; n = 55) showed a diameter > 80 cm, 12 (21.82 %) hosted available holes for nesting, and 9 (16.36 %) hosted holes with nests (all with a diameter > 80 cm).

In total, we detected 73 available holes for nesting. Among them 28 (38.4 %) hosted bird nests: 9 of rose-ringed parakeet (32.1 % of occupied nests); 16 of starling (57.1 %). We also detected 3 hole nests (10.7 %), of house sparrow (*Passer domesticus*) (Linnaeus, 1758), a synanthropic species, recently declining in density and distribution at the continental scale (SUMMER-SMITH, 2003): these data were not included in the following analyses. Forty-five holes remained empty. Data on mean tree diameter and mean tree height of available holes and occupied nests for these three species are given in in Tables 1 and 2.

The mean height of starling nests in tree cavities was significantly lower when compared to mean height of rose-ringed parakeet nests ($Z = -2.159$, $p < 0.05$, Mann-Whitney U test) and lower than the mean of all available holes ($Z = -2.873$, $p < 0.01$, Mann-Whitney U test), while nests of rose-ringed parakeet were not significantly

TABLE 2

Number of available and occupied hole nests, their density (D; in nests/ha) in *Cedrus libanotica* patch and mean nest height (MEAN NEST NH; in m, and standard deviation, s.d.) for the two cavity nesters studied: rose-ringed parakeet (*Psittacula krameri*) and starling (*Sturnus vulgaris*). (*) included three nests of house sparrow (*Passer domesticus*).

	N	D	MEAN NEST NH (s.d.)
All available holes	73	146	7.82 (2.97)
Rose-ringed parakeet hole nests	9	18	8.17 (2.83)
Starling hole nests	16	32	5.38 (2.80)
total hole nests (*)	28	56	6.66 (3.06)

different when compared to the mean height of all available holes ($Z = 0.175$, $p = 0.845$).

Analyzing the frequency distribution of data, we corroborate the previous results. In particular, we observed a shift between the frequency distribution of height classes of nest holes between rose-ringed parakeet and starling (Fig. 1). The

frequency distribution of total available holes was not significantly different from the frequency distribution of rose-ringed parakeet ($Z = 0.349$, $p = 1$), i. e. parakeets used nest sites according to availability, while our results show a trend towards a significant difference between starling nests and total available holes ($Z = 1.278$, $p = 0.076$, Kolmogorov-Smirnov two sample test),

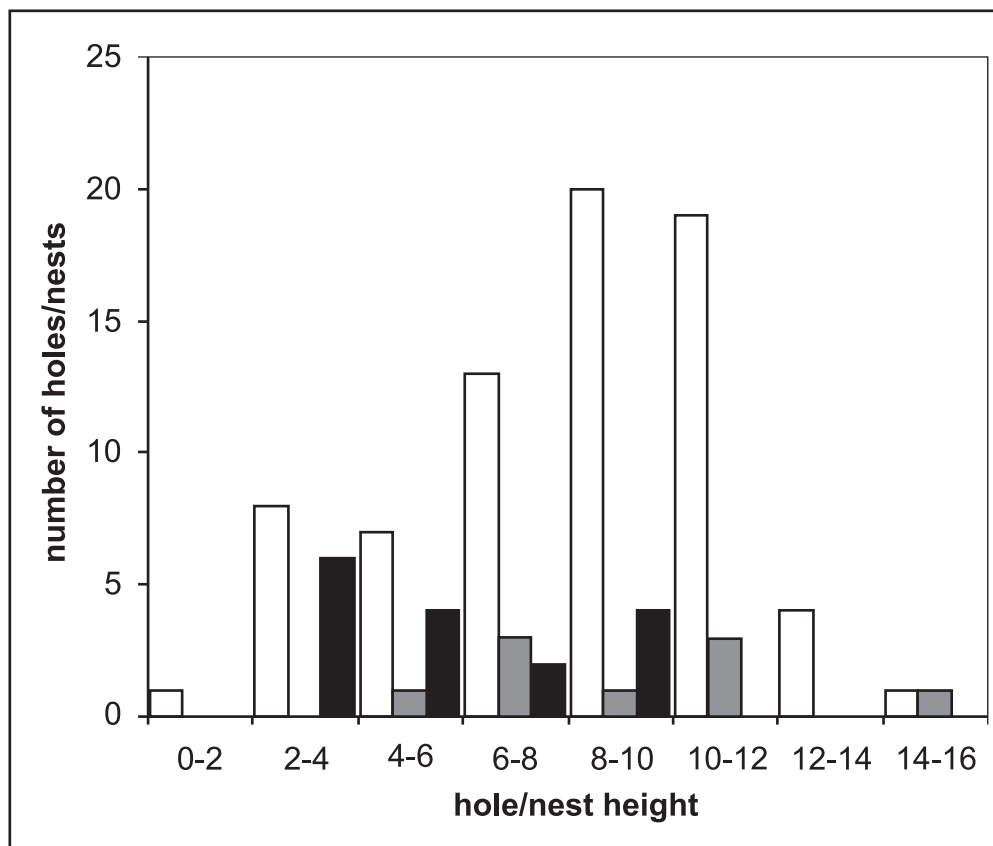


Fig. 1. – Available (in white) and occupied holes (nests) subdivided for categories (grey: rose-ringed parakeet, *Psittacula krameri*; black: starling, *Sturnus vulgaris*).

i.e. starlings showed a preference. In starlings we observed a higher frequency of nest holes at lower height classes whereas the frequency distribution of total available holes was lower, i.e. nesting cavities of starlings were significantly lower than parakeet nests (Fig. 1).

The Feinsinger index showed a higher value in rose-ringed parakeet (0.659) when compared to starling (0.581), indicating that parakeets are more generalists than starlings in regard to nest site choice. Niche overlap index between these two species was 0.625.

The analysis of co-occurrence performed on the distribution of the 19 trees colonized by at least one species and with at least one empty hole available to be colonized, showed that the two species were spatially segregated (observed C-score index = 60.00; mean of simulated indices = 20.25; Variance of simulated indices = 102.25; $p_{(\text{obs} \geq \text{exp})} = 0.002$).

DISCUSSION

In this study, we assessed nest site choice of two synanthropic cavity-nesters, the (native) starling and the (introduced) rose-ringed parakeet. These two species are often considered to be urban exploiters, i.e. belonging to a guild of species commonly found in urban parks and suburban landscapes, and are adapted to edge habitats, human dwellings and small-sized forest patches occurring in urban parks (ADAMS, 1994; BLAIR, 2001).

Parakeets and starlings reached high breeding densities in our study area (18 and 32 nests/ha, respectively), and this is probably due to plentiful availability of large trees (*Cedrus libanotic*) with many holes (146 tree holes/ha). In this urban park, only ornamental and allochthonous trees showed a mean diameter at breast height larger than 80 cm, since trees belonging to the natural vegetation (mainly oaks, *Quercus* spp.) rarely have a diameter greater than 50 cm (BATTISTI, 1986). The occurrence of large trees in historical

urban parks has been highlighted as an important feature to allow the breeding of hole-nesting birds (HINSLEY *et al.*, 1995; MIKUSIŃSKI *et al.*, 2001). In our study, the detected synanthropic hole-nesting birds utilized only a limited number of trees (< 20%), with a significantly larger mean diameter when compared to the total number of available trees. Thus, our results show that ornamental allochthonous tree species can have a high ecological value for urban hole-nesting birds, many of them species of high ecological interest and conservation concern due to their sensitivity to coppice management, forest fragmentation, isolation and degradation (e.g. CIESLAK, 1985; HELLE, 1985; OPDAM *et al.*, 1985; MATTHYSEN *et al.*, 1995; BELLAMY *et al.*, 1996; ZANGHERI *et al.*, 2013).

The starling is one of the most common secondary cavity-nesters in Europe, breeding in central Italy from 1970s (ANGELICI & PAZIENTI, 1985) and nowadays occurs almost throughout the whole country (CECERE *et al.*, 2005). For this species, a significant correlation between cavity availability and species abundance has been reported (STRUBBE & MATTHYSEN, 2007). This species is known to compete with other cavity nesters for nest-site (e.g. woodpeckers: INGOLD, 1994). When introduced, starling is also considered an aggressive secondary cavity nester (PELL & TIDEMANN, 1997; KOENIG, 2003; MARTIN *et al.*, 2004).

Differing from starlings, the rose-ringed parakeet is an allochthonous species, widely introduced in urban areas in Italy since the 1980s (SPANÒ & TRUFFI, 1986; MORI *et al.*, 2013; for Rome: ANGELICI, 1984; BRUNELLI *et al.*, 2011). Although some studies on parakeet nesting behaviour and habitat choice have been conducted in Northern Europe (e.g. CZAIJKA *et al.*, 2011), such information is still lacking from Mediterranean areas. In Northern Europe, starlings are considered to be vulnerable to competition with rose-ringed parakeets (STRUBBE & MATTHYSEN, 2007, 2009a, 2009b, STRUBBE *et al.*, 2010). However, STRUBBE and MATTHYSEN (2007), BRAUN *et al.* (2009) and CZAIJKA *et*

al. (2011) found a niche separation in regard to tree size and tree species between the nests of parakeets and starlings in German and Belgian city parks, suggesting that differing nesting site preferences may reduce competition between these species. Our data, obtained from a single ornamental tree species (*Cedrus libanotica*), suggest that in our study area, parakeets and starlings may compete for nesting cavities as the starling shows a higher specialization in nest height selection, breeding at lower heights than rose-ringed parakeets. Also, we observed a partial niche overlap in nest choice between these two species, suggesting a moderate inter-specific competition. As the height at which cavities are located may be related to predation risk (NILSSON, 1984), our data suggest that parakeet competition may force starlings to breed in lower, and thus less-safe cavities.

Our evidence for possible competition between these two species when occurring in syntopy is further supported by the results of statistical analysis for co-occurrence. It is possible, however, that our data may be affected by a local effect (the detection of competition among bird species is largely affected by the scale of investigation; BENNETT, 1990). Therefore, it is possible that geographical and ecological contexts and circumstances are of great importance to predict whether a certain species may be affected by competition (KOENIG 2003). For example, studying the competition between nuthatch (*Sitta europaea*) and rose-ringed parakeet, NEWSON *et al.* (2011) suggested the possibility that competitive exclusion occurred at a minority of sites where availability of nest cavities was limited.

We propose that further research should be carried out because in our study direct competition (e.g. aggressive interactions) between these two species has not yet been observed, nor is it clear whether the pattern in nest site choice found here actually influences the starling's reproductive success (KERPEZ & SMITH, 1990; PELL & TIDEMANN, 1997; STRUBBE & MATTHYSEN, 2007).

Our data also suggest that rose-ringed parakeet may be included in a proposed 'grey list' of non-native species (ESSL *et al.*, 2008), i.e. a list that includes those introduced species for which there is evidence that native bird populations may be affected by their presence, but for which more research seems necessary to decide whether the increase and spread of this species may warrant further conservation actions (BAUER & WOOG, 2011).

Finally, the present study could also provide evidence that an exotic ornamental tree such as *Cedrus libanotica* to some extent favours the success of introduced bird species, because the rose-ringed parakeets do not nest on buildings (contrarily to native starlings and sparrows). This fact suggests suitable future conservation actions to control parakeet populations through the management of this exotic ornamental tree.

ACKNOWLEDGEMENTS

Two anonymous reviewers have largely improved a first draft of the manuscript. We would acknowledge also Dr. PhD. Leonardo Vignoli (University of Rome III) for your support in statistical analyses.

REFERENCES

- ADAMS LW (1994). Urban wildlife habitats. University of Minnesota press, Minneapolis.
- ANGELICI FM (1984). Il Parrocchetto dal collare *Psittacula krameri* (Scopoli) è presente in libertà anche a Roma. *Avifauna*, 7: 179-180.
- ANGELICI FM & PAZIENTI A (1985). Tre nuove colonie di Storno *Sturnus vulgaris* nella città di Roma. *Rivista italiana di Ornitologia*, 55: 181-182.
- BATTISTI C (1986). Censimento degli uccelli nidificanti in un parco urbano (Villa Doria Pamphili, Roma). *Avocetta*, Italian Journal of Ornithology, 10: 37-40.
- BAUER H-G & WOOG F (2008). Non-native and naturalized bird species (neozoa) in Germany,

- part I: occurrence, population size and status. *Vogelwarte*, 46: 157–194
- BAUER G & WOOG F (2011). On the ‘invasiveness’ of non-native bird species. *Ibis*, 153: 204–206
- BENNETT WA (1990). Scale of investigation and the detection of competition : an example from the house sparrow and house finch introductions in North America. *The American Naturalist*, 135: 725–747.
- BLACKBURN TM, LOCKWOOD JL & CASSEY P (2009). *Avian Invasions. The Ecology and Evolution of Exotic Birds*. Oxford: Oxford University Press.
- BRAUN M, CZAJKA C & WINK M (2009). Gibt es eine Brutplatzkonkurrenz zwischen Star und Halsbandsittich? *Vogelwarte*, 47: 361–362.
- BEISSINGER SR & OSBORNE DR (1982). Effects of urbanization on avian community organization. *Condor*, 84: 75–83.
- BELLAMY PE, HINSLEY SA & NEWTON I (1996). Factors influencing bird species numbers in small woods in south-east England. *Journal of Applied Ecology*, 33: 249–262.
- BIBBY CJ, BURGESS ND, HILL DA & MUSTOE SH (2000). *Bird census techniques*. II Ed., Academic Press, Londra, UK.
- BIRDLIFE INTERNATIONAL (2004). *Birds in Europe: population estimates, trends and conservation status*. BirdLife Conservation Series, 12, BirdLife International, Canbridge, UK.
- BLAIR RB (2001). Birds and butterflies along urban gradients in two ecoregions of the United States. *In: LOCKWOOD JL & MCKINNEY ML (Eds.), Biotic homogenization*. Kluwer, Norwell, MA: 33–56.
- BLANC A & WALTERS JR (2008). Cavity excavation and enlargement as mechanisms for indirect interactions in an avian community. *Ecology*, 89: 506–514.
- BRUNELLI M, SARROCCO S, CORBI F, SORACE A, BOANO A, DE FELICI S, GUERRIERI G, MESCHINI A & ROMA S (2011). *Nuovo Atlante degli Uccelli Nidificanti nel Lazio*. Edizioni ARP (Agenzia Regionale Parchi), Roma.
- BUTLER, CJ (2005). Feral parrots in the Continental United States and United Kingdom: past, present, and future. *Journal of Avian Medicine and Surgery*, 19:142–149.
- CASSEY P, BLACKBURN TM, RUSSEL GJ, JONES KE & LOCKWOOD JL (2004). Influences of the transport and establishment of exotic bird species: an analysis of the parrots (Psittaciformes) of the world. *Global Change Biology*, 10: 417–426.
- CECERE JC, SORACE A & DE SANTIS E (2005). Distribuzione dello Storno *Sturnus vulgaris* nella città di Roma. *Alula*, 12: 85–86.
- CELESTI GRAPOW L (1995). *Atlante della flora di Roma. La distribuzione delle piante spontanee come indicatore ambientale*. Comune di Roma, Argos edizioni, Roma.
- CIESLAK M (1985). Influence of forest size and other factors on breeding bird species number. *Ekologia Polska*, 33: 103–121.
- CIGNINI B & ZAPPAROLI M (1996). *Atlante degli uccelli nidificanti a Roma*. F.lli Palombi Editore, Roma.
- CLERGEAU P, CROCI S, JOKIMÄKI J, KAISANLAHTI-JOKIMÄKI M-L & DINETTI M (2006). Avifauna homogenization by urbanisation: Analysis at different European latitude. *Biological Conservation*, 127: 336–344.
- CRAMP S & PERRINS CM (1993). *The Birds of the Western Palearctic*. Vol. VII. Oxford Univ Press, Oxford.
- CZAJKA C, BRAUN MP & WINK M (2011). Resource use by non-native Ring-Necked Parakeets (*Psittacula krameri*) and native Starlings (*Sturnus vulgaris*) in Central Europe. *The Open Ornithology Journal*, 4: 17–22.
- DAVIS MA (2003) Biotic Globalization: Does Competition from Introduced Species Threaten Biodiversity? *BioScience*, 5: 481–489.
- DORNEY JR, GUNTENSPERGEN GR, KEUGH JR & STERNS F (1984). Composition and structure of an urban woody plant community. *Urban Ecology*, 8: 69–90.
- DYTHAM C (2011). *Choosing and using statistic. A Biologist’s guide*. Wiley-Blackwell, UK.
- EBENHARD T (1988). Introduced birds and mammals and their ecological effects. *Swed. Wildlife Research*, 13: 1–107.
- EDELMAN AJ, KOPROWSKI JL & BERTELSEN S (2009). Potential for nest site competition between native and exotic tree squirrels. *Journal of Mammalogy*, 90:167–174.
- ESSL F, KLINGENSTEIN F, NEHRING S, OTTO C, RABITSCH W & STÖHR O (2008). Schwarze Listen invasiver Arten – ein Instrument zur Risikobewertung für die Naturschutz-Praxis. *Natur Landschaft*, 83: 418–424.

- FALK JH (1976). Energetics of suburban lawn ecosystems. *Ecology*, 57: 141-150.
- FEARE CJ (1984). *The starling*. Oxford University Press, New York.
- FEINSINGER P, SPERS EE & POOLE RW (1981). A simple measure of niche breadth. *Ecology*, 62: 27-32.
- GOTELLI NJ (2000). Null model analysis of species co-occurrence patterns. *Ecology*, 81: 2606-2621.
- GOTELLI NJ & ENTSMINGER GL (2001). *EcoSim: Null models software for ecology*. Version 7.0. Acquired Intelligence Inc. & Kesey-Bear. <http://homepages.together.net/~gentsmin/ecosim.htm>.
- HELLE P (1985). Effects of forest fragmentation on bird densities in northern boreal forests. *Ornis Fennica*, 62: 35-41.
- HINSLEY SA, BELLAMY PE, NEWTON I & SPARKS TH (1995). Habitat and landscape factors influencing the presence of individual breeding bird species in woodland fragments. *Journal of Avian Biology*, 26: 94-104.
- KERPEZ, TA & SMITH NS (1990). Competition between European starlings and native woodpeckers for nest cavities in Saguaros. *Auk*, 107: 367-375.
- KESTENHOLZ M, HEER L & KELLER V (2005). Non-indigenous bird species established in Europe – a review. *Ornithologische Beob.* 102: 153–180.
- KOENIG WD (2003). European Starlings and their effect on native cavity-nesting birds. *Conserv. Biol.* 17: 1134–1140.
- KOTAKA, N & MATSUOKA, S (2002). Secondary users of great spotted woodpecker (*Dendrocopos major*) nest cavities in urban and suburban forests in Sapporo City, northern Japan. *Ornithol. Sci.* 1: 117-122.
- KREBS CJ (1989). *Ecological methodology*. Harper Collins Publishers, New York.
- JUNIPER T & PARR M (1998). *Parrots: a guide to the Parrot of the World*. Pica press.
- LÖVEI GL (1997). Global change through invasion. *Nature*, 388: 627–628.
- MARTIN K & EADIE JM (1999). Nest webs: A community-wide approach to the management and conservation of cavity-nesting forest birds. *Forest Ecology and Management*, 115: 243-257.
- MARTIN K, AITKEN KEH & WIEBE KL (2004). Nest sites and nest webs for cavity-nesting communities In Interior British Columbia, Canada: nest characteristics and niche partitioning. *The Condor*, 106: 5-19.
- MARTIN TE & LI P (1992). Life history traits of open- vs. cavity-nesting birds. *Ecology*, 73: 579-592.
- MATTHYSEN E, LENS L, VAN DONGEN S, VERHEYEN GR, WAUTERS LA, ADRIAENSEN F & DHONDT AA (1995). Diverse effects of forest fragmentation on a number of animal species. *Belgian Journal of Zoology*, 125: 175-183.
- MCKINNEY ML (2002). Urbanization, biodiversity, and conservation. *BioScience*, 52: 883-890.
- MENNECHEZ G & CLERGEAU P (2006) Effect of urbanisation on habitat generalists: starlings not so flexible? *Acta Oecologica*, 30: 182-191.
- MIKUSINSKI G, GROMADZKI M & CHYLARECKI P (2001). Woodpeckers as Indicators of Forest Bird Diversity. *Conservation Biology*, 15: 208-217.
- MORI E, DI FEBBRARO M, FORESTA M, MELIS P, ROMANAZZI E, NOTARI A & BOGGIANO F (2013). Assessment of the current distribution of free-living parrots and parakeets (Aves: Psittaciformes) in Italy: a synthesis of published data and new records. *Italian Journal of Zoology*, 80: 158-167. <http://dx.doi.org/10.1080/11250003.2012.738713>
- NEWSON SE, JOHNSTON A, PARROTT D & LEECH DI (2011). Evaluating the population-level impact of an invasive species, Ring-necked Parakeet *Psittacula krameri*, on native avifauna. *Ibis*, 153: 509-516.
- NILSSON, SG (1984). The evolution of nest-site selection among hole-nesting birds: the importance of nest predation and competition. *Ornis Scandinavica*, 15: 167-175.
- OPDAM P, RIJSDIJK G & HUSTINGS F (1985). - Bird communities in small woods in an agricultural landscape: effects of area and isolation. *Biological Conservation*, 34: 333-352.
- PELL, AS & TIDEMANN, R (1997). The impact of two exotic hollow-nesting birds on two native parrots in savannah and woodland in eastern Australia. *Biological Conservation*, 79: 145-153.
- PRANTY B (2002). The use of Christmas Bird Count data to monitor populations of exotic birds. *American Birds*, 56: 24–28.
- REBELE F (1994). Urban ecology and special features of urban ecosystems. *Global Ecology and Biogeographic letters*, 4: 173-187.
- ROBINSON RA, SIRIWARDENA GM & CRICK HQP (2005) Status and population trends of Starling

- Sturnus vulgaris* in Great Britain: Bird Study 52: 252-260.
- SMITH, KW (2006). The implications of nest site competition from starlings *Sturnus vulgaris* and the effect of spring temperatures on the timing and breeding performance of great spotted woodpeckers *Dendrocopus major* in southern England. *Annales Zoologici Fennici*, 43: 177-185.
- SNOW DW & PERRINS CM (1998). The Birds of the Western Palearctic. Concise edition. Vol. I, Non Passerines. Oxford University Press, Oxford.
- SPSS Inc. (2003) SPSS for Windows – Release 13.0 (1 Sep 2004), Leadtools (c), Lead Technologies Inc
- SPANÒ S & TRUFFI G (1986). Il parrocchetto dal collare, *Psittacula krameri*, allo stato libero in Europa, con particolare riferimento alle presenze in Italia e primi dati sul pappagallo monaco, *Myiopsitta monachus*. *Rivista italiana di Ornitologia*, 56: 231-239.
- STONE L & ROBERTS A (1990). The checkerboard score and species distributions. *Oecologia*, 85: 74-79.
- STRUBBE D & MATTHYSEN E (2007). Invasive ring-necked parakeets *Psittacula krameri* in Belgium: habitat selection and impact on native birds. *Ecography*, 30: 578-588.
- STRUBBE D & MATTHYSEN E (2009a). Establishment success of invasive ring-necked and monk parakeets in Europe. *Journal of Biogeography*, 36: 2264-2278.
- STRUBBE D. & MATTHYSEN E. (2009b). Experimental evidence for nest-site competition between invasive Ring-necked Parakeets (*Psittacula krameri*) and native Nuthatches (*Sitta europaea*). *Biological Conservation*, 142: 1588–1594.
- STRUBBE D, MATTHYSEN E & GRAHAM CH (2010). Assessing the potential impact of invasive ring-necked parakeets *Psittacula krameri* on native nuthatches *Sitta europaea* in Belgium. *Journal of Applied Ecology*, 47: 549-557.
- SUMMER-SMITH JD (2003). The decline of the House Sparrow: a review. *British Birds*, 96: 439-446.
- ZANGARI L, FERRAGUTI M, LUISELLI L, BATTISTI C & BOLOGNA MA (2013). Comparing patterns in abundance and diversity of hole-nesting birds in Mediterranean habitats. *Revue d'Écologie (Terre Vie)*, 68: 275-282.

Received: June 16th, 2013

Accepted: May 16th, 2014

Branch editor: Isa Schön

A case of partial albinism in the yellow-belly flounder, *Rhombosolea leporina* GÜNTHER, 1862 (Pleuronectiformes: Pleuronectidae) collected from Manukau Harbour, Auckland, New Zealand

Laith A. Jawad

Manukau, Auckland, New Zealand, e-mail: laith_jawad@hotmail.com

ABSTRACT. A partial albino specimen of *Rhombosolea leporina* with a total length of 295 mm was collected from Manukau Harbour, south of Auckland City, New Zealand. This is the first record of abnormal pigmentation in the wild yellow-belly flounder from New Zealand waters. The specimen is patterned with a white blotch on the caudal peduncle area of the ocular side. Causes for such colour aberration are discussed.

KEY WORDS: Abnormality, flatfish, vertebral deformity, albino specimen

INTRODUCTION

The yellow-belly flounder, *Rhombosolea leporina* is a right-sided eye flounder endemic to New Zealand. The adults occur at depths of 30-40 metres, where the water is brackish and very turbid (FRANCIS, 2012). It is a commercially valuable species, with one kilogram worth over NZ\$20 (17.3 US\$).

The peculiar colouration of this species has attracted the attention of biologists for a long time. The colouration pattern is considered as a tool to avoid predators, catch prey, and for conspecific communication (MILLS & PATTERSON, 2009). There are three basic types of colour abnormalities in fishes: ambicolouration, albinism, and xanthochroism. Ambicolouration is an excess of pigmentation on the blind side of flatfish. Xanthochroism is a rare condition in which the melanophores are missing, though other pigments are present, typically producing a golden-orange colour (COLMAN, 1972).

Malpigmentation is the typical anomaly of flatfishes. It is characterized by either a deficiency of pigment cells on portions of the ocular side (albinism, pseudoalbinism, or hypomelanism), or the presence of dark pigmentation on the normally light-coloured bellyside of the fish, also called ambicoloration (BOLKER & HILL, 2000).

Colour abnormalities are well documented for flatfish (e.g., DÍAZ DE ASTARLOA, 1995; BOLKER & HILL, 2000; CHAVES et al., 2002; Purchase et al., 2002; MACIEIRA et al., 2006), while abnormal pigmentation in other fish groups is rare (HERNÁNDEZ & SINOVCIC, 1987; JAWAD et al., 2007, 2013; JAWAD & AL-KHARUSI, 2013).

Flounders are famous for their ability to match their background by changing their ocular-side pigmentation. Such alterations are based on rapid changes in the morphology of melanophores, specifically in the distribution of pigment-containing melanosomes within the cytoplasm (BURTON, SUGIMOTO & OSHIMA 2002). In addition to this cause of changes, flounder pigmentation also changes during ontogeny, beginning during larval development and then, noticeably, at metamorphosis (SUGIMOTO & OSHIMA, 2002).

In New Zealand, JAWAD et al. (2007) is the only published work on alteration of colouration of fishes other than flatfish, while ARCHEY (1924) and COLMAN (1972) represent the only work on flatfishes. ARCHEY (1924) reported on a xanthochroic specimen of the yellow-belly flounder *R. leporina* and COLMAN (1972) examined partial and complete albinism cases in *R. plebeia* obtained from Wellington and Firth of Thames waters, respectively. In the present

study, a report on partial albinism in the yellow-belly flounder *R. leporina* is presented.

MATERIAL AND METHODS

On 10th October 2013, an abnormally-pigmented specimen of *Rhombosolea leporina* with a total length of 295 mm was obtained from a commercial catch in Auckland City. This specimen originated from Manukau Harbour, south of Auckland City, and was caught with a

set net. In addition, normal specimens of 280 mm total length were obtained from the same catch and used for comparisons. Total length was measured to the nearest 1 mm and the specimens photographed. Counts and measurements were made on both the miscoloured and normal specimens. All specimens were kept frozen and later radiographed, fixed in 10% formaldehyde solution and stored in 70% ethanol and deposited in the fish collection of Auckland War Memorial Museum (AIM MA33573).



Fig. 1. – Normal specimen of *Rhombosolea leporine*, 280 mm total length.



Fig. 2. – Abnormal specimen of *Rhombosolea leporine*, 295 mm total length.

RESULTS

The normal colouration of this species (Fig. 1) is green to olive above and cream-yellow below with numerous small black spots (< 1 mm in diameter) (FRANCIS, 2012). The edge of the dorsal fin rays is creamy –yellow. The pectoral fin is slightly darker than the body. The blind side of the miscoloured specimen (Fig. 2) exhibits the normal colouration. The caudal peduncle and the caudal fin are the areas that display partial albinism. The white patch starts from the end of the anal fin and goes up and forward reaching the last few dorsal fin rays, and extends to the caudal fin, covering the whole area of the caudal

peduncle and the base of the caudal fin. A faint brown triangular blotch with an area of 33 mm² is found at the posterior dorsal end of the caudal peduncle area. The caudal fin rays appeared to be less dark than the anterior part of body with the dark colour being paler towards the posterior end of the caudal fin. The area from the posterior edge of the operculum to the line passing through the deepest point of the body, and from the base of the dorsal fin to the ventral edge of the anal fin had a faint brown colouration. The edge of the pectoral fin appeared darker than the fin itself. The dorsal edges of the dorsal fin rays are black. No other external deformations are seen in the colour or in the fish body structure.

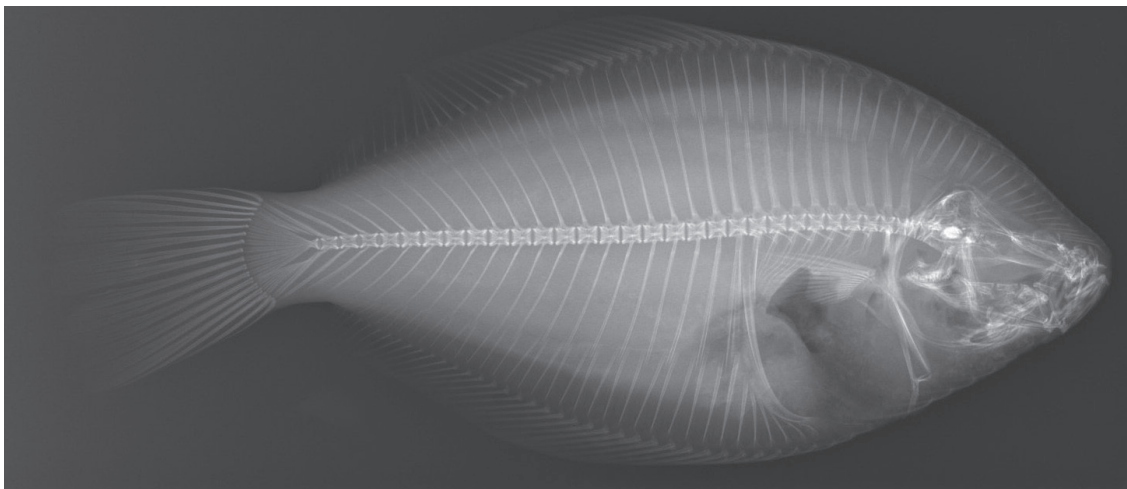


Fig. 3. – Radiograph of a normal specimen of *Rhombosolea leporine*, 295 mm total length.

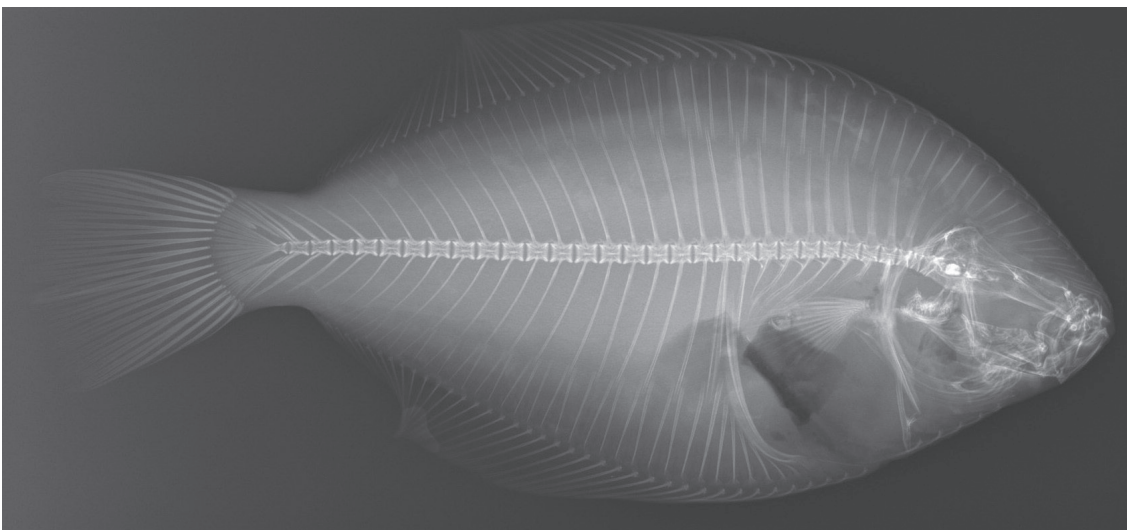


Fig. 4. – Radiograph of the abnormal specimen of *Rhombosolea leporine*, 295 mm total length.

From examination of the radiographs of the normal specimen (Fig. 3) and that of the abnormal specimen (Fig. 4), it is clear that in the abnormal specimen the ultimate and penultimate vertebrae are fused together and the anterior part of the centre of the ultimate vertebra is missing. Other osteological features of the skeleton appear to be normal.

DISCUSSION

DAWSON (1967) suggested that partial albinism occurs as a result of a wound or the effects of adverse environmental factors. It was not clear whether the occurrence of abnormal pigmentation in the present specimen was caused by bites received from other fish. There were no visible signs of injuries that might cause such anomaly.

Abnormal pigmentation is frequently accompanied by morphological variation and vertebral deformities (DÍAZ DE ASTARLOA, 1998). No noticeable variation in morphological or meristic characteristics was found in the abnormal specimen of *R. leporine*, but a slight vertebral fusion of the ultimate and penultimate vertebrae was noticed.

The incomplete pigmentation of flatfishes is almost always associated with head or vertebral anomalies or some other variation in the morphology of the specimens, such as migration of the eye, scales and associated structures (DÍAZ DE ASTARLOA, 1995, 1998).

Pigmentation anomalies can occur on both sides of the body. Hypomelanosis results in white patches or areas devoid of normal pigmentation on the ocular side of the body (VENIZELOS & BENETTI, 1999). Such aberrations in flatfishes may occur during metamorphosis and when the eye migrates to the other side of the head (GARTNER, 1986), depending upon the asymmetry of organizational environments that potentially regulate latent chromatophore precursor survival, proliferation and differentiation (HAMRE et al. 2007; BOLKER & HILL, 2000). Such regulatory

asymmetry may be due to differences in the expression and distribution of secretory proteins involved in the precursor differentiation into mature chromatophores (YAMADA et al., 2010). Accordingly, the partially un-pigmented ocular side could be due to abnormalities in the asymmetry of the regulatory system (BARTON, 2010). This has not yet been studied for wild fish in general and in the flatfish species of New Zealand in particular. Thus, further experimental research is needed to test this hypothesis.

CONCLUSIONS

The partial albino case in a specimen of *Rhombosolea leporina* obtained from Manikau Harbour, south of Auckland City, New Zealand is considered to be the first reported case of its kind in New Zealand. The pattern of body coloration is similar to the partial albinism occurring in other fish species sporting parts of the body completely devoid of chromatophores. Possible causes for such colour aberration are discussed and include abnormalities in the asymmetry of the regulatory system of the chromatophores.

ACKNOWLEDGEMENTS

My sincere thanks are due to the Auckland War Memorial Museum, Natural Science, for depositing the abnormal specimen in their collection, to the radiology team at Green Lane Hospital, Auckland and in particular to Kathryn Bush for doing the x-ray of the normal and abnormal specimens of fish, to Daniel Pauly, Fisheries Centre, University of British Columbia, Canada for reading the manuscript and finally to my daughter, Warda Jawad, for photographing the specimens.

REFERENCES

- ARCHEY G, 1924. An abnormally coloured specimen of the yellowbelly (*Rhombosolea millari* Waite). N.Z. J. Sci. Tech. 6: 342.

- BARTON D, 2010. Flatfish (Pleuronectiformes) chromatic biology. *Rev. Fish Biol. Fish.* 20: 31-46.
- BOLKER J & HILL CR, 2000. Pigmentation development in hatchery-reared flatfishes. *J. Fish Biol.* 56: 1029-1052.
- BURTON D, 2002. The physiology of flatfish chromatophores. *Microsc. Res. Tech.* 58: 481-487.
- CHAVES PT, GOMES I D, FERREIRA EA, AGUIAR KD & SIRIGATE P, 2002. Ambicoloration in the flatfish *Symphurus tessellatus* (Cynoglossidae) from southern Brazil. *Acta Biol. Parana., Curitiba*, 31 (1-4): 59-63.
- COLMAN JA, 1972. Abnormal pigmentation in the sand flounder. *N. Z. J. Mar. fresh. Res.* 6: 208-213.
- DAWSON CE, 1967. Three new records of partial albinism in American Heterosomata. *Trans. Amer. Fish. Soc.* 96: 400-4.
- DÍAZ DE ASTARLOA JM, 1995. Ambicoloration in two flounders, *Paralichthys patagonicus* and *Xystreuris rasile*. *J. Fish Biol.* 47: 168-170.
- DÍAZ DE ASTARLOA JM, 1998. An ambicolorate flounder *Paralichthys isosceles* (Pleuronectiformes: Paralichthyidae), collected off Península Valdez (Argentina). *Cybiurn* 22: 187-191.
- FRANCIS M, 2012. Coastal fishes of New Zealand. Craig Potton Publishing, New Zealand.
- GARTNER JV, 1986. Observations on anomalous conditions in some flatfishes (Pisces: Pleuronectiformes), with a new record of partial albinism. *Environ. Biol. Fish.* 17: 141-152.
- HAMRE K, HOLEN E & MOREN M, 2007. Pigmentation and eye migration in Atlantic halibut (*Hippoglossus hippoglossus* L) larvae: new findings and hypothesis. *Aquacult. Nutr.* 13: 65-80.
- HERNÁNDEZ VA & SINOVCIC G, 1987. A note on a partial albino specimen of the species *Liza (Liza) ramada* (Risso, 1826) caught from the middle Adriatic. *Institut Za Oceanog. Ribarstvo* 68: 1-4.
- JAWAD LA, 2013. A reported case of malpigmentation in the spangled emperor *Lethrinus nebulosus* (Forsskål, 1775) collected from the Arabian Sea Coasts of Oman. *Thalassia Salentina* 35: 29-35
- JAWAD LA & AL-KHARUSI LH, 2013. A reported case of abnormal pigmentation in the Epaulet grouper *Epinephelus stoliczkae* (Day, 1875) collected from the Sea of Oman. *Anales Biología* 35: 41-44.
- JAWAD LA, AHYONG ST & HOSIE A, 2007. Malformation of the lateral line and ambicoloration in the triplefin *Grahamina capito* (Jenyns, 1842) (Pisces: Tripterygiidae) from New Zealand. *Ann. Mus. Civ. Stor. Nat. Ferrara* 9/10: 89-97.
- MACIERA RM, JOYEUX J.-C & PEREIRA CL, 2006. Ambicoloration and morphological aberration in the sole *Achirus declivis* (Pleuronectiformes: Achiridae) and two other cases of colour abnormalities in a chrid soles from south eastern Brazil. *Neot. Ichthyol.* 4: 287-290.
- MILLS MG & PATTERSON LB, L.B. 2009. Not just black and white: pigment pattern development and evolution in vertebrates. *Seminars in Cell and Developmental Biology* 20: 72-81.
- PURCHASE CF, BOYCE DL & BROWN JA, 2002. Occurrence of hypomelanization in cultured yellowtail flounder *Limanda ferruginea*. *Aquacult. Res.* 33: 1191-1193.
- SUGIMOTO M & OSHIMA N, 2002. Introduction: biology of pigment cells in fish. *Microsc. Res. Tech.* 58: 433-434.
- VENIZELOS A & BENETTI DD, 1999. Pigment abnormalities in flatfish. *Aquacult.* 176: 181-188.
- YAMAD Y, OKAUCHI M & ARAKI K, 2010. Origin of adult-type pigment cells forming asymmetric pigment patten in Japanese flounder (*Paralichthys olivaceus*). *Dev. Dyn.* 239: 3147-3162.

Received: January 8th, 2014

Accepted: May 16th, 2014

Branch editor: Marleen de Troch

Soft tissue discrimination with contrast agents using micro-CT scanning

Emilie Descamps¹, Alicja Sochacka¹, Barbara De Kegel¹, Denis Van Loo^{2,3}, Luc Van Hoorebeke² & Dominique Adriaens^{1,*}

¹ Research Group Evolutionary Morphology of Vertebrates, Ghent University, K.L. Ledeganckstraat 35, 9000 Gent, Belgium

² UGCT, Department of Physics and Astronomy, Ghent University, Proeftuinstraat 86, 9000 Gent, Belgium

³ Department of Soil Management, Ghent University, Coupure Links 653, 9000 Gent, Belgium

* Corresponding author: dominique.adriaens@ugent.be

ABSTRACT. The use of high resolution, three-dimensional visualization has been receiving growing interest within life sciences, with non-invasive imaging tools becoming more readily accessible. Although initially useful for visualizing mineralized tissues, recent developments are promising for studying soft tissues as well. Especially for micro-CT scanning, several X-ray contrast enhancers are performant in sufficiently contrasting soft tissue organ systems by a different attenuation strength of X-rays. Overall visualization of soft tissue organs has proven to be possible, although the tissue-specific capacities of these enhancers remain unclear. In this study, we tested several contrast agents for their usefulness to discriminate between tissue types and organs, using three model organisms (mouse, zebrafish and *Xenopus*). Specimens were stained with osmium tetroxide (OsO₄), phosphomolybdic acid (PMA) and phosphotungstic acid (PTA), and were scanned using high resolution microtomography. The contrasting potentials between tissue types and organs are described based on volume renderings and virtual sections. In general, PTA and PMA appeared to allow better discrimination. Especially epithelial structures, cell-dense brain regions, liver, lung and blood could be easily distinguished. The PMA yielded the best results, allowing discrimination even at the level of cell layers. Our results show that those staining techniques combined with micro-CT imaging have good potential for use in future research in life sciences.

KEY WORDS: 3D visualization, micro-CT scanning, soft tissue, contrast agents, vertebrates

INTRODUCTION

Light microscopic histology is commonly used to analyze the organization and internal structure of biological tissues. However, despite its advantage in providing high resolution images, it requires elaborate preparation and full destruction of the specimen. It also often generates marked and heterogeneous distortions (JONES et al., 1994; CARDEN et al., 2003; DESCAMPS et al., 2012). To properly understand tissue organization, life sciences research in developmental biology or comparative biology currently requires accurate, high resolution three-dimensional (3D) imaging of these tissues within a whole organism topography. The latter has gained interest with the increasing development of valuable new automated imaging

techniques, which facilitate visualization, processing and analysis of 3D images (see also ZANETTE et al., 2013). Those methods include X-ray micro Computed Tomography (μ CT) scanning (MASSCHAELE et al., 2007; CNUUDE et al., 2011), magnetic resonance imaging (MRI) (TYSZKA et al., 2005; POHLMANN et al., 2007), Optical Projection Tomography (OPT) (SHARPE et al., 2002), absorption and phase-contrast synchrotron X-ray imaging (BETZ et al., 2007; BOISTEL et al., 2011) and Light Sheet (based) Fluorescence Microscopy (LSFM) (SANTI, 2011; BUYTAERT et al., 2012; DESCAMPS et al., 2012).

μ CT scanning is the oldest tomographic imaging technique and most frequently applied to image 3D tissue organization in a non-invasive way (RITMAN, 2011). It allows the

discrimination of soft from hard tissue, relying on the differences in photon attenuation levels of these tissue types (RITMAN, 2004; MIZUTANI & SUZUKI, 2012). Bone, with its calcium phosphate minerals, attenuates X-rays more intensely than the surrounding soft tissues (such as cartilage, nerves, blood vessels and muscles). As the latter are mainly composed of low-atomic-number elements (carbon, hydrogen, oxygen), their comparable levels of hydration result in low contrast levels (MIZUTANI & SUZUKI, 2012). Although recent studies show that proper boundary conditions of tissue sampling (such as stabilized humid environment) allow contrast between some soft and hard tissues (NAVEH et al., 2014), a more detailed discrimination requires the use of contrast agents (high-atomic-number elements) that bind to components of these soft tissues (MIZUTANI et al., 2008; METSCHER, 2009a; MIZUTANI & SUZUKI, 2012; PAUWELS et al., 2013), or the use of phase contrast imaging (RITMAN, 2004; BETZ et al., 2007; MIZUTANI & SUZUKI, 2012). As with the contrast agents used in transmission electron microscopy (TEM), these agents bind differently to soft tissue types in whole mount samples, thereby allowing μ CT scanning to provide 3D data on soft tissue topography. Because of this potential, staining techniques with contrast enhancement agents have been tested for their ability to improve tissue discriminations and organ boundaries (DOBRIVOJEVIC et al., 2013). Soft tissue contrast agents that have been used on biological specimens include osmium, gold, silver, iodine, platinum, mercury, tungsten, molybdenum and lead (MIZUTANI & SUZUKI, 2012; ZANETTE et al., 2013). Although some of these agents allow the visualization of particular tissues or cells (such as liposome-rich cells being contrasted with an iodinated contrast agent) (SCHAMBACH et al., 2010), other agents generate a more overall contrasting of certain tissue types (*e.g.* myelinated brain tissue versus grey matter) (EFIMOVA et al., 2013).

Studying the 3D organization of organs within an organism using μ CT scanning particularly benefits from contrast agents that meet two criteria: (1) they can be administered in a simple

manner by submersing complete specimens in an aqueous solution containing elements with a high atomic number, and (2) they penetrate easily through the thick layers of tissues (PAUWELS et al., 2013). If the agents could also be washed away after scanning, this would be an additional advantage in the study of internal structures of rare specimens, such as type material from collections. METSCHER (2009b) provided a first empirical approach to developing simple protocols for staining small but complete organisms, without using the toxic osmium tetroxide (a commonly used but highly toxic contrast agent for TEM). MIZUTANI & SUZUKI (2012) gave an overview of commonly-used contrast agents, and their general contrasting potentials. In a more extensive comparison of contrast agents that meet the first two criteria mentioned above, PAUWELS et al. (2013) compared the contrasting enhancement of 28 different chemicals on samples larger than 1 cm³. All three studies showed that the best contrasts are obtained by using aqueous solutions of osmium tetroxide (OsO₄), phosphomolybdic (PMA) or phosphotungstic acid (PTA), or inorganic iodine (in different solutions). Whereas MIZUTANI & SUZUKI (2012) reviewed the features of these agents, as they are known from their application in TEM, METSCHER (2009a) provided overview images of reconstructed whole mount specimens. The latter author did indicate, among other things, that with PTA, cartilage matrix does not stain strongly. PAUWELS et al. (2013) compared the contrasting enhancement of muscle tissue versus adipose tissue, and tested penetration capacities of the contrast solutions. More recently, GIGNAC & KLEY (2014) tested Lugol's iodine staining on larger specimens, to analyse its contrasting potential across different tissue types.

Although much progress has been made on the use of these contrast agents, and their application in μ CT scanning has become common practice (ZANETTE et al., 2013), little is known about the binding affinities of these agents for particular tissues in large tissue blocks or whole organisms, and thus their potential to allow automated segmentation of individual organs or tissues based on voxel grey values. Applications of

contrast-enhancing elements in TEM suggest that OsO_4 labels lipids in cell membranes (CARSON & HLADIK, 2009), and hence its application with μCT scanning should visualize all cells rather equally. Although this would theoretically make discrimination between cell types rather difficult, it has allowed discrimination between neural and vascular tissue (HALL et al., 1945; WATSON, 1958; HAYAT, 2000; AOYAGI et al., 2010; WATLING et al., 2010; MIZUTANI & SUZUKI, 2012). JOHNSON et al. (2006) showed that OsO_4 allows different organs to be distinguished in early embryos, however, the discriminating power across different tissue types was not explored in detail. In adult mice, OsO_4 proved to be suitable for visualizing tongue musculature, although only for smaller tissue specimens due to limited penetration (AOYAGI et al., 2013). PTA on the other hand is known to adhere to various proteins and is considered to be suitable for visualizing connective tissue (KIERNAN, 1981; METSCHER, 2009a). PMA allowed the identification of cartilage structures in mollusks (GOLDING & JONES, 2007). Iodine is considered not to adhere to specific chemical components but rather uniformly to tissue constituents (MIZUTANI & SUZUKI, 2012), although a binding affinity of iodine trimers to glycogen and lipids has been suggested (BOCK, 1972; METSCHER, 2009b). Also a higher affinity with liposome-rich cells (BARON, 1994; SCHAMBACH et al., 2010), connective tissue of muscle fascia, individual muscle fibers (JEFFERY et al., 2011; TSAI & HOLLIDAY, 2011; WILHELM et al., 2011; BAVERSTOCK et al., 2013), and blood has been suggested (DEGENHARDT et al., 2010). Still, METSCHER (2009b) indicated that, based on his experiments with embryos of both vertebrates and invertebrates, none of the contrast agents used (OsO_4 , PTA and iodine solutions) was tissue-specific.

Some apparently conflicting, or rather inconsistent results regarding the tissue-discriminating potentials of these contrast agents thus remain, especially when applied to complete organisms. Because of that, we wanted to focus more on differences in contrasts

between tissue types and organs, and compare the degrees to which tissue and organ boundaries can be discriminated. We compared the effect of OsO_4 , PTA and PMA using embryonic mice (stages E14.5 and E15.5), and contrasted that to a recently published similar test using Lugol's iodine staining (GIGNAC & KLEY, 2014). More specifically, we tested whether OsO_4 generates a non-discriminative contrast of all soft tissues, or whether some tissues can be discriminated consistently across the complete organism. As it has been claimed in literature that PTA, and PMA solutions have similar discriminative potentials to the highly toxic OsO_4 , we tested whether that was indeed the case at the level of tissue types. As the best results were obtained with PTA and PMA, we also compared them across other taxa, using a juvenile zebrafish and *Xenopus* tadpoles. With respect to PMA and PTA, if indeed they bind specifically to proteins, including collagen, we would expect protein-rich tissues (such as blood and muscle tissue) and dense connective tissues (such as the dermis, ligaments and tendons) to show higher levels of affinity with the contrast agents (and lower levels in, for example, cartilage, which is lower in protein levels). The potential of the different contrast agents to discriminate between myelinated and non-myelinated nerves was not tested in this study, as myelination in mice only starts at the E16.5 stage (thus later than the one studied here) (HARDY & FRIEDRICH, 1996). As we used complete organisms exceeding 1 cm^3 , we tested whether these agents penetrate sufficiently to allow tissue discrimination throughout the whole body. This paper further discusses the different characteristics of each contrast agent, and describes how they could be applied for tissue differentiation and (semi-)automated segmentation when using μCT scanning.

MATERIALS AND METHODS

Specimens

We used five mice (*Mus musculus*), two tadpoles (*Xenopus laevis*) and one juvenile

zebrafish (*Danio rerio*). The mice were obtained from the Department for Molecular Biomedical Research (DMBR) at the VIB and Ghent University (Belgium). The embryos were removed from the mother on embryonic day E14.5 (E15.5 for PMA-stained mouse), collected in phosphate-buffered saline (PBS) and fixed overnight in 4% paraformaldehyde at room temperature. The *Xenopus laevis* tadpoles were also reared at the DMBR, euthanized with an overdose of MS-222 (ethyl 3-aminobenzoate methanesulfonate salt, Sigma Aldrich, E10521) and fixed in 4% paraformaldehyde in PBS at stage 48. The juvenile zebrafish was obtained through the commercial trade (Florida). It was euthanized with an overdose of MS-222 and fixed in 4% paraformaldehyde. All experimental procedures were performed in accordance with the Experimental Animal Ethics Committee of Ghent University.

Contrast stains

Contrast agents were obtained from VWR International (PMA and PTA) and Laborimpex NV (OsO_4). All mouse embryos ($n = 5$, average total length: ± 10 mm) were stained overnight (14 hours), except for the PMA mouse, which was stained for six days. The *Xenopus* tadpoles (average total length: ± 10 mm) were stained with PTA for 24 hours and the juvenile zebrafish (total length: 22 mm) was stained with PMA for six days. The staining times were chosen arbitrarily, but were sufficiently long to allow appropriate penetration. The protocols followed METSCHER (2009a), except for the PTA and PMA staining (PMA was not used by the latter). PTA and PMA staining was performed with 2.5% solution in demineralized water. The OsO_4 staining was done in a 1% osmium tetroxide (OsO_4) solution.

Micro-CT imaging

The mouse and zebrafish specimens were kept in vials with a saturated atmosphere of ethanol vapour to prevent shrinkage from dehydration.

Although X-ray attenuation of water and ethanol is low, experience showed that better contrast results were obtained without the specimens being fully submerged. For the *Xenopus* tadpoles, to avoid specimen movement during acquisition of the μCT images, they were embedded in Epon (Fluka, 45359) (after dehydration in an ethanol series). The specimens were all scanned at the μCT scanning facilities of UGCT (Ghent University, Belgium). The setup consisted of a dual-head microfocus X-ray source (FeinFocus FXE160.51 transmission tube and FeinFocus FXE160.48 directional tube head), a high precision Micos UPR160 F Air rotation stage, an interchangeable detector and in-house-developed acquisition software (DIERICK et al., 2010). For these samples, only the Varian PaxScan 2520V and the PerkinElmer XRD 1620 CN3 CS a-Si flat panel detectors were used. For all scans, the transmission tube head was used. All mouse embryos, except the one stained with PMA, were scanned using a tube voltage and target current of 100 kV and 60 μA , respectively. For each individual, a series of 1001 projections with an exposure time of one second per projection was recorded using the Varian detector and covering 360 degrees, resulting in voxel sizes of 5.95 μm (each dimension of the isometric voxels). The PMA-stained mouse was scanned at 100 kV and 90 μA , using the PerkinElmer detector. A series of 1441 projection images was recorded at an exposure time of two seconds per projection image, covering 360 degrees resulting in voxel sizes of 6.24 μm . Identical settings were used for the juvenile zebrafish allowing a better comparison between the two PMA-stained specimens. The voxel sizes for the zebrafish were 5.82 μm . For the *Xenopus* tadpole, the X-ray tube was operated at 80 kV tube voltage and 37.5 μA target current. Using the PerkinElmer detector, a total of 1001 projection images was recorded at a total exposure time of 6 seconds per image, covering 360 degrees and resulting in voxel sizes of 3.40 μm . Reconstruction of the tomographic projection data was performed using the in-house-developed CT-software Octopus (VLASSENBOECK et al., 2007) and VGStudioMAX.

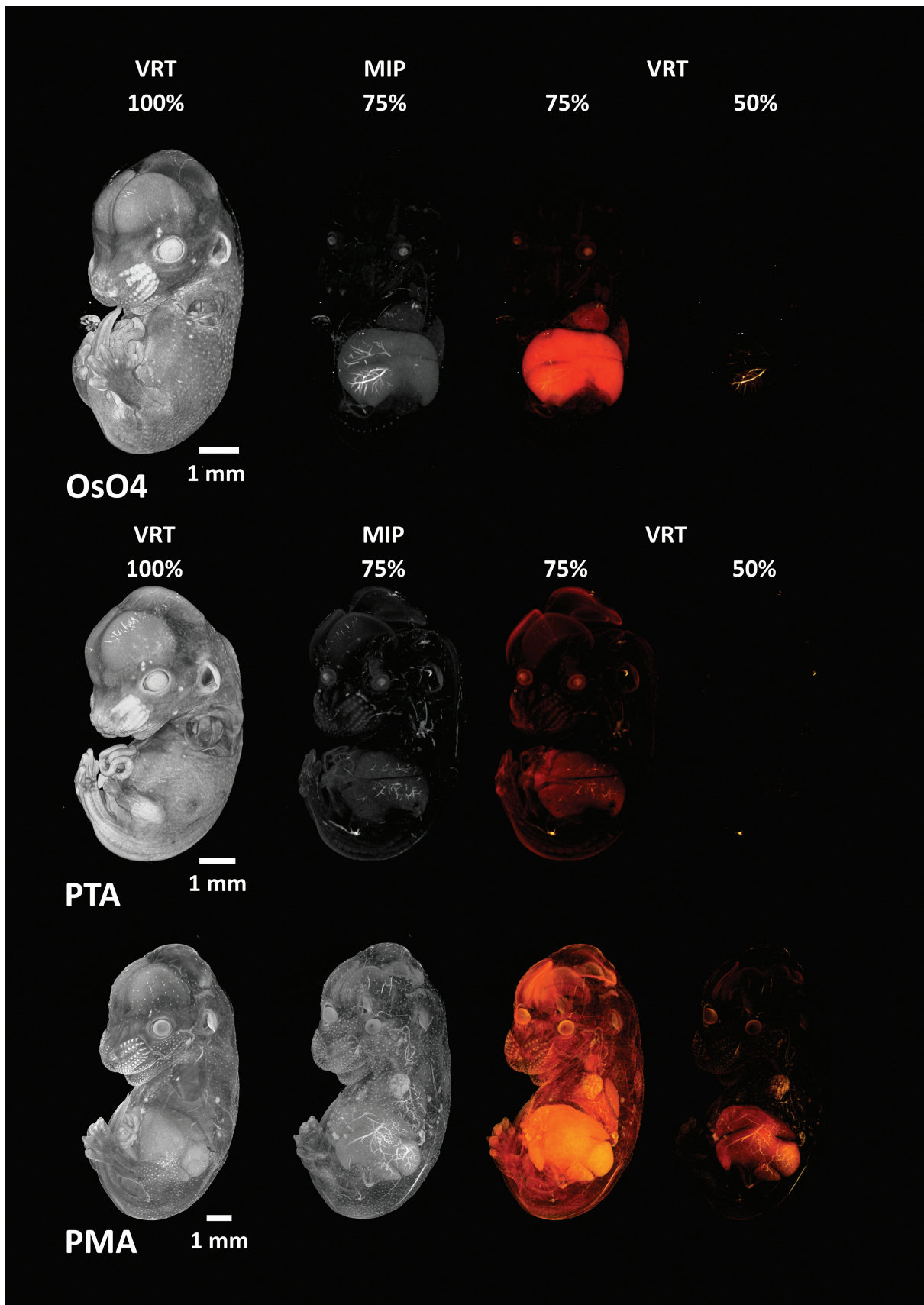


Fig. 1. – Volume rendering images of the mouse embryos stained with three different contrast agents, using maximum intensity projection (MIP) and texture volume rendering (VRT) at 100% (left), 75% and 50% of the total color value range (OsO₄ – osmiumtetroxide, PTA – phosphotungstic acid, PMA – phosphomolybdic acid).

Image analysis

The TIFF virtual images were imported in the software Amira (version 5.5.0, 64-bit, Mercury Computer Systems). Volume rendering (Volren) of the total color value range was performed. To visualize an overview of the level of discrimination between tissue types and organs, volume rendering images were generated where the lower threshold was set to 50% and 75% of the total color range of the tissues, allowing a qualitative comparison across contrast stains within the mouse embryos (Fig. 1), and across the species (Fig. 2). As this is an arbitrary manner of setting thresholds, these figures should not be considered in any quantitative way but purely for visualization of overall results. These were visualized using the texture-rendering option

(VRT), whereas the 75% threshold was also visualized using maximum intensity projection (MIP). The latter has proven to be more accurate for visualizing the vasculature than texture-based volume rendering (RUBIN et al., 1994; FISHMAN et al., 2006). Virtual slices (sagittal and frontal) were generated at similar anatomical positions in the three mouse embryos for a more detailed comparison across the three contrast agents (Fig. 3). For a more detailed visualization of organ discrimination, volume rendering images (using VRT) and virtual cross sections were generated of specific regions of interest (Figs 4-7). Where pixels were rather coarse on these virtual sections, a low pass filter was applied for improved visualization. For the anatomical nomenclature, we used on-line and published databases on mouse brain anatomy (SCHAMBRA,

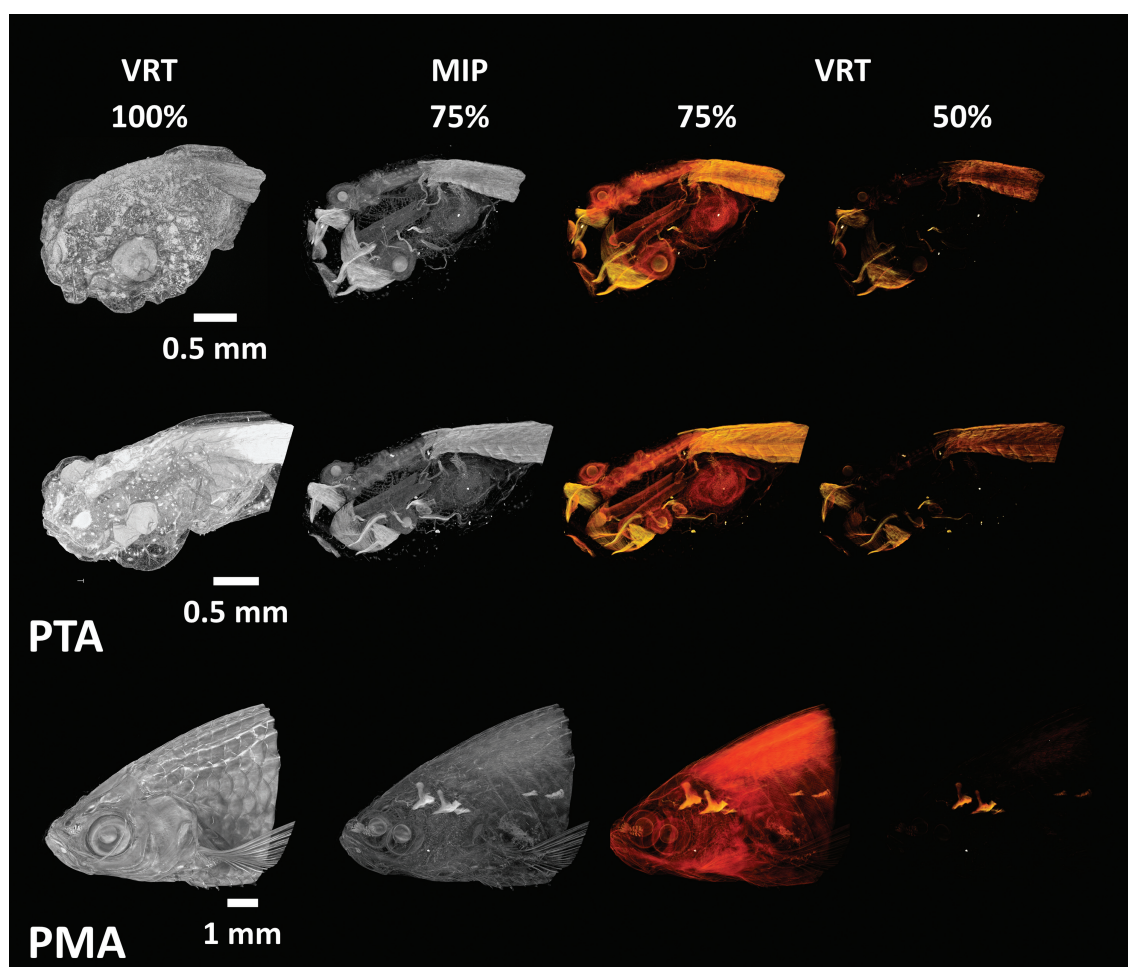


Fig. 2. – Volume rendering images of *Xenopus laevis* tadpoles (upper two rows) stained with PTA and juvenile zebrafish (*Danio rerio*) stained with PMA, using maximum intensity projection (MIP) and texture volume rendering (VRT) at 100% (left), 75% and 50% of the total color value range (PTA – phosphotungstic acid, PMA – phosphomolybdenic acid).

2008; ALLEN INSTITUTE FOR BRAIN SCIENCE, 2014), zebrafish brain (WULLIMANN et al., 1996; ULLMANN et al., 2010) and vascular anatomy (ISOGAI et al., 2001), and *Xenopus* anatomy (WIECHMANN & WIRSIG-WIECHMANN, 2003).

RESULTS

Overall staining patterns

A difference in the overall contrast between voxel color values for the tissue types and organs could be observed (Figs 1-3). While the voxel size of the PMA-stained mouse embryo was the highest of all (6.24 μm vs 5.95), the quality of the virtual sections was substantially better. The arbitrary thresholds of a 75% color value range

showed that for PMA, most organs were still stained, whereas for PTA and OsO_4 , hardly any structures were visible (Fig. 1). At the 50% color value range, only PMA allowed the visualization of multiple organs. In all stains, the liver seemed to absorb the highest levels of contrast agents. MIP-rendering allowed better visualization of tissues that had higher color intensities, especially for blood within the blood vessels. This allowed clearer visualization of the vascularization of the liver with all stains.

In the zebrafish and *Xenopus* tadpoles, overall staining patterns in relation to the 75% and 50% thresholds were somewhat different (Fig. 2). For the PTA-stained tadpoles, several organs were clearly visible even at the 50% threshold, especially muscle tissue and eye lenses. For the

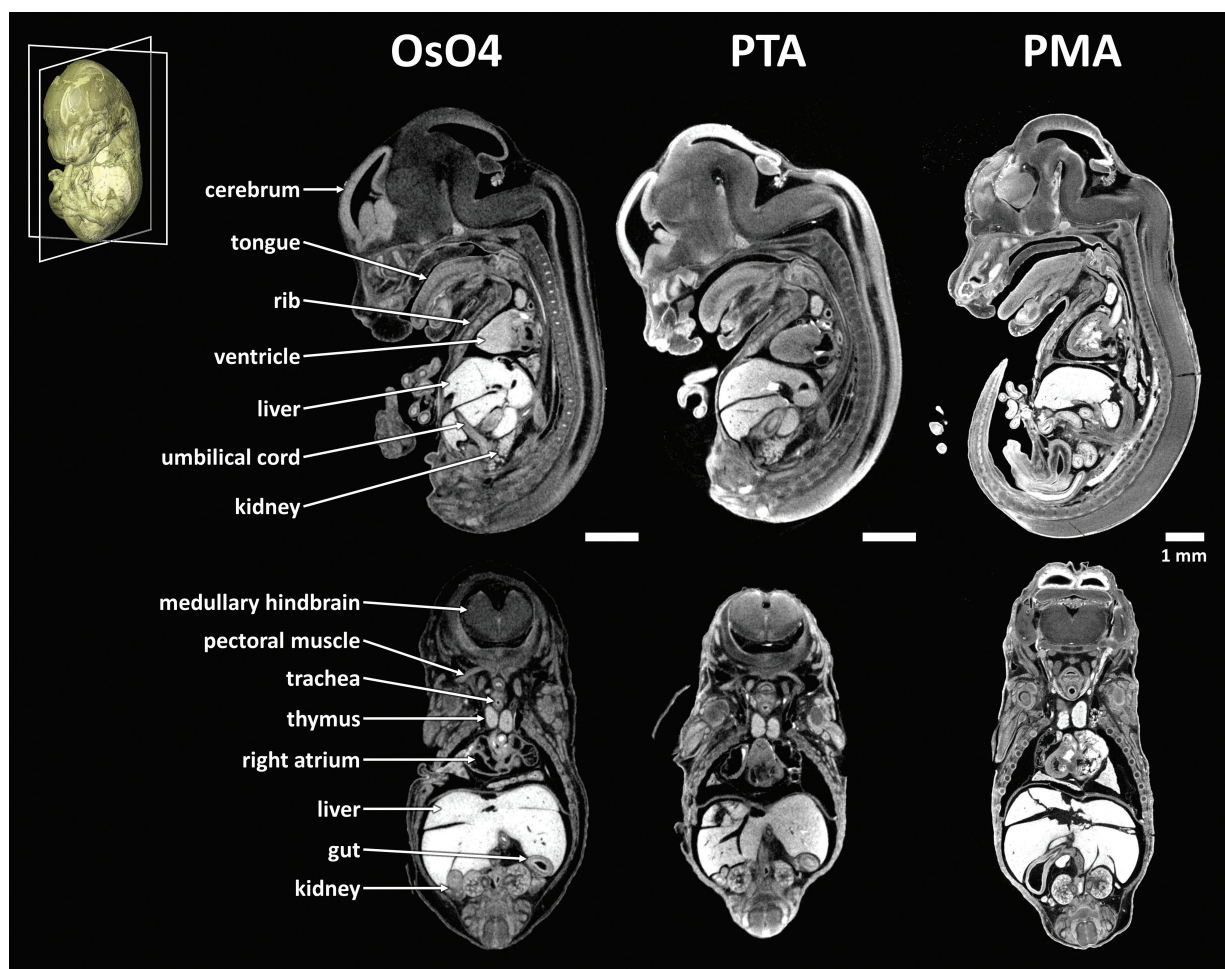


Fig. 3. – Virtual sagittal (top) and frontal (bottom) sections at similar position in the mouse embryos stained with three different contrast agents (OsO_4 –osmiumtetroxide, PTA–phosphotungstic acid, PMA–phosphomolybdenic acid). Inset shows the relative position of the sections.

PMA-stained zebrafish, on the other hand, hardly any structure was visible at the 50% threshold, only condensations of blood in cranial sinuses.

Discrimination of tissue types and organs

An overview of the tissue types and organs that could clearly be distinguished with each of the contrast agents is given in Tables 1 and 2.

OsO₄

In the mouse embryos, structures that were most intensely stained were the eye lenses, liver, heart, lungs (small cavities were visible, suggesting bronchioli were present, together with bronchi and trachea), thymus and blood (Figs 1, 3, 4). Also part of the intervertebral discs, more specifically the nucleus pulposus, seemed to be

intensely stained (Fig. 4B). In most cases, not only the blood but also the actual blood vessels and the heart were clearly visible in the virtual sections (Fig. 4A). What seemed to be glomeruli in the metanephros were clearly visible, as well as the adrenal gland next to the kidney (Fig. 4A). This higher intensity of the voxel values could be the consequence of an increased vascularization and thus merely demonstrate presence of blood rather than higher affinities for these tissues. Virtual sections showed that penetration of the stain was homogenous, as centrally-located organs were clearly identifiable (Figs 3, 4A). As is the case for most other contrast agents, OsO₄ stained epithelial structures very well (e.g. olfactory epithelium, follicles of the vibrissae, and the gut and tracheal mucosa). In the brain, particular regions (such as the cerebral periventricular layers, mammillary mantle zone and the trigeminal ganglion) could be discerned. Of the musculoskeletal system, cartilage (e.g.

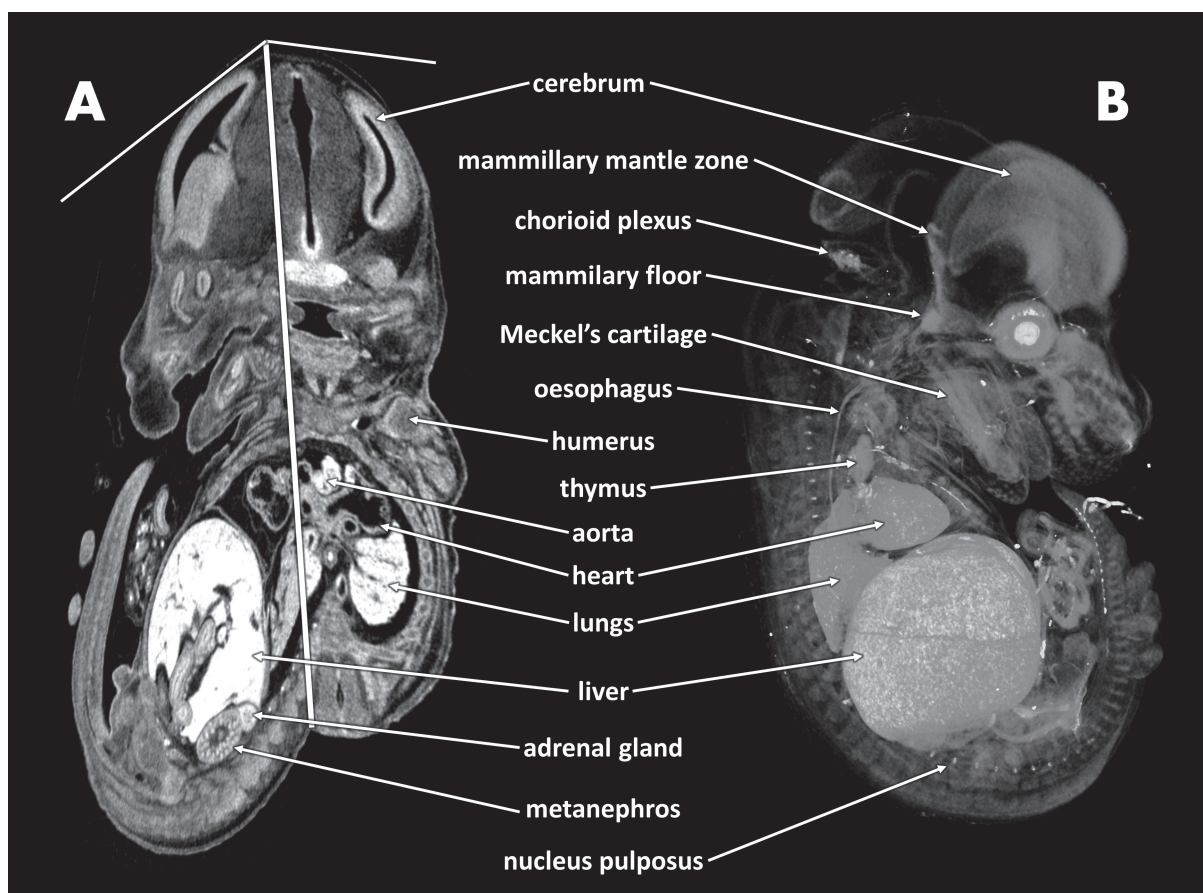


Fig. 4. – Organ and tissue specific voxel intensities of mouse embryo (stage E14.5) stained with osmium tetroxide: (A) virtual frontal and parasagittal section and (B) volume rendering image (right lateral view).

TABLE 1

Summary of the published binding preferences of contrast agents and the level of visualization obtained in this study.

Contrast agent	Binding preference	Visualised soft tissue structures
OsO ₄	Lipids, proteins and nucleic acids	Eye lens, liver, heart, lungs, thymus, blood and blood vessels, metanephros, adrenal gland, nucleus pulposus, epithelia, cell dense brain regions, muscle, cartilage
PTA	Connective tissue (collagen)	Eye lens, liver, heart, lungs, thymus, blood, blood vessels, metanephros, epithelia, glands, cell dense brain regions, muscle, cartilage
PMA	Collagen (phospholipids?)	Eye retina, liver, lungs, thymus, blood and blood vessels, metanephros, epithelia, glands, cell dense brain regions, muscle, cartilage

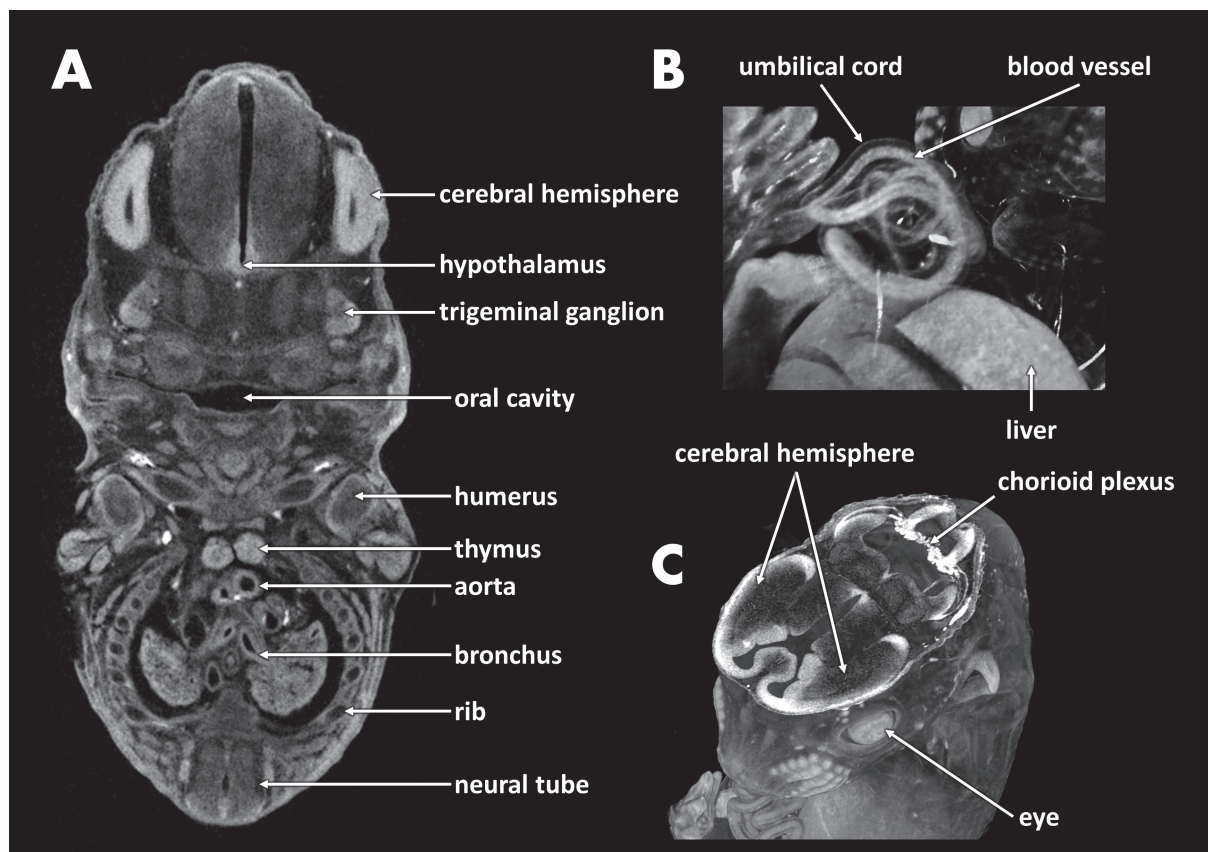


Fig. 5. – Organ and tissue specific voxel intensities of mouse embryo (stage E14.5) stained with phosphotungstic acid: (A) virtual frontal section at similar level as in Fig. 4, (B) volume rendering image of the umbilical region, and (C) cut through volume rendering through the brain.

TABLE 2

Overview of the tissue and/or organ specificity of the contrast agents used in this study ('-' indicates hardly visible, '+' indicates weak discrimination potential, '++' and '+++' indicate moderate and very good discrimination potential, respectively).

Tissue/Organ	OsO ₄	PTA	PMA
Cartilage	+	+	++
Muscles	++	++	+++
Blood/vessels	++	++	++
Liver	+++	+++	+++
Eye/eye lens	++	+++	+++
Epithelial structures	++	+++	+++
Cell-dense nervous tissue	+++	+++	+++
Lungs	+++	+++	+++
Connective tissues	++	++	++

Meckel's cartilage) and muscle tissue could be distinguished (Fig. 4B). Ossification zones, as observed with the other stains, could not be discerned with OsO₄.

PTA

Tissues or organs that showed the highest color intensities in the mouse embryo were eye lenses, liver, blood, and epithelial structures (olfactory epithelium, follicles of vibrissae) (Figs 1, 2, 5). Some parts of the brain showed higher levels of X-ray attenuation, such as the periventricular layers of the cerebral hemispheres, the trigeminal ganglion and the hypothalamus (Fig. 5A). The myelencephalic chorioid plexus was intensely stained, which could be due to the staining of the blood it contained (Fig. 5C). Postcranially, spinal ganglia were visible. In general, blood showed highest intensities on the virtual sections, and blood vessels could be distinguished (*e.g.* the umbilical vessels embedded within the umbilical cord, leaving the mucoid tissue poorly stained) (Fig. 5B). Other organs that were clearly visible were the thymus, lungs (trachea, bronchi, bronchioli), kidney (glomeruli were visible) and adrenal gland. Of the musculoskeletal system, cartilage and muscles (*e.g.* eye muscles) were

visible. Cartilage of ribs and limbs could be clearly discriminated, whereas the contrast between vertebral cartilages and surrounding tissues was less prominent. The presence of ossifications (which arise at about this E14.5 stage) could be derived from the differences in the grey value intensity of the cartilage matrix. At locations where ossification was to be expected, cartilage matrix was stained less (*e.g.* base of scapula, upper half of humeral diaphysis, proximal parts of ribs) (PATTON & KAUFMAN, 1995; MA *et al.*, 2003).

In the PTA-stained tadpoles, contrasts between the different tissue types was consistent between the two specimens analyzed (Fig. 2). As in the mouse embryos, muscles (individual fibers and myosepta), eye lenses (superficial layer), blood and blood vessels (including the heart tissue), epithelia (olfactory epithelium, gill and gut mucosa) and the brain were more intensely stained (Fig. 6). However, discrimination between specific brain regions was not as clear as in the mouse embryos. Also discernible were the mucosal layers of the filtering plates, which comprise a central portion of connective tissue, covered by one or two layers of epithelial cells covered by mucus (BRUNELLI *et al.*, 2004) (Fig. 6C). The thick oral plates were intensely stained

(Fig. 6D). Cartilage could be distinguished as the perichondral connective tissue was visible, as well as what appeared to be individual chondrocytes (Fig. 6C, inset). In the notochord, the cell membranes of notochordal cells could also be discerned on the virtual sections.

PMA

In the mouse embryo, the brightest structures were the eyes (retina only), the liver, particular brain regions (such as the inferior colliculus, mammillary mantle zone, periventricular layers of the cerebral hemispheres) (Figs 1, 7A), blood and blood vessels, lungs (with distinct bronchioli), epithelia (olfactory, tracheal and gut mucosa, epidermis with follicles of vibrissae and regular hair), and muscles (including the

heart) (Figs 1, 7). In addition, several glandular structures could be clearly distinguished, such as the thymus, salivary glands, adrenal gland (Fig. 7A), and the pancreas. Distinct from the other contrast agents, in the eye, PMA stained only the photoreceptor layer intensely, whereas the lens and optic nerve were clearly less stained (Fig. 7B, C).

Cartilaginous structures were also stained, although it was not clear whether chondrocytes or the matrix were the brighter on the CT sections. Also here, we could distinguish cartilage that had started to become ossified (based on the topography of suspected ossification), whereas for PMA there were cartilaginous regions where the matrix was not stained or was poorly stained (Fig. 7D). Whether this corresponds to resorbed cartilage or not, could not be verified here. It

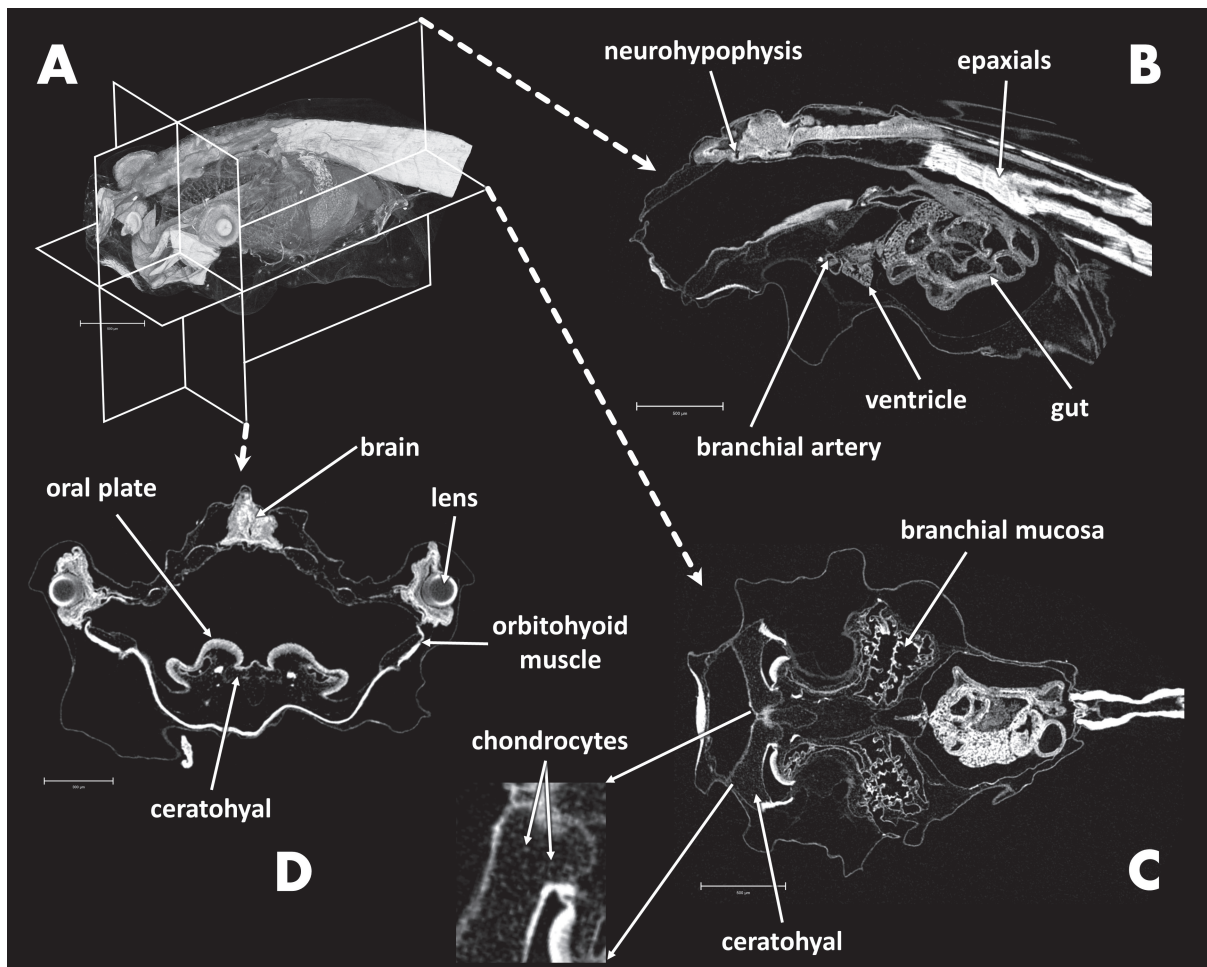


Fig. 6. – Organ and tissue specific voxel intensities of *Xenopus laevis* tadpole (stage 48) stained with phosphotungstic acid: (A) volume rendered overview, (B) mediasagittal virtual section, (C) horizontal virtual section through the ceratohyal cartilages, and (D) transverse section through the eye lenses.

may be that the thin, but more intensely-stained superficial layer surrounding the darker cartilage corresponds to bone, whereas the layer in the same position around other cartilage corresponds to perichondrium (where this layer is thicker and less demarcated) (Fig. 7D).

Similar, highly qualitative results were obtained in the zebrafish juvenile (Fig. 8). Most spectacular results involved the level of detail in some organs and tissues. As in the mouse embryos, it was not the eye lens and eye nerve that were stained the most, but the remaining parts. It was even possible to distinguish all cellular layers of the retina (Fig. 8B, C). Blood also stained most intensely, visualizing the cranial sinuses in the specimen studied (Fig. 2). The keratinized pharyngeal pads were also clearly visible (Fig. 8A, E). Individual muscle fibers and myosepta were very clearly distinguishable (Fig. 8A, D). In the vertebral column, the notochord and its notochordal strand were obvious (Fig. 8A). In

the brain, functional parts (rather than just layers) could be distinguished, of which some clearly stained more intensely (*e.g.* periventricular grey zone and torus longitudinalis of the optic tectum, eminentia granularis, intermediate thalamic nucleus, corpus cerebelli, medial octavolateralis nucleus, pituitary, etc.) (Fig. 8E). Bone could be distinguished, whereas cartilage was less obvious than in the mouse embryos. The hemibranchs appeared clearly as well (Fig. 8E). In the ventral branchial region, individual follicles of the thyroid gland were intensely stained (Fig. 8E).

DISCUSSION

Limited contrast between tissue types and organs with OsO_4 ?

OsO_4 is a highly toxic contrast agent interacting with unsaturated lipids, sometimes also interacting with proteins (WIGGLESWORTH,

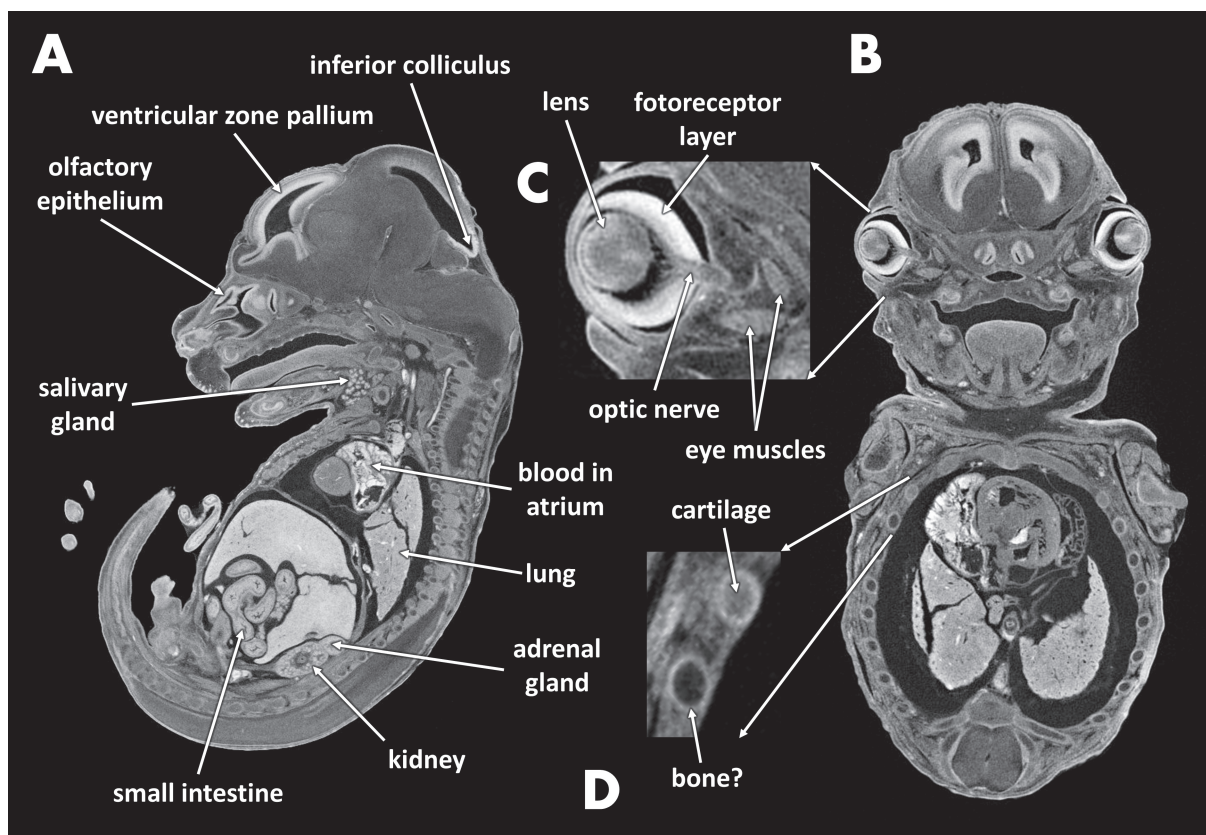


Fig. 7.—Organ and tissue specific voxel intensities of mouse embryo (stage E15.5) stained with phosphomolybdenic acid: (A) virtual sagittal section through the kidney, (B) virtual frontal section through the optic nerves, (C) detail of the section at the eye, and (D) detail of the section at the ribs.

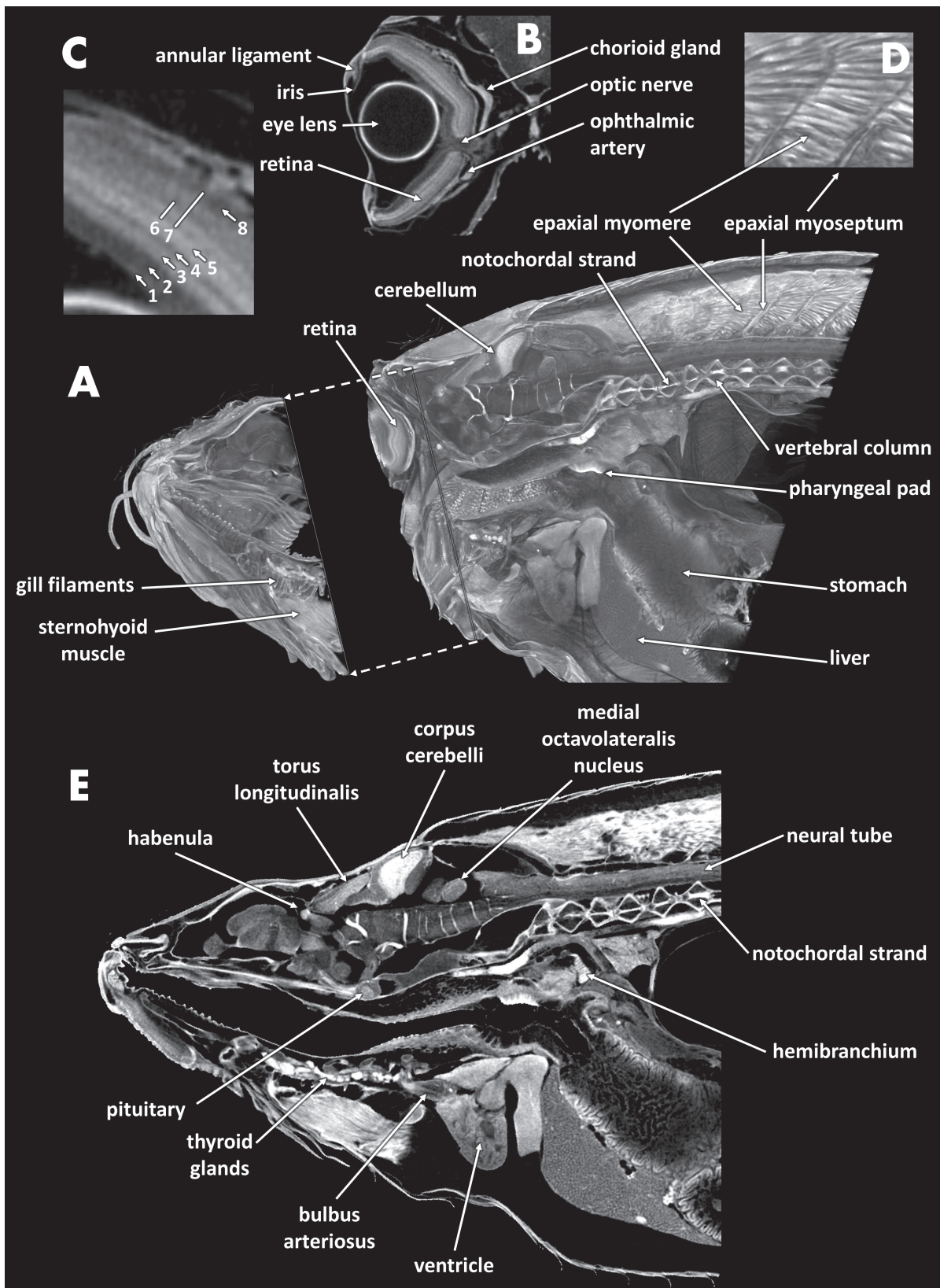


Fig. 8. – Organ and tissue specific voxel intensities of juvenile zebrafish stained with phosphomolybdenic acid: (A) volume rendering with mediosagittal cut-through and transverse cut-through at the level of the eyes, (B) detail of the eye, (C) higher detail of the retinal layers, (D) detail of epaxial muscle fibers and myosepta, (E) virtual mediosagittal section (Legend for Fig. C: 1 – ganglionic layer, 2 – inner plexiform layer, 3 – inner nuclear layer, 4 – outer plexiform layer, 5 – outer nuclear layer, 6 – cones photoreceptor layer, 7 – rods photoreceptor layer, 8 – pigmented layer).

1975; HAYAT, 2000; DI SCIPIO et al., 2008). As such, a staining with limited contrast in grey values of the voxels across the tissue types and organs was expected, as OsO_4 was expected to show an overall and similar affinity with all cell types (*i.e.* the phospholipids in their membranes). However, the overall result of the OsO_4 -stained mouse embryos was fairly good, allowing the discrimination of most tissues and organs (*e.g.* liver, blood, eye lens, heart, lungs, thymus). The intense staining of the liver, as was observed by JOHNSON et al. (2006), could be explained by its rich content in lipids and lipoproteins. The intense affinity with blood also confirms our hypothesis, *i.e.* that erythrocytes have high OsO_4 affinity through their combined high protein (hemoglobin) and phospholipid content (enucleated cells with few organelles).

As with the other contrast agents, there was a non-homogenous visualization of blood vessels, and in several cases even a distinct unilateral difference in staining intensity. This asymmetry was not seen in other structures. This indicates that the blood, and not the blood vessels, stained intensely (as was expected), as postmortem precipitation of red blood cells due to gravity may explain the observed patterns.

Discrimination between particular brain regions was possible, partly due to the vascularization conditions (*e.g.* chorioid plexus). On the other hand, the intense staining of the periventricular strata in the dorsal telencephalic pallium (which was a consistent observation across the contrast agents used) requires an alternative explanation. Because myelin is phospholipid-dense, OsO_4 is known to bind intensely to it (DI SCIPIO et al., 2008). In mouse embryos, however, myelin only starts to be produced by oligodendrocytes from the E16.5 stage on (we used E14.5 and E15.5 stages) (HARDY & FRIEDRICH, 1996). Still, the virtual sections gave similar results to histological sections stained with haematoxylin with respect to nuclear-dense versus less-dense zones (SCHAMBRA, 2008). Haematoxylin is known to stain nuclei due to its affinity with nucleic acids. The fact that the telencephalic

periventricular zone is a cell-dense area where cell proliferation takes place, may then explain its intense staining with OsO_4 (SEKI et al., 2011; ALLEN INSTITUTE FOR BRAIN SCIENCE, 2014). This seems to be confirmed by similar observations in brain regions of the other stained embryos, as well as the zebrafish.

The lung tissue also stained intensely, which could be explained by the glycoprotein-containing mucus, as well as the surfactant (a phospholipid-protein complex) (BATENBURG & HAAGSMAN, 1998). However, lung surfactant production only starts around stage E17 in fetal mice (CONDON et al., 2004), whereas alveoli are formed from the E18.5 stage on (WARBURTON et al., 2010). As such, the observed cavities embedded within the lung tissue most likely represent bronchioles.

Additional structures that could be demarcated after OsO_4 staining were epithelial tissues, muscles and cartilaginous elements (*e.g.* the observed Meckel's cartilage and ribs) (Fig. 4). We hypothesized that cartilage would not stain well, considering it is less dense in proteins or phospholipids. However, cartilage does contain a variety of proteoglycans in its matrix, of which the protein content is high (KNUDSON & KNUDSON, 2001), and the matrix contains lipids (STOCKWELL, 1979). Both the glycosaminoglycans (components of the proteoglycans) and lipids might explain the moderate affinity for OsO_4 .

Tissue/organ discriminative potentials of OsO_4 compared to that of non-toxic alternatives

As METSCHER (2009a) indicated, other contrast agents can replace the toxic OsO_4 and still give similar or even better results. Prior to the comparison of these agents in our study, we needed to consider some differences in the procedures of staining and CT scanning of the PMA mouse embryo (compared to the other mouse embryos). Firstly, the incubation period was longer (six days for the PMA embryo versus

14 hours for the other embryos), and the amount of photonic data (photon statistics) per voxel was substantially higher (due to longer exposure time and higher μA values). This implies that for each voxel, a higher rate of photonic data can be gathered during the scan, which could explain the apparently better quality of the virtual sections through the PMA mouse, even though absolute voxel resolution was similar (more photonic data per voxel reduces the amount of noise compared to the actual voxel value). This could explain why, within the same organ, the quality in these sections was better for the PMA dataset (Fig. 3). However, this does not explain the substantially higher discriminative power between the different tissue types and organs, which could then be explained by the longer incubation time and very likely the better contrast staining of PMA. As a result, from our study we cannot draw any quantitatively-supported conclusions on that, but only report that PMA clearly shows indications of being qualitatively better able to discriminate between tissue types and organs (also see below on the penetration aspects of the agents).

Comparing the results of OsO_4 with those of PTA and PMA, several similarities could be observed. For all agents, it was the liver, blood, lungs, cell-dense brain regions and epithelial structures that showed the most intense staining. Also other organs such as the heart, cartilages, muscles, thymus, etc. could be discriminated, albeit with a lower intensity. In the PTA and PMA embryos, the cartilage regions undergoing ossification could be distinguished (darker central matrix of the cartilaginous structures), which was not the case for the OsO_4 mouse (Fig. 7D).

However, there were also some marked differences with the OsO_4 staining. PTA stained epithelial lining in a rather consistent way, and olfactory epithelium, integumentary, respiratory and digestive epithelia (both for the mouse embryos as for the *Xenopus* tadpoles) were intensely stained. GIGNAC & KLEY (2014) showed that Lugol's iodine also has a higher affinity for epithelial tissue. Muscle tissue was stained with

high intensity in the *Xenopus* tadpoles, which was not the case in the mouse embryos (Figs 5B, 6). We hypothesized that a high protein content of muscle tissue (densely-packed myofilaments) would result in highly-contrasted muscle tissue. In both the tadpoles and zebrafish, muscle fibers were clearly differentiated. In mice, however, differentiation of myotubules into myofibres only starts from the 19th day of gestation on (WIRSÉN & LARSSON, 1964). As such, myofilament density in E14.5 and E15.5 embryos would have been low, which could explain the relatively lower intensity of the involved voxels. Muscle tissue also stains intensely with iodine, as shown in literature (COX & JEFFERY, 2011; JEFFERY et al., 2011; GIGNAC & KLEY, 2014). The latter study even suggested that it can enable distinction between red and white muscle tissue, based on different carbohydrate contents.

Cartilaginous structures stained weakly, although cartilage is a connective tissue composed of, among other substances, collagen fibrils. A previous histochemical study already showed a similar outcome after PTA was added to sections comprising cartilage (QUINTARELLI et al., 1971). They suggested that the intensity of staining of cartilage with PTA decreases with a progressive increase in hydrogen-ion concentration of the PTA dye bath. PMA gave a much broader voxel intensity range, which yielded images that showed a high contrasting resolution between tissues, better than for all the other agents (Fig. 7). This was even more pronounced in the juvenile zebrafish, where, for example, details at the level of retinal cell layers could be discerned (Fig. 8B, C). The observed pattern may reflect distinct distributions of phospholipid densities in these layers (ROY et al., 2011). Also epithelial lining of the digestive and respiratory system was more pronounced in the mouse embryos, including now also the distinction of glandular epithelia (e.g. salivary gland). Whether the gland content or its epithelial lining was more intensely stained could not be verified here, however. It can also not be excluded that the glands were only visible in the PMA embryo, which was at the E15.5 stage (at which salivary glands become canalized

with proliferating epithelial cells), whereas the other embryos were at the E14.5 stage (where the glands are still solid, multilobular glands) (TUCKER, 2007). Also in the zebrafish, thyroid glands could be observed (Fig. 7E). Another similarity with the OsO_4 staining was that in the PMA zebrafish brain, brain regions that were cell-rich stained more intensely (e.g. central part of the corpus cerebelli) (CHENG, 2013). This confirms the above conclusion that it is not myelin itself that was visualized in the OsO_4 mouse embryo, but brain cell nuclei. This is in contrast to the study by GIGNAC & KLEY (2014), who could clearly distinguish myelinated from non-myelinated fibers in American alligators stained with Lugol's iodine. JEFFERY et al. (2011) reported that this Lugol's iodine preferentially binds to connective tissues surrounding the muscle fibers and suggested that iodine binds to glycogen molecules in the muscle cells. Glycogen has indeed a high iodine-binding capacity, yielding a glycogen-iodine complex (LECKER et al., 1997). Also ethanol solutions of iodine (I_2/E) showed a strong staining of muscle tissue in insects, allowing the visualization of individual muscle fibers (METSCHER, 2009a; WILHELM et al., 2011).

Although PMA and PTA allowed better discrimination between tissue types and organs based on voxel grey values, OsO_4 still proved to be sufficiently powerful to distinguish and demarcate most of the organs based on their topography within the body and spatial relation to surrounding organs. As this study was not a quantitative analysis of contrast variation in voxel intensity values (as was done by GIGNAC & KLEY, 2014), the assessment of the quality of contrast staining is based on the combination of voxel contrast and topographic anatomy. This is essential to anatomists who need to interpret 3D soft anatomy using CT data. Still, higher voxel contrasts can be especially useful for automated segmentation of tissue types or organs based on grey value thresholds.

Consistent tissue/organ discrimination of PMA and PTA?

Both PTA and PMA yielded excellent contrast between different tissues in the mouse embryo, as well as in the *Xenopus* tadpole and zebrafish, although the PMA results were superior (see above).

Tungsten is known to specifically bind to fibers of connective tissues, such as collagen (KIERNAN, 1981). In the mouse embryos, the perichondral layer of connective tissue (e.g. surrounding the ribs) consistently stained more intensely (Figs 5A, 6C, 7D). In zebrafish, the myoseptal connective tissue sheets and ligaments also stained very well with PMA (Fig. 8D). On the other hand, the epidermal epithelia in the mouse embryos stained more intensely than the collagen-rich dermal layer. Although several epithelial structures showed a high affinity for all three of the contrast agents, PTA and PMA have been shown to enable consistent visualization of collagenous tissue. Also muscle tissue stained consistently well, especially in the tadpoles and zebrafish with fully-differentiated muscle fibers (Figs 6, 8). In both, the individual fibers could be visualized. Similar levels of details have been obtained using OsO_4 in mouse tongue muscles (AOYAGI et al., 2013), and with I_2/KI in crocodile and mouse cranial muscles (JEFFERY et al., 2011; TSAI & HOLLIDAY, 2011; GIGNAC & KLEY, 2014). Also heart muscle tissue was clearly visible in our PTA and PMA specimens. The heart is mainly composed of cardiac muscle cells, embedded within a network of collagen-rich connective tissue in the extracellular space of the myocardium (WEBER et al., 1994). This, together with the thin endomysial layer of connective tissue, may explain the high affinity for PMA.

For all contrast agents tested, blood and liver stained at high intensities in a consistent manner (see above). Also consistent, both in staining and moderate intensity level, was the visualization of epithelial structures using PMA and PTA. Especially the olfactory, digestive, respiratory and integumentary epithelia (follicles of vibrissae)

were always prominently visible, in all specimens and taxa studied. Also glandular structures could be identified in both PTA and PMA, but were most prominent in the PMA specimens.

Cartilage stained moderately with PMA and PTA in all three taxa studied. Similar results were obtained by METSCHER (2009a). In *Xenopus* tadpoles, individual chondrocytes could be visualized (Fig. 6C), whereas in the mouse embryos it was the matrix that showed X-ray attenuation. This is in concordance with what METSCHER (2009a) found after staining fish specimens with PTA. GOLDING et al. (2007) showed a high affinity of PMA for the surrounding soft tissues of mollusk cartilages, where the matrix itself did not stain.

Tissue/organ discrimination dependent on penetration potentials?

The capacities of these agents to visualize soft tissues in larger specimens can be expected to be inversely related to their potential to penetrate tissues (larger molecules have higher attenuation but penetrate less well). However, PAUWELS et al. (2013) quantified penetration rates of 12 different contrast agents, showing that the relation is not that simple. A correlation analysis done on the atomic number and penetration rate (data from table 1 and 2 of that study, penetration rate calculated from the 24h data in table 2) actually showed a positive correlation (Pearson correlation coefficient of 0.73, $p=0.02$). In that study, the samples (mice paws) were already fully stained after 24 hours of staining with iodine (KI), whereas PMA showed the slowest penetration rate (of OsO_4 , PMA and PTA). As the authors indicated, other factors, such as concentration of the contrast solution, solvent, tissue composition and pretreatment protocols will also have played a role in these penetration rates. In our study, pretreatment tissue composition was kept constant with the mouse embryos, as was to some degree the concentration. However, controlling for the other factors remains practically impossible.

Osmium, which was not included in the latter study, has an atomic number that is slightly heavier than that of tungsten (76 vs 74), and substantially higher than that of molybdenum (42). For application in mouse embryos, it was even advised to remove the epithelial layers prior to staining (JOHNSON et al., 2006). Although this was not performed in our study (and in both studies, specimens were kept in a 1% osmium solution overnight), the OsO_4 was shown to have homogeneously penetrated throughout the specimen. Also, specimens used by JOHNSON et al. (2006) were even slightly younger, and hence smaller than the ones used in our study. AOYAGI et al. (2010) stained E13 stage mouse for 24h in a 1% osmium solution, obtaining better contrast than we did in our study. Previous studies had already shown that the penetration speed depends on the tissue density, and that the diffusion rate depends on the OsO_4 concentration (BURKL & SCHIECHL, 1968). It is therefore suggested that a higher concentration and a longer duration of treatment with OsO_4 would resolve the problem of low contrast, and increase the intensity of the overall staining. The quality of a staining is also dependent on other factors, such as the embedding procedure.

Penetration of PTA has been reported to be much slower than that of iodine (METSCHER, 2009b). Unlike inorganic iodine (I_2KI or I_2E), PTA is a larger molecule (KEGGIN, 1934), which requires a longer incubation to penetrate deeply into the specimens. The longer incubation period (i.e. six days) for PMA in our study, in contrast to the shorter incubation period (i.e. overnight) for the other contrast agents, may thus also explain the better results observed with PMA. Further testing of the effect of incubation times on tissue-specific contrasting and color value heterogeneity in voxel data could clarify this issue.

As mentioned previously, Lugol's iodine (I_2KI) is a much smaller molecule and it is known to diffuse rapidly and deeply into fixed tissues (METSCHER, 2009a, b). DEGENHARDT et al. (2010) also showed that it better penetrates and stains soft tissues. One should, however,

also consider the artefacts being induced, as shrinkage and tissue distortions were observed with higher iodine concentrations, showing an inherent trade-off between contrast and tissue preservation (DEGENHARDT et al., 2010; VICKERTON et al., 2013). However, GIGNAC & KLEY (2014) showed optimal incubation times in Lugol's iodine of two weeks for larger specimens, without the extensive shrinkage reported by VICKERTON et al. (2013). Whether or not shrinkage was also induced by the other staining agents, was not apparent but was also not quantified.

CONCLUSIONS

In conclusion, this study provides further insight into the potential of contrast agents for soft tissue discrimination in μ CT voxel data. We were able to demonstrate that OsO_4 , PTA and PMA provide moderate to very good contrast among tissue and organ structures, both in mouse embryos and in other vertebrates. In our study, PTA and PMA proved to be suitable, less-toxic alternatives to OsO_4 . Especially PMA consistently yielded very good results, which could partially be explained by the longer incubation time applied. Most agents stained certain tissue types or organs more intensely in a rather consistent manner (e.g. liver, lungs, cell-dense brain regions, epithelial structures), whereas other tissue and organ types could be distinguished based on a moderate contrast, combined with their topography with respect to other organs. Further studies would be needed to quantify contrasting potentials of these agents for tissue types, in relation to, for example, incubation time. Based on the information obtained, we further confirmed the substantial potential for these contrast agents to allow detailed 3D anatomical analysis using μ CT scanning.

ACKNOWLEDGEMENTS

This work was supported by the Concerted Research Actions (GOA - 01G01908) of Ghent

University. The Fund for Scientific Research Flanders (FWO) is acknowledged for the doctoral grant to D. Van Loo (G.0100.08). The authors thank the Department for Molecular Biomedical Research (DMBR) of the University Ghent for providing the mouse embryos and *Xenopus* tadpoles.

REFERENCES

- ALLEN INSTITUTE FOR BRAIN SCIENCE. (2014). "Allen mouse brain atlas." from <http://mouse.brain-map.org>.
- AOYAGI H, IWASAKI SI & NAKAMURA K (2013). Three-dimensional observation of mouse tongue muscles using micro-computed tomography. *Odontology*.
- AOYAGI H, TSUCHIKAWA K & IWASAKI S (2010). Three-dimensional observation of the mouse embryo by micro-computed tomography: Composition of the trigeminal ganglion. *Odontology* 98(1): 26-30.
- BARON RL (1994). Understanding and optimizing use of contrast material for ct of the liver. *American Journal of Roentgenology* 163(2): 323-331.
- BATENBURG JJ & HAAGSMAN HP (1998). The lipids of pulmonary surfactant: Dynamics and interactions with proteins. *Progress in Lipid Research* 37(4): 235-276.
- BAVERSTOCK H, JEFFERY NS & COBB SN (2013). The morphology of the mouse masticatory musculature. *Journal of Anatomy* 223(1): 46-60.
- BETZ O, WEGST U, WEIDE D, HEETHOFF M, HELFEN L, LEE WAHK & CLOETENS P (2007). Imaging applications of synchrotron x-ray phase-contrast microtomography in biological morphology and biomaterials science. I. General aspects of the technique and its advantages in the analysis of millimetre sized arthropod structure. *Journal of Microscopy* 227(1): 51-71.
- BOCK WJ, SHEAR, R.C. (1972). A staining method for gross dissection of vertebrate muscles. *Anat. Anz.* Bd. 130: 222-227.
- BOISTEL R, SWOGER J, KRŽIČ U, FERNANDEZ V, GILLET B & REYNAUD EG (2011). The future of three-dimensional microscopic imaging in marine biology. *Marine Ecology* 32(4): 438-452.
- BRUNELLI E, PERROTTA E & TRIPEPI S (2004). Ultrastructure and development of the gills in *rana*

- dalmatina* (amphibia, anura). Zoomorphology 123(4): 203-211.
- BURKL W & SCHIECHL H (1968). A study of osmium tetroxide fixation. Journal of Histochemistry & Cytochemistry 16(3): 157-161.
- BUYTAERT J, DESCAMPS E, ADRIAENS D & DIRCKX JJJ (2012). The opfos microscopy family: High-resolution optical-sectioning of biomedical specimens. Anatomy Research International 2012: 9 pages.
- CARDEN A, RAJACHAR RM, MORRIS MD & KOHN DH (2003). Ultrastructural changes accompanying the mechanical deformation of bone tissue: A raman imaging study. Calcif. Tissue Int. 72: 166-175.
- CARSON FL & HLADIK C (2009). Histotechnology: A self-instructional text. American Society for Clinical Pathology Press, Hong Kong.
- CHENG K. (2013). "Zebrafish atlas." 2014, from <http://zfatlas.psu.edu/>.
- CNUUDE V, BOONE M, DEWANCKELE J, DIERICK M, VAN HOOREBEKE L & JACOBS P (2011). 3d characterization of sandstone by means of x-ray computed tomography. Geosphere 7(1): 54-61.
- CONDON JC, JEYASURIA P, FAUST JM & MENDELSON CR (2004). Surfactant protein secreted by the maturing mouse fetal lung acts as a hormone that signals the initiation of parturition. PNAS 101(14): 4978-4983.
- COX PG & JEFFERY N (2011). Reviewing the morphology of the jaw-closing musculature in squirrels, rats, and guinea pigs with contrast-enhanced microct. Anatomical Record-Advances in Integrative Anatomy and Evolutionary Biology 294(10): 915-928.
- DEGENHARDT K, WRIGHT AC, HORNG D, PADMANABHAN A & EPSTEIN JA (2010). Rapid 3d phenotyping of cardiovascular development in mouse embryos by micro-ct with iodine staining. Circulation: Cardiovascular Imaging 3(3): 314-322.
- DESCAMPS E, BUYTAERT J, DE KEGEL B, DIRCKX J & ADRIAENS D (2012). A qualitative comparison of 3d visualization in *xenopus laevis* using a traditional method and a non-destructive method. Belgian Journal of Zoology 142(2): 101-113.
- DI SCIPIO F, RAIMONDO S, TOS P & GEUNA S (2008). A simple protocol for paraffin-embedded myelin sheath staining with osmium tetroxide for light microscope observation. Microscopy Research and Technique 71(7): 497-502.
- DIERICK M, VAN LOO D, MASSCHAELE B, BOONE M & VAN HOOREBEKE L (2010). A labview® based generic ct scanner control software platform. Journal of X-Ray Science and Technology 18(4): 451-461.
- DOBRIVOJEVIC M, BOHACEK I, ERJAVEC I, GORUP D & GAJOVIC S (2013). Computed microtomography visualization and quantification of mouse ischemic brain lesion by nonionic radio contrast agents. Croatian Medical Journal 54(1): 3-11.
- EFIMOVA OI, KHLEBNIKOV AS, SENIN RA, VORONIN PA & ANOKHIN KV (2013). Contrasting of biological samples for x-ray synchrotron microtomography. Bulletin of Experimental Biology and Medicine 155(4): 413-416.
- FISHMAN EK, NEY DR, HEATH DG, CORL FM, HORTON KM & JOHNSON PT (2006). Volume rendering versus maximum intensity projection in ct angiography: What works best, when, and why1. Radiographics 26(3): 905-922.
- GIGNAC PM & KLEY NJ (2014). Iodine-enhanced micro-ct imaging: Methodological refinements for the study of the soft-tissue anatomy of post-embryonic vertebrates. J Exp Zool B Mol Dev Evol 322(3): 166-176.
- GOLDING RE & JONES AS (2007). Micro-ct as a novel technique for 3d reconstruction of molluscan anatomy. Molluscan Research 27: 123-128.
- HALL, C, JAKUS M & SCHMITT F (1945). The structure of certain muscle fibrils as revealed by the use of electron stains. Journal of Applied Physics 16: 459-465.
- HARDY RJ & FRIEDRICH VL, JR. (1996). Oligodendrocyte progenitors are generated throughout the embryonic mouse brain, but differentiate in restricted foci. Development 122: 2059-2069.
- HAYAT MA (2000). Principles and techniques of electron microscopy: Biological applications. Cambridge University Press. p.564.
- ISOGAI S, HORIGUCHI M & WEINSTEIN BM (2001). The vascular anatomy of the developing zebrafish: An atlas of embryonic and early larval development. Developmental Biology 230(2): 278-301.
- JEFFERY NS, STEPHENSON RS, GALLAGHER JA, JARVIS JC & COX PG (2011). Micro-computed tomography with iodine staining resolves the arrangement of muscle fibres. J Biomech 44(1): 189-192.

- JOHNSON JT, HANSEN MS, WU I, HEALY LJ, JOHNSON CR, JONES GM, CAPECCHI MR & KELLER C (2006). Virtual histology of transgenic mouse embryos for high-throughput phenotyping. *Plos Genetics* 2(4): 471-477.
- JONES AS, MILTHORPE BK & HOWLETT CR (1994). Measurement of microtomy induced section distortion and its correction for 3-dimensional histological reconstructions. *Cytometry* 15: 95-105.
- KEGGIN J (1934). The structure and formula of 12-phosphotungstic acid. *Proceedings of the Royal Society of London. Series A* 144(851): 75-100.
- KIERNAN JA (1981). *Histological and histochemical methods. Theory and practice.* Pergamon Press, Oxford.
- KNUDSON CB & KNUDSON W (2001). *Cartilage proteoglycans.* Cell & Development Biology, Elsevier.
- LECKER DN, KUMARI S & KHAN A (1997). Iodine binding capacity and iodine binding energy of glycogen. *Journal of Polymer Science Part A: Polymer Chemistry* 35(8): 1409-1412.
- MA S, CHARRON J & ERIKSON RL (2003). Role of *plk2 (snk)* in mouse development and cell proliferation. *Molecular and Cellular Biology* 23(19): 6936-6943.
- MASSCHAELE BC, CNUUDE V, DIERICK M, JACOBS P, VAN HOOREBEKE L & VLASSEN BROECK J (2007). UgcT: New x-ray radiography and tomography facility. *Nuclear Instruments and Methods in Physics Research Section A: Accelerators, Spectrometers, Detectors and Associated Equipment* 580(1): 266-269.
- METSCHER BD (2009a). MicroCT for comparative morphology: Simple staining methods allow high-contrast 3d imaging of diverse non-mineralized animal tissues. *BMC Physiol* 9: 11.
- METSCHER BD (2009b). MicroCT for developmental biology: A versatile tool for high-contrast 3d imaging at histological resolutions. *Developmental Dynamics* 238(3): 632-640.
- MIZUTANI R & SUZUKI Y (2012). X-ray microtomography in biology. *Micron* 43(2-3): 104-115.
- MIZUTANI R, TAKEUCHI A, UESUGI K, TAKEKOSHI S, OSAMURA RY & SUZUKI Y (2008). X-ray microtomographic imaging of three-dimensional structure of soft tissues. *Tissue Engineering Part C-Methods* 14(4): 359-363.
- NAVEH GR, BRUMFELD V, DEAN M, SHAHAR R & WEINER S (2014). Direct microCT imaging of non-mineralized connective tissues at high resolution. *Connect Tissue Res* 55(1): 52-60.
- PATTON JT & KAUFMAN MH (1995). The timing of ossification of the limb bones, and growth-rates of various long bones of the fore and hind limbs of the prenatal and early postnatal laboratory mouse. *Journal of Anatomy* 186: 175-185.
- PAUWELS E, VAN LOO D, CORNILLIE P, BRABANT L & VAN HOOREBEKE L (2013). An exploratory study of contrast agents for soft tissue visualization by means of high resolution x-ray computed tomography imaging. *Journal of Microscopy* 250(1): 21-31.
- POHLMANN A, MÖLLER M, DECKER H & SCHREIBER WG (2007). Mri of tarantulas: Morphological and perfusion imaging. *Magnetic Resonance Imaging* 25(1): 129-135.
- QUINTARELLI G, ZITO R & CIFONELLI J (1971). On phosphotungstic acid staining. I. *Journal of Histochemistry & Cytochemistry* 19(11): 641-647.
- RITMAN EL (2004). Micro-computed tomography-current status and developments. *Annual Review of Biomedical Engineering* 6: 185-208.
- RITMAN EL (2011). Current status of developments and applications of micro-ct. *Annual Review of Biomedical Engineering*, Vol 13 13: 531-552.
- ROY MC, NAKANISHI H, TAKAHASHI K, NAKANISHI S, KAJIHARA S, HAYASAKA T, SETOU M, OGAWA K, TAGUCHI R & NAITO T (2011). Salamander retina phospholipids and their localization by maldi imaging mass spectrometry at cellular size resolution. *Journal of Lipid Research* 52(3): 463-470.
- RUBIN GD, DAKE MD, NAPEL S, JEFFREY RB, MCDONNELL CH, SOMMER FG, WEXLER L & WILLIAMS DM (1994). Spiral ct of renal artery stenosis: Comparison of three-dimensional rendering techniques. *Radiology* 190(1): 181-189.
- SANTI PA (2011). Light sheet fluorescence microscopy: A review. *Journal of Histochemistry & Cytochemistry* 59(2): 129-138.
- SCHAMBACH SJ, BAG S, SCHILLING L, GRODEN C & BROCKMANN MA (2010). Application of micro-ct in small animal imaging. *Methods* 50(1): 2-13.

- SCHAMBRA U (2008). Prenatal mouse brain atlas. Springer Science+Business Media, LLC, New York.
- SEKI T, SAWAMOTO K, PARENT JM & ALVAREZ-BUYLLA A (2011). Neurogenesis in the adult brain i: Neurobiology. Springer, Tokyo.
- SHARPE J, AHLGREN U, PERRY P, HILL B, ROSS A, HECKSHER-SORENSEN J, BALDOCK R & DAVIDSON D (2002). Optical projection tomography as a tool for 3d microscopy and gene expression studies. *Science* 296(5567): 541-545.
- STOCKWELL RA (1979). Biology of cartilage cells. Cambridge University Press.
- TSAI HP & HOLLIDAY CM (2011). Ontogeny of the alligator cartilago transiliens and its significance for sauropsid jaw muscle evolution. *Plos One* 6(9).
- TUCKER AS (2007). Salivary gland development. *Seminars in Cell & Developmental Biology* 18(2): 237-244.
- TYSZKA JM, FRASER SE & JACOBS RE (2005). Magnetic resonance microscopy: Recent advances and applications. *Current Opinion in Biotechnology* 16(1): 93-99.
- ULLMANN JF, COWIN G, KURNIAWAN ND & COLLIN SP (2010). A three-dimensional digital atlas of the zebrafish brain. *Neuroimage* 51(1): 76-82.
- VICKERTON P, JARVIS J & JEFFERY N (2013). Concentration-dependent specimen shrinkage in iodine-enhanced microct. *J Anat* 223(2): 185-193.
- VLASSEN BROECK J, DIERICK M, MASSCHAELE B, CNUDE V, VAN HOOREBEKE L & JACOBS P (2007). Software tools for quantification of x-ray microtomography. *Nuclear Instruments & Methods in Physics Research Section a-Accelerators Spectrometers Detectors and Associated Equipment* 580(1): 442-445.
- WARBURTON D, EL-HASHASH A, CARRARO G, TIOZZO C, SALA F, ROGERS O, DE LANGHE S, KEMP PJ, RICCARDI D, TORDAY J, BELLUSCI S, SHI W, LUBKIN SR & JESUDASON E (2010). Lung organogenesis. *Organogenesis in Development* 90: 73-158.
- WATLING C, LAGO N, BENMERAH S, FITZGERALD J, TARTE E, MCMAHON S, LACOUR S & CAMERON R (2010). Novel use of x-ray micro computed tomography to image rat sciatic nerve and integration into scaffold. *Journal of Neuroscience Methods* 188(1): 39-44.
- WATSON ML (1958). Staining of tissue sections for electron microscopy with heavy metals. *The Journal of Biophysical and Biochemical Cytology* 4(4): 475-478.
- WEBER KT, SUN Y, TYAGI SC & CLEUTJENS JPM (1994). Collagen network of the myocardium: Function, structural remodeling and regulatory mechanisms. *Journal of Molecular and Cellular Cardiology* 26(3): 279-292.
- WIECHMANN AF & WIRSIG-WIECHMANN CR (2003). Color atlas of *xenopus laevis* histology. Kluwer Academic Publishers, Boston.
- WIGGLESWORTH V (1975). Lipid staining for the electron microscope: A new method. *Journal of Cell Science* 19(3): 425-437.
- WILHELM G, HANDSCHUH S, PLANT J & NEMESCHKAL HLEO (2011). Sexual dimorphism in head structures of the weevil *rhopalapion longirostre* (olivier 1807) (coleoptera: Curculionoidea): A response to ecological demands of egg deposition. *Biological Journal of the Linnean Society* 104(3): 642-660.
- WIRSÉN C & LARSSON KS (1964). Histochemical differentiation of skeletal muscle in foetal and newborn mice. *Journal of Embryology and Experimental Morphology* 12: 758-&.
- WULLIMANN MF, RUPP B & REICHERT H (1996). Neuroanatomy of the zebrafish brain: A topological atlas. Birkhäuser Verlag, Basel.
- ZANETTE I, DAGHFOUS G, WEITKAMP T, GILLET B, ADRIAENS D, LANGER M, CLOETENS P, HELFEN L, BRAVIN A, PEYRIN F, BAUMBACH T, DISCHLER J-M, VAN LOO D, PRAET T, POIRIER-QUINOT M & BOISTEL R (2013). Looking inside marine organisms with mri and x-ray tomography. In: Reynaud EG (Eds.). *Imaging marine life*. Wiley & Sons: 123-186.

Received: March 12th, 2014

Accepted: April 25th, 2014

Branch editor: Isa Schön

Facultative endosymbionts of aphid populations from coastal dunes of the North Sea

Eduardo de la Peña^{1,2,*}, Viki Vandomme^{1,3} & Enric Frago⁴

¹ Ghent University, Department of Biology, Terrestrial Ecology Unit, K.L. Ledeganckstraat 35, 9000 Gent, Belgium

² Instituto de Hortofruticultura Subtropical y Mediterránea "La Mayora", Universidad de Málaga – Consejo Superior de Investigaciones Científicas, E-29750 Algarrobo-Costa (Málaga), Spain

³ Royal Belgian Institute of Natural Sciences, Vautierstraat 29, 1000 Brussels, Belgium

⁴ Laboratory of Entomology, Wageningen University, P.O. Box 8031, 6700 EH Wageningen, the Netherlands

* Corresponding author: eduardo.delapena@ugent.be

ABSTRACT. Aphids establish symbiotic associations with a diverse assemblage of mutualistic bacteria. Some of them are not required for the host's survival but still have a crucial impact on the biology and ecology of their host. Facultative symbionts may modify important host-life-history traits and affect the interactions of aphids with other members of the community. So far several species of aphid have been reported to occur in coastal dunes. Given the extreme environmental conditions of this type of habitat and the wide distribution along the European coast of some aphid species, these aphids would be expected to show variation in their facultative endosymbionts. However, there is currently no information available for these species. To address this question, we collected specimens from different populations of aphids (i.e. *Schizaphis rufula*, *Laingia psammae* and *Rhopalosiphum padi*) associated with the dune grass *Ammophila arenaria* in several locations of the North and the Irish Sea. By means of specific diagnostic PCR's we checked for the presence of facultative bacterial endosymbionts in these populations. Results of this explorative assessment showed variation in the endosymbiont community according to species and location. All populations sampled along the North Sea coast were associated with the facultative endosymbiont *Serratia symbiotica*. *Hamiltonella defensa* was only detected in some specimens coming from the population in Het Zwin, Belgium. *Regiella insecticola* and the γ -proteobacteria X-type were only found associated with the population of *Schizaphis rufula* in De Panne, Belgium. Although further experiments are necessary to characterize the nature of these symbiotic relationships, our correlation analyses showed a significant co-occurrence of *S. symbiotica* with *H. defensa* and *R. insecticola* with X-type proteobacteria suggesting reciprocal regulatory functions. No significant correlation was detected between the number of mummies (i.e. carcasses of aphids parasitized by wasps) and the occurrence of bacterial symbionts. The potential role of these symbionts in coastal dune ecosystems is discussed.

KEY WORDS: wasps, parasitoids, heat shock, specific primers, top-down, bottom-up control

INTRODUCTION

Aphids are one of the most common insect groups studied for symbiotic associations (OLIVER et al., 2010; MORAN et al., 2008). Aphids engage in symbiotic associations with a diverse assemblage of heritable bacteria. In addition to the obligate endosymbiont *Buchnera aphidicola*, aphids may carry one or more facultative bacterial symbionts. Although these symbionts are not required for the survival of the aphid, they may transfer beneficial features to their

hosts such as increased resistance against natural enemies and pathogens, protection from heat shocks, and more importantly influence survival and fitness on specific host plants (OLIVER et al., 2010; LEONARDO & MONDOR, 2006).

Several aphid species have been reported to occur along the Western European Atlantic coast and the North Sea, including *Schizaphis rufula* (WALKER, 1849), *Laingia psammae* (THEOBALD, 1922), *Metapolophium sabiahe* (PRIOR, 1976) and *Rhopalosiphum padi* (1758) (BRÖRING

& NIEDRINGHAUS, 1989; VANDEGEHUCHTE et al., 2010). These species are usually found on *Ammophila arenaria* (L.) Link but also on other dune grasses thriving in pioneer dunes e.g. *Elymus farctus*, *Festuca rubra* and *Leymus arenaria*. From laboratory observations we know that these aphid species reproduce freely on young *Ammophila arenaria* shoots and spikes (VANDEGEHUCHTE et al., 2009; VANDEGEHUCHTE et al., 2010) but the factors underlying their ecology and population dynamics in the field remain relatively unexplored. Aphid populations colonizing coastal dunes do not commonly reach high densities as they are controlled either by natural enemies or by constitutive and induced plant defenses regulated by plant mutualists such as fungal endophytes (VANDEGEHUCHTE et al., 2013; DE LA PEÑA et al., 2006). Moreover, for some aphid species the endosymbiont community plays an important role in defining the host-plant range and the ability to exploit

certain plant species (LUKASIC et al., 2013, MORAN et al., 2008). Therefore, to understand aphid-plant interactions in coastal dunes the endosymbiont community in dune aphids needs to be characterized.

Coastal dunes are extreme environments, where both plant and animal species have to cope with several environmental stresses such as sand accretion, salt spray, extreme temperature variability, wind, etc (MAUN 2009). In addition to these abiotic factors, aphids have to deal with the host-plant defences, other herbivore competitors exploiting the same host-plants, and their natural enemies. Mutualism with facultative (i.e. non-essential) heritable bacteria may influence the biology of these insects, and can have major (positive and negative) effects on the host's fitness (MORAN et al., 2008). Facultative symbionts of aphids can confer protection against insect parasitoids and also



Fig. 1. – The five geographic locations sampled, and the aphid species found, in this study. 1. Ynyslas (Wales, UK): *Schizaphis rufula*. 2. Westhoek (Belgium): *S. rufula* and *Rhopalosiphum padi*. 3. Ter Yde: *S. rufula*. 4. Sluis-Het Zwin (the Netherlands): *S. rufula* and *Laingia psammae*. 5. Duinnoord (the Netherlands): *S. rufula*.

increase resistance to extreme temperatures. Recent research suggests that in the pea aphid, *Acyrtosiphon pisum*, the population structure of some species of facultative symbionts is mostly influenced by climate. In particular, symbiont species that confer resistance to heat shocks have been found to be commonly associated with aphids from arid regions (HENRY et al., 2013).

With such *a priori* knowledge it is not far-fetched to assume that dune aphids rely on such mutualistic interactions to better survive and we report here the first records on dune aphid-endosymbiotic bacteria associations in several locations of the Atlantic and North Sea coast in Western Europe.



Fig. 2. – A. Foredunes with vigorous *Ammophila arenaria* where the different populations of aphids were collected. B. Infestation of marram leaves by the aphid *Schizaphis rufula*. C-D. Symptoms of aphid multiplication: yellowing of leaf tips.

MATERIAL AND METHODS

Sampling surveys and establishment of cultures of aphid isolates

In total, five locations with active dune systems dominated by *A. arenaria* were sampled along the coast of the North Sea and the Irish Sea (Fig. 1). The first sampling survey took place in June 2011. In the field, plants were visually inspected to detect aphid populations feeding on *A. arenaria* shoots (Figs 2-3). Once aphids were detected, they were manually collected and transferred to an eppendorf tube filled with 100% ethanol. From each site we collected aphids from at least four different plants. During this first sampling survey individuals of the species *S. rufula* were retrieved from De Panne, Ter Yde and Het Zwin. In De Panne (Belgium), individuals of the species *R. padi* were also detected and sampled. Once in the lab, the identity of 10-15 aphids from each location was double-checked and this bulk sample was further used for DNA extraction.

Since the preliminary assessment based on bulk samples revealed the presence of bacterial endosymbionts, in a second sampling survey, aphids were individually screened for symbiont infection to assess the frequency of infection by different endosymbiotic bacteria within a site. In October 2011, the same populations were revisited and aphids were taken to the laboratory alive in order to establish cultures of the different isolates. Also in October 2011, parasitoid impact was assessed by counting the number of mummies (i.e. carcasses of aphids parasitized by parasitoid wasps) and healthy aphids on the surveyed plants and locations. Once in the lab, leaves infested with aphids were transferred to *A. arenaria* seedlings that had been previously prepared as in DE LA PEÑA et al. (2010). To ensure aphids were kept in conditions as natural as possible, we reared them in sympatric *A. arenaria* plants. In our second survey, we did not detect *R. padi* as in the preliminary survey, and instead we detected *L. psammae* (Fig. 3) in plants from the location sampled in the Netherlands. From each site and species, we established between ten to

fifteen aphid lines (i.e. from a single female), which we kept in the laboratory under long photoperiod (16/8h light/dark regime) to ensure continuous asexual reproduction. In order to assess the degree of incidence of endosymbionts per species and population we checked for the presence of the different endosymbionts in 10 aphid-lines per population.

With the data for *S. rufula* from the second sampling survey, a Spearman correlation analysis was conducted to infer patterns in the simultaneous occurrence of the different facultative endosymbionts and the number of mummies (i.e. carcasses of aphids that have been parasitized by wasps) detected in the field.

Extraction of DNA and PCR for molecular identifications

Genomic DNA was extracted using the NucleoSpin® Tissue Kit (Macherey-Nagel). The facultative endosymbiont communities of

the different aphid populations were assessed with diagnostic PCRs (Polymerase Chain Reaction)s using specific primers for the 16S ribosomal RNA genes for the following bacterial species (commonly found in the pea aphid, *Acyrtosiphon pisum* model system): *Hamiltonella defensa*, *Regiella*, *Serratia symbiotica*, *Rickettsia*, *Spiroplasma* and the and the bacterial compliment X-type- a γ -Proteobacteria- (see FERRARI et al., 2012 and MCCLEAN et al., 2011 for further information). The amplification of the 16S ribosomal RNA gene was done using a universal bacterial primer 10F, 35R. These primers are able to detect a wide range of Eubacteria. This initial amplification was followed by a diagnostic PCR using specific primers (Table 1) to detect the specific bacterial endosymbionts. PCRs were performed in a final volume of 10 μ L containing ≤ 20 ng/ μ l of genomic DNA, 1 x PCR buffer, 1.5 mM MgCl₂, 0.2mM each dNTP, 0.25mM each primer and 1U of *Taq* DNA polymerase. Thermal profile for amplification included an initial denaturation step at 95 °C for 5 min, followed by 30 cycles

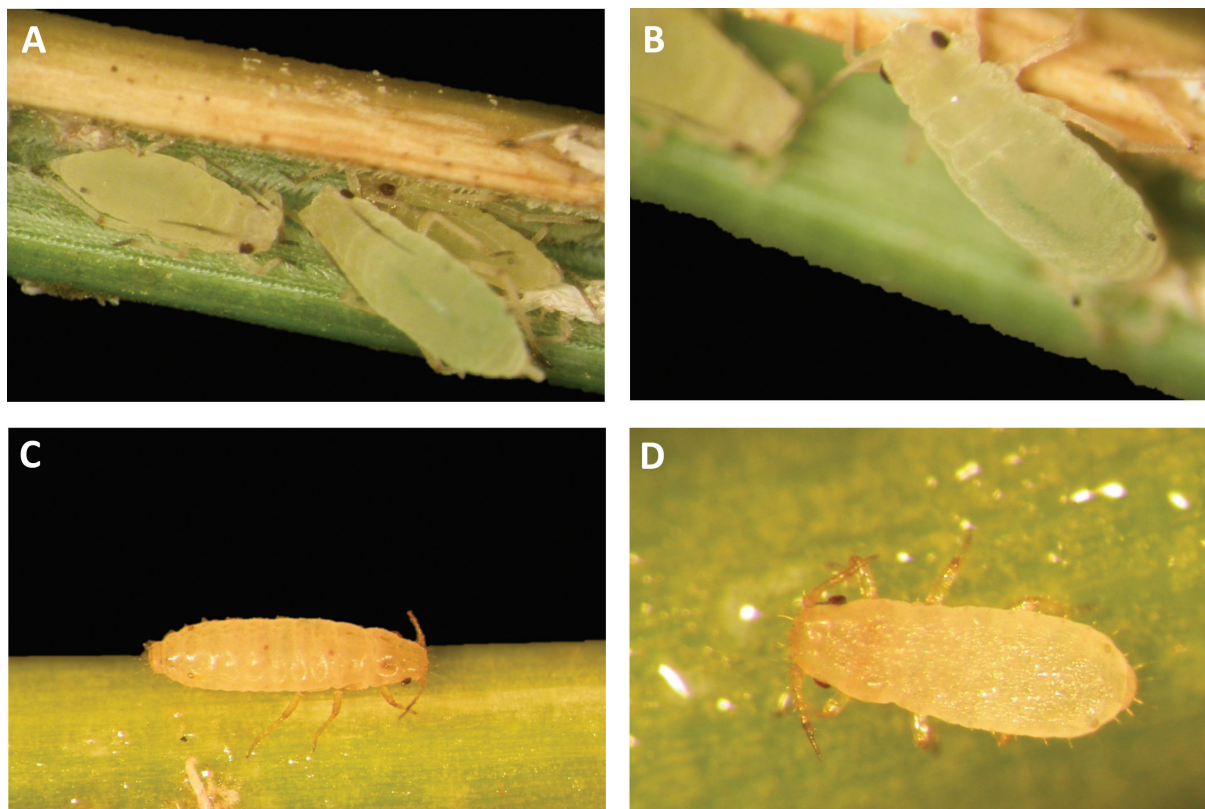


Fig. 3. – *Schizaphis rufula* (A, B) and *Laingia psammae* (C, D) on leaves of *Ammophila arenaria*.

TABLE 1

Specific primers and PCR conditions for diagnostic symbiont detection. From MCLEAN et al., 2010 and FERRARI et al., 2011.

Symbiont species	Forward primer	Reverse primer	PCR programm
<i>Hamiltonella defensa</i>	10F 5'- AGTTTGATCATGGCTCA- GATT-3'	T419R 5'- AAATGGTATTCGCATT- TATCG-3'	1
<i>Regiella insecticola</i>	10F	U443R 5'- GGTAACGTCAATCGATAAG- CA-3'	1
<i>Serratia symbiotica</i>	10F	R443R 5'- CTTCTGCGAGTAACGTCAA- TG-3'	1
X-Type	10F	X420R 5'- GCAACACTCTTTGCAT- TGCT-3'	1
<i>Rickettsia</i>	16SA1 5'- AGAGTTTGATCMTGGCT- CAG-3'	Rick16SR 5'- TTTGAAAGCAATTCCGAG- GT-3'	1
<i>Spiroplasma</i>	10F	TKSSsp 5'- ATCATCAACCCTGCCTTT-3'	2

Cycling conditions:

Programm 1: 94°C 2 min, 10 cycles of (94°C 1min, 65°Cà55°C in 1°C steps each cycle 1min, 72°C 2min), 25 cycles of (94°C 1min, 55°C 1min, 72°C 2min), 72°C 6min.

Programm 2: 94°C 2 min, 35 cycles of (94°C 1 min, 54°C 1 min, 72°C 2 min), 72°C 6 min.

of 30 s at 94°C, 30 s at Ta (γ -Proteobacteria 50°C, *Hamiltonella defensa* 57°C, *Regiella insecticola*, *Serratia symbiotica* 57°C, X-type 57°C, *Rickettsia* 45°C, *Spiroplasma* 45°C) and 1 min at 72°C; a final step at 72 °C for 10 min was used to complete primer extension. PCR products were visualized after electrophoresis on a 1.2% agarose gel stained with GelRed. Since some PCR reactions produced faint bands, all PCR reactions were repeated twice to discard potential false positives. Furthermore, some of the PCR products were sequenced to confirm their identity based on sequence homologies (from GenBank) (BENSON et al., 2013). For

this purpose, PCR products were purified using Exonuclease I and the purification kit FastAP™ (Fermentas). The purified PCR products were sequenced on both strands by Macrogen (Seoul, Korea) using the PCR primers.

RESULTS

The results of the assessment of the aphid populations collected during the sampling surveys showed that facultative endosymbionts are common and widespread in aphid populations occurring in coastal dunes (Table 2). PCR

TABLE 2

Overview of endosymbionts in *Schizaphis rufula*, *Rhopalosiphum padi* and *Laingia psammae* based on the results of PCR amplifications using specific primers and posterior confirmation through sequence blasting.

Species	Location	<i>Hamiltonella defensa</i>	<i>Regiella</i>	Type-X	<i>Serratia symbiotica</i>	<i>Rickettsia</i>	<i>Spiroplasma</i>
<i>S. rufula</i>	Duin-Noord, Netherlands	No	No	No	Yes	No	No
<i>S. rufula</i>	Belgium, Het Zwin	Yes	No	No	Yes	No	No
<i>S. rufula</i>	Belgium, Ter Yde	No	No	No	Yes	No	No
<i>S. rufula</i>	Belgium, De Panne	No	Yes	Yes	Yes	No	No
<i>S. rufula</i>	Wales (UK), Ynyslas	No	No	No	No	No	No
<i>R. padi</i>	Belgium, De Panne	No	No	No	Yes	No	No
<i>L. psammae</i>	Belgium, De Panne	No	No	No	Yes	No	No

amplifications using specific primers for *H. defensa* yielded positive results (i.e. with an amplification band of ca. 490 bp) in one population, i.e. Het Zwin (the Netherlands). *Serratia symbiotica* was detected in all specimens tested except for the population of *S. rufula* from Ynyslas (Wales). The population of *R. padi* was found to be only associated with *S. symbiotica*. In all cases amplification bands had a size of ca. 890bp.

In the second assessment, using 10 aphid-lines, a different pattern in the results was observed (Fig. 4). Again, only the *S. rufula* population from Het Zwin was infected with *H. defensa*. *Serratia symbiotica* was once more the most common facultative endosymbiont although this time, the bacterium was not detected in specimens of *S. rufula* from Ter Yde. In this second study, we also detected *R. insecticola* and the γ -proteobacteria X-type in some specimens from the population in De Panne, yielding amplification bands near 470 bp and 450bp respectively.

The identity of some of the positive samples was further confirmed by sequencing the PCR products and DNA blasting (BENSON et al., 2013). These sequences are available in GenBank and correspond with accession numbers KJ943256-KJ943268.

The Spearman correlation analysis (Table 3) showed a significant co-occurrence of *S. symbiotica* with *H. defensa*, and *R. insecticola* with the endosymbiont X-type. The incidence of mummies in the field was not correlated with any of the endosymbionts detected.

DISCUSSION

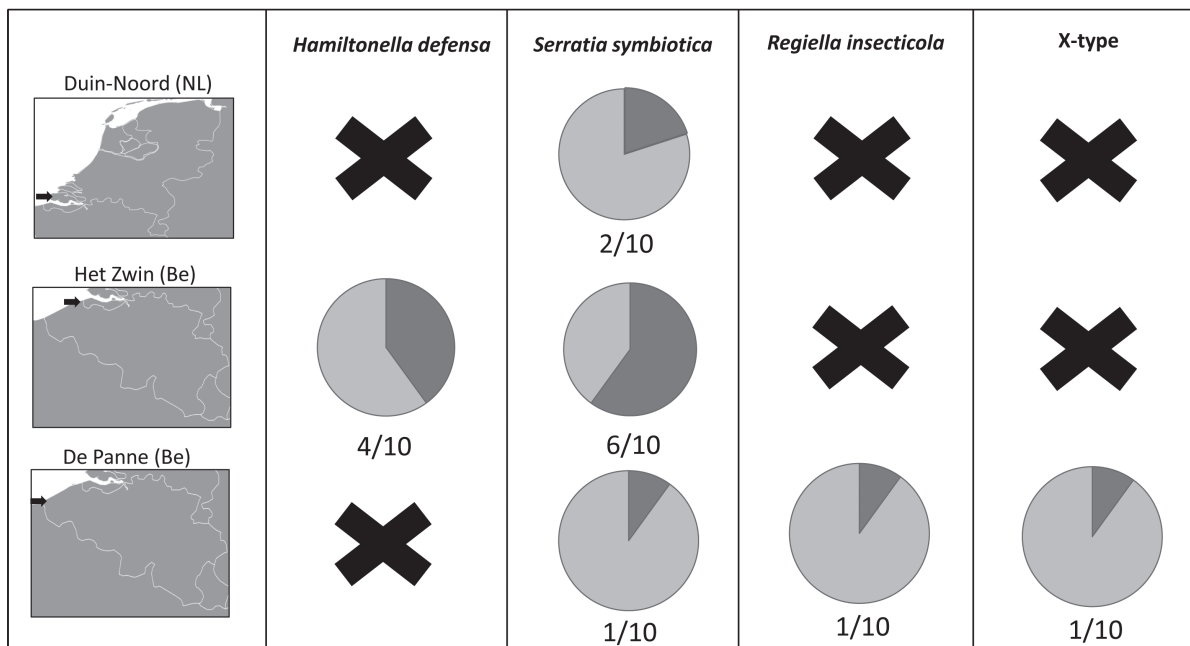
By means of diagnostic PCRs we assessed the occurrence of facultative endosymbionts in different species and populations of aphids from coastal dunes. The results of this first assessment not only show that facultative endosymbionts are common elements in these aphids, but also showed variation in the endosymbiont community according to species and location. All populations, except *S. rufula* from Wales, were associated with facultative endosymbionts and by combining the results of the two sampling surveys, four different taxa of facultative endosymbionts were detected: *H. defensa*, *S. symbiotica*, *R. insecticola* and the γ -proteobacteria X-type. Based on a relatively small sample (i.e. 10 aphid-lines per population/species) we have shown that even within a population, there may be abundant variation in the occurrence of facultative endosymbionts; specimens coming from different *A. arenaria*

TABLE 3

Spearman coefficients for the correlation between facultative endosymbionts (i.e. *Hamiltonella defensa*, *Serratia symbiotica*) and the number of mummies observed in *Schizaphis rufula*.

	<i>H. defensa</i>	<i>S. symbiotica</i>	<i>R. insecticola</i>	X-type	Mummies
<i>H. defensa</i>		0.61 <0.0001	-0.05 0.74	-0.05 0.74	0.14 0.35
<i>S. symbiotica</i>	0.61 <0.0001		-0.08 0.59	-0.08 0.59	0.08 0.62
<i>Regiella insecticola</i>	-0.05 0.74	-0.08 0.59		0.99 <0.0001	0.21 0.18
X-type	-0.05 0.74	-0.08 0.59	0.99 <0.0001		0.21 0.18
Mummies	0.14 0.35	0.08 0.62	0.21 0.18	0.21 0.18	

Schizaphis rufula



Laingia psammae

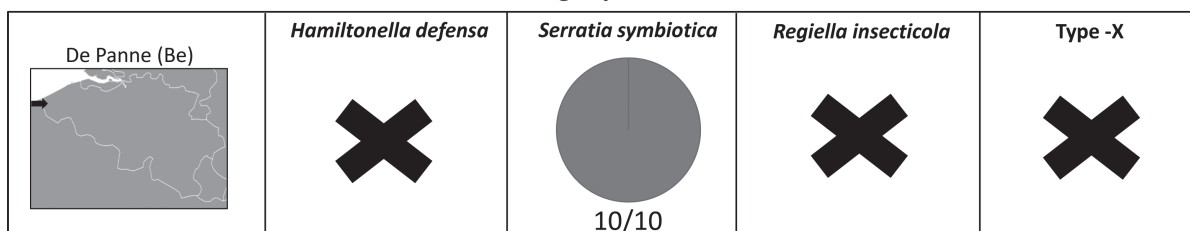


Fig 4. – Frequency of facultative endosymbionts in two species of aphids found in coastal dunes: *Schizaphis rufula* and *Laingia psammae*.

plants, only separated a few meters, showed dissimilar endosymbiotic profiles. Moreover, the results showed that different species of dune aphids shared facultative endosymbionts. For instance, *L. psammae*, *R. padi* and *S. rufula* were all infected with *S. symbiotica*. Also temporal variation in the occurrence of endosymbionts cannot be excluded since different endosymbionts were detected in the samples collected in June and in October.

These findings open interesting future research avenues. For instance, *H. defensa* is an endosymbiont already reported in aphids and other sap-feeding insects as protecting its hosts from parasitoid wasps (OLIVER, 2010; NYABUGA et al., 2010; MCCLEAN et al., 2011; LUKASIK et al., 2013). As observed in the field, the sampled populations were frequently parasitized by parasitoid wasps but only a few individuals from Het Zwin revealed the presence of *H. defensa*. Since not all *H. defensa* strains are known to confer resistance to parasitoids and the effect also varies among aphid species (DEGNAN et al., 2009; VORBURGER et al., 2009) the meaning of the interaction for this Belgian aphid population needs further experimental examination. The correlation analysis did not show any relationship between *H. defensa* and the number of mummies detected in the field. However, these results should be taken with caution due to the limited number of observations and also because a lack of correlation cannot exclude causality. The same type of ideas can be put forward regarding *R. insecticola* as this endosymbiont is known to protect aphids from different natural enemies. Preliminary experimental manipulations with *R. insecticola* in other aphid species have demonstrated that it confers resistance against aphid fungal pathogens (FERRARI et al., 2004; SCARBOROUGH et al., 2005). Nonetheless, it has also been shown that this endosymbiont protects *Myzus persicae* and *Aphis fabae* against parasitoids (VORBURGER et al., 2009).

Serratia symbiotica was consistently detected in the three species (*S. rufula*, *R. padi*, *L. psammae*) collected in coastal dunes from both sampling

dates. Dune habitats are not only harsh for the plant community but also for the associated insects. For example, oscillations in temperature of ca. 25°C are common during the summer and dune sand can easily reach temperatures above 50°C (MAUN 2009). Besides different life history traits and behavioral adaptations to such rapid environmental changes, symbiotic relationships with facultative bacteria may ameliorate such harsh environmental conditions. The facultative endosymbiont *S. symbiotica* has been reported to be pivotal in protection against heat shocks in several species of aphids; in arid areas a relatively high proportion of aphids are found to be carrying this symbiont (HENRY et al., 2013; BRUMIN et al., 2011; BURKE et al., 2010). Whether this is the case for dune species requires further investigation. Nonetheless, it is noteworthy that the three aphids species do carry this symbiont.

A regulatory role of some endosymbionts has been reported in the literature. For instance, in the pea aphid comparison of strains with similar genetic background with or without *Rickettsia* showed a remarkable interaction between this endosymbiont and other endosymbiotic bacteria, including *Buchnera aphidicola* (SAKURAI et al., 2005). From other systems, we also know that the γ -proteobacteria X-type plays a pivotal role in the regulation of resistance against parasitoid wasps during abiotic stress (GUAY et al., 2009). Whether this applies to the species included in this study is a question that needs further analysis. In this direction points the correlation of *R. insecticola* with the endosymbiont X-type and *H. defensa* with *S. symbiotica*.

Regarding the aphid species studied here, we still have very limited knowledge on the factors determining their population dynamics on dune grasses. Experimental evidence shows that population growth in *S. rufula* and *R. padi* is negatively affected by the presence of plant parasitic nematodes in grass roots (DE LA PEÑA et al., 2009; VANDEGEHUCHTE et al., 2011). Other experiments have shown that fungal endophytes are also involved in the control

of aphid populations through belowground / aboveground plant-mediated interactions (JABER & VIDAL 2009; DE LA PEÑA unpublished). In the field, we found significant numbers of aphid mummies, indicating that aphid control by parasitoid wasps occurs in the dunes. Preliminary research addressing the host-range of *S. rufula* has also shown that the species is able to feed on several grasses (PETTERSSON 1971), but given the differences in the composition of the endosymbiont community it would be interesting to address the question of whether aphid host-range is influenced by these endosymbionts. Putting all these pieces together, it is clear that in order to understand the ecology of aphids on dune grasses a multitrophic perspective needs to be taken to further understand how all these players modulate each other (VANDEGEHUCHTE et al., 2013).

More and more empirical evidence reveals the pivotal role of facultative bacteria in mediating indirect interactions in insect communities through changes in plant physiology (FRAGO et al., 2013). The results of our initial assessment showed an unexpected diversity of facultative endosymbionts in dune aphids. The further study of these inconspicuous organisms in coastal dunes will provide new insights into the functioning of these ecosystems. Finally, it is important to highlight that the aphid species included in this study are not only relevant for the dune system; they offer an interesting system to address general eco-evolutionary questions regarding bacterial endosymbionts, the community in which they are embedded, and their abiotic environment.

ACKNOWLEDGEMENTS

Eduardo de la Peña has enjoyed during the course of this research a post-doctoral fellowship of the Flemish Foundation for Scientific Research (FWO, Belgium) and a Ramón y Cajal research contract (Subprograma Ramón y Cajal, Ministerio de Economía y Competitividad, Spain). Enric Frago is currently funded by Marie Curie Intra-European Fellowship within the 7th

European Community Framework Programme. The authors would like to thank Prof. Frédérick Hendrickx for his useful suggestions while preparing the manuscript and Graeme Rycyk for his suggestion regarding English usage.

REFERENCES

- BENSON DA, CAVANAUGH M, CLARK K, KARSCH-MIZRACHI I, LIPMAN DJ, OSTELL J, SAYERS EW. (2013) GenBank. Nucleic Acids Research Jan; (D1) D36-42.
- BRÖRING U. & NIEDRINGHAUS (1989) Die epigäische Hemipterenfauna (Heteroptera, Auchenorrhyncha) der Tertiärdünen Ostfriesischer Düneninseln. - Braunschw. naturk. Schr. 3: 387-398.
- BRUMIN M, KONTSEDALOV S, GHAMIN M. (2011) *Rickettsia* influences thermotolerance in the whitefly *Bemisia tabaci* B biotype. Insect Science 18, 57-66.
- BURKE G, HIEHN O, MORAN N (2010) Effects of facultative symbionts and heat stress on the metabolome of pea aphids. The ISME Journal 4:242-252.
- DE LA PEÑA E, KARSSSEN G, MOENS M (2007) Diversity and distribution of root lesion nematodes associated to *Ammophila arenaria* in Europe dunes. Nematology, 9: 881-901.
- DE DE LA PEÑA E, BONTE D, MOENS M (2009) Evidence of population differentiation in the dune grass *Ammophila arenaria* and its associated root-feeding nematodes. Plant and Soil 324 (1-2): 307-316.
- DE LA PEÑA E, RODRÍGUEZ-ECHEVERRÍA S, VAN DER PUTTEN WH, FREITAS H, MOENS M (2006) Mechanism of control of root-feeding nematodes by arbuscular mycorrhizal fungi in the dune grass *Ammophila arenaria*. New Phytologist, 169:829-840.
- DEGNAN PH, YU Y, SISNEROS N, WING RA, MORAN NA (2009) *Hamiltonella defensa*, genome evolution of protective bacterial endosymbiont from pathogenic ancestors. Proceedings of the National Academy of Sciences 106 (22): 9063-9068.
- FERRARI J, DARBY AC, DANIELL TJ, GODFRAY HCJ, DOUGLAS AE (2004) Linking the bacterial community in pea aphids with host-plant use and

- natural enemy resistance. *Ecological Entomology* 29: 60-65.
- FERRARI J, WEST JA, GODFRAY HCJ (2011) Population genetic structure and secondary symbionts in host-associated populations of the pea aphid complex. *Evolution* 66(2): 375-390.
- FRAGO E, DICKE M, GODFRAY HCJ (2012) Insect symbionts as hidden players in insect-plant interactions. *Trends in Ecology & Evolution*, 27(12): 705-711.
- GUAY JF, BOUDREAU S, MICHAUD D, CLOUTIER C (2009) Impact of environmental stress on aphid clonal resistance to parasitoids: Role of *Hamiltonella defensa* bacterial symbiosis in association with a new facultative symbiont of the pea aphid. *Journal of Insect Physiology* 55: 919-926.
- HENRY LM, PECCOUD J, SIMON JC, HADFIELD JD, MAIDEN MJC, FERRARI J, GODFRAY HCJ (2013). Horizontally transmitted symbionts and host colonization of ecological niches. *Current biology* 23(17), 1713-7.
- JABER LR, VIDAL S (2009) Interactions between and endophytic fungus, aphids and extrafloral nectaries: do endophytes induce extrafloral-mediated defenses in *Vicia faba*. *Functional Ecology* 23(4), 707-714.
- LEONARDO T E & MONDOR EB (2006). Symbiont modifies host life history traits that affect gene flow. *Proceedings of the Royal Society of London B – Biological Sciences* 273: 1079-1084.
- LUKASIK P, DAWID MA, FERRARI J, GODFRAY HCJ (2013) The diversity and fitness effects of infection with facultative endosymbionts in the grain aphid, *Sitobion avenae*. *Oecologia* 173: 985-996.
- MAUN M (2009) *The biology of coastal sand dunes*. Oxford University press.
- MCCLEAN AHC, VAN ASCH M, FERRARI J, GODFRAY HCJ (2011) Effects of bacterial secondary symbionts on host plant use in pea aphids. *Proc. R. Soc. B*, 278: 760-766.
- MORAN NA, MCCUTCHEON JP, NAKABACHIA (2008) Genomics and evolution of heritable bacterial symbionts. *Annual Review of Genetics*. 42:165-90.
- NYABUGA FN, OUTREMAN Y, SIMON J, HECKEL DG, WEISSER W (2010) Effects of pea aphid secondary endosymbionts on aphid resistance and development of the aphid parasitoid *Aphidius ervi*: a correlative study. *Entomologia Experimentalis et Applicata* 136: 243-253.
- OLIVER KM, DEGNAN PH, BURKE GR, MORAN NA (2010) Facultative symbionts in aphids and the horizontal transfer of ecological important traits. *Annu. Rev. Entomol.* 55:247-266.
- PETTERSSON J (1971) Studies on four grass-inhabiting species of *Schizaphis* (Hem: Aphidoidea) II. Morphological descriptions of populations of *S. dubia* Huc., *S. arrenatheri* n. sp., *S. rufula* (Walk.) and *S. longicaudata* H.R.L. *Swedish Journal of Agricultural Research* I: 115-132.
- SAKURAI M, KOGA R, TSUCHIDA T, MENG X, FUKATSU T (2005) *Rickettsia s* symbiont in the pea aphid *Acyrtosiphon pisum*: novel cellular tropism, effect on host fitness and interaction with the essential symbiont *Buchnera*. *Applied Environmental Microbiology* 7: 4069-4075.
- SCARBOROUGH CL, FERRARI J, GODFRAY HCJ (2005) Aphid protected from pathogen by endosymbiont. *Science* 310: 1781-1781.
- VANDEGEHUCHTE M, DE LA PEÑA E, BONTE D (2010) Aphids on *Ammophila arenaria* in Belgium: first reports, phenology and host range expansion. *Belgian Journal of Zoology*, 140: 77-79.
- VANDEGEHUCHTE M, DE LA PEÑA E, BONTE D (2010) Interactions between root and shoot herbivores of *Ammophila arenaria* in the laboratory do not translate into correlated abundances in the field. *Oikos*, 119: 1011-10
- VANDEGEHUCHTE M, DE LA PEÑA E, BONTE D (2013). Non-local genotypes of a resident grass species reduce invertebrate species richness. *Insect Conservation and Diversity* 5(6): 453-460.
- VORBURGER C, SANDROCK C, GOUSKOV A, CASTAÑEDA L, FERRARI J (2009) Genotypic variation and the role of defensive endosymbionts in an all-parthenogenetic host-parasitoid interaction. *Evolution* 63: 1439-50.
- VORBURGER C, GEHRER L, RODRIGUEZ P (2010) A strain of the bacterial symbiont *Regiella insecticola* protect against insect parasitoids. *Biology letters* 6: 109-112.

Received: November 29th, 2013

Accepted: May 27th, 2014

Branch editor: Frederik Hendrickx

An ecological study of *Electra posidoniae* Gautier, 1954 (Cheilostomata, Anasca), a bryozoan epiphyte found solely on the seagrass *Posidonia oceanica* (L.) Delile, 1813

Gilles Lepoint ¹, Olivier Mouchette ¹, Corine Pelaprat ² & Sylvie Gobert ¹

¹ Oceanology, Centre MARE, University of Liège, Belgique

² STARESO (STAtion de REcherches Sous-marines et Océanographiques), Calvi, Corse, France

ABSTRACT. The bryozoan *Electra posidoniae* Gautier is found solely on the leaves of the Neptune grass *Posidonia oceanica* (L.) Delile, dominating the leaf epifauna of this seagrass. Epiphytes of marine angiosperms (or seagrasses) often play an important role in ecosystem functioning, for example as food web suppliers. As dysfunction of the epiphytic component is often implied in human-induced seagrass decline, it is important to understand the dynamics and life traits of this community in pristine areas. This study involved the monthly assessment of colonization dynamics, biomass seasonality, and diet composition through measurements of stable isotopes, in *E. posidoniae* at a depth of 10 m in the Revellata Bay (Corsica, Mediterranean Sea). Ancestrulae (i.e. colony founders) appeared towards the end of winter and were very selective in their settlement position along the leaves of *P. oceanica*. A maximum of 100,000 colonies per square meter was recorded. Colonies of *E. posidoniae* dominated the epiphytic community biomass in early spring, but were overtaken by epiphytic algae in June. Food shortage could be involved in this reduction in dominance. Although stable isotope ratios of C, N and S showed that this suspension feeder mainly relies on the water column for its food, other food sources such as re-suspended epiphytic diatoms could be important in late spring (i.e. after the phytoplanktonic bloom). Additionally, a contribution of seagrass phytodetritus to the diet of this species cannot be excluded. The species was almost absent in winter, raising the question of its recruitment in spring. This study confirms the quantitative importance of this species in the seagrass meadow and explores its role in the relationship between the water column and this seagrass ecosystem.

KEY WORDS: biofouling, bryozoan, seagrass, stable isotopes, Neptune grass, NW Mediterranean

INTRODUCTION

The Neptune grass *Posidonia oceanica* (L.) Delile forms large submarine seagrass meadows in the coastal zone at a depth of up to 40 m and, in consequence of its large size and its relatively long life span, is fouled by many epiphytic species (PERES & PICARD, 1964). This epiphytic community is a central component of the seagrass meadow ecosystem in terms of diversity (PERES & PICARD, 1964; BOROWITZKA et al., 2006). Species living as epiphytes of marine angiosperms (or seagrasses) often play an important role in ecosystem functioning. They are important contributors to primary production (BOROWITZKA et al., 2006) and key components

of the food web (LEPOINT et al., 2000; TOMAS et al., 2005; GACIA et al., 2009; VIZZINI, 2009; MICHEL, 2011). They contribute to benthic-pelagic coupling (LEMMENS et al., 1996) and to nitrogen and carbon cycling within the meadow (ALCOVERRO et al., 2004; MATEO et al., 2006). Because epiphytic component dysfunction is often implied in human-induced seagrass decline (BALATA et al. 2010), it is important to understand dynamics and life traits of this community.

Leaf epiphytic communities are typically dominated by photophilous brown macroalgae, red algae of the taxon Ceramiales, and calcareous red algae (MAZZELLA et al., 1989). Nevertheless, some animal species, such as bryozoans,

hydrozoans or sedentary polychaetes, are also found fixed on leaves of *P. oceanica* (PERES & PICARD, 1964; HAYWARD, 1975; BOERO et al., 1985; LEPOINT et al., 1999). The most abundant and the most characteristic of these animals is *Electra posidoniae* Gautier 1954 (Fig. 1), an anascan bryozoan specialized in epiphytic colonisation and strictly restricted to the leaves of *P. oceanica* (GAUTIER, 1961). This species is frequently found almost entirely covering the internal faces of leaves (DALLA VIA et al., 1998). It is recognised as a true species differing both morphologically and genetically from the “cosmopolitan” *Electra pilosa* species complex (NIKULINA et al., 2007). *E. posidoniae* displays life history traits that could be considered as hyper-adapted to epiphytism on leaves of *Posidonia*. For example, the settlement of ancestrulae (i.e. colony founders) is highly selective in terms of substrate choice (never found on any substrate besides Neptune grass leaves), of leaf face choice (generally the inner side), of place on the leaf face (generally in the middle of the leaf width), and in term of orientation (generally aligned to allow colony growth towards the leaf apex) (MATRICARDI et al., 1991; DALLA VIA et al., 1998). Moreover, colonies are constituted of zooids with multiseriate encrusting morphology (MCKINNEY & JACKSON, 1989); this morphology is particularly efficient in the colonisation of

newly-formed leaves. Colonies tend to grow parallel to the leaf veins and are flexible because they are lightly calcified (GAUTIER, 1961). This morphology is adapted to substrate deformation (i.e. leaf flexibility), reducing the risk of colony breaking. Finally, zooids are large compared to other epiphytic bryozoans and rapidly colonize the available substrate; this is probably a competitive advantage over other epiphytic taxa (LEPOINT et al., 2014).

Electra posidoniae is a common suspension feeder in the Mediterranean sublittoral benthos, probably contributing to the energetic and material coupling between the water column and the benthic compartment, in a similar way to other suspension feeders in other seagrass meadows (LEMMENS et al. 1996). However, in the oligotrophic Mediterranean, microphytoplankton (i.e. diatoms) is a very seasonal resource, restricted primarily to the beginning of spring. In late spring and summer, smaller phytoplanktonic species dominate and are not necessary available or suitable for bryozoan feeding. For this reason food shortage is often observed in some Mediterranean suspensivores (COMA & RIBES 2003). Alternative food sources could exist for *E. posidoniae*, for example microepiphytes (bacteria, protists or diatoms), (NOVAK, 1984; MABROUK et al., 2011), which could constitute a

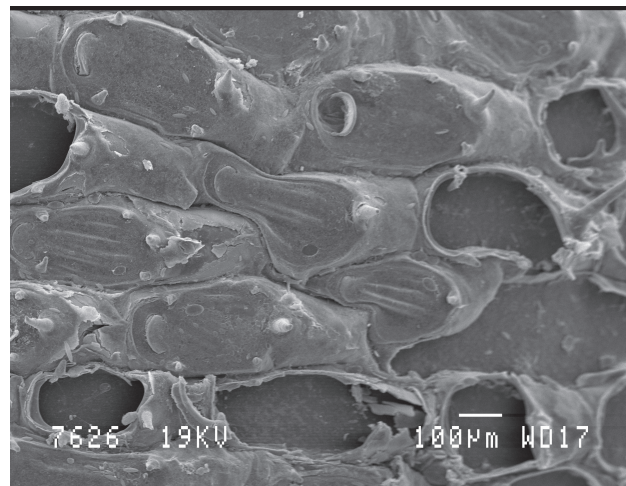
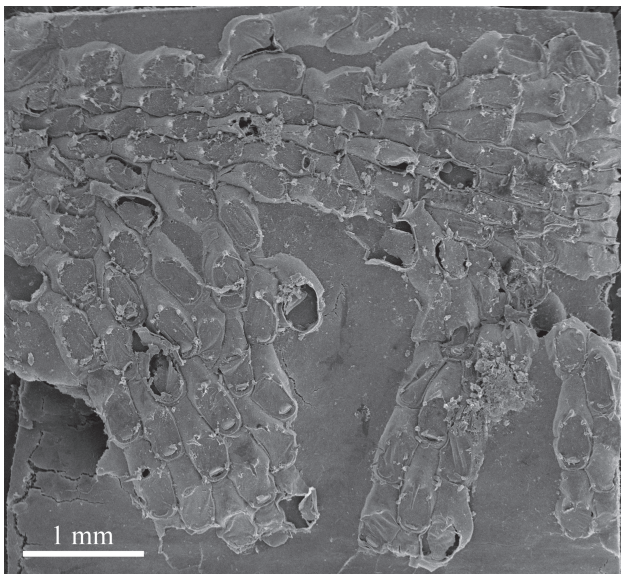


Fig. 1. – SEM microphotographs of a colony of *Electra posidoniae* on a leaf of *Posidonia oceanica* (a) with a more detailed view of some zooids (b). Photography: F. REMY.

food source when detached from their substrate. Moreover, seagrass meadows are known to produce large amounts of phytodetritus, which fuels detritic food webs (CEBRIAN & LARTIGUE, 2004). This detritus may sometimes form a large part of the suspended particulate organic matter (SPOM), depending on hydrodynamic conditions (DAUBY et al., 1995).

To the best of our knowledge, the seasonal population dynamics of *E. posidoniae* have not previously been quantitatively assessed. Therefore, our first aim in this study was to assess these dynamics at monthly intervals in terms of biomass, leaf covering and colony numbers. Assessments were made over a period of one year at a 10 m depth. Secondly, stable isotope analyses were conducted to estimate the contribution of alternative food sources (i.e. *Posidonia* detritus, detached microepiphytes) to the diet of *E. posidoniae*. Thirdly, we have attempted to quantify the potential role of *E. posidoniae* in the benthic-pelagic coupling.

MATERIAL AND METHODS

Sampling

Within a permanent quadrat (3 x 3 m), five shoots of *P. oceanica* were harvested at monthly intervals in the Revellata Bay (Calvi Bay, NW Corsica) near the oceanographic station STARESO (University of Liège) at a depth of 10 m. Samples were taken between November 2002 and November 2003. Shoots were immediately frozen at -18°C until analysis.

Shoot density, measured at monthly intervals using a circle with a diameter of 40 cm randomly set in the meadow (n=10 counts /campaign), was 452 ± 127 shoots.m⁻².

Sample processing

Shoots were dissected to separate the leaves, and the length and width of each leaf were

recorded to calculate the surface area of one leaf side. Total leaf surface per shoot was calculated as the sum of each leaf surface multiplied by two to account for each leaf side.

Each month, for each shoot, the numbers of colonies and ancestrulae (i.e. the colony founder) of *E. posidoniae* were recorded, and assigned to a leaf face (internal or external).

Colonies were collected with a razor blade, oven-dried at 50°C and weighed to obtain the total dry mass per shoot (mgDM.shoot⁻¹). The remaining epiphytes were scraped off with a razor blade. Cleaned leaves and remaining epiphytes were also oven-dried and weighed.

To estimate cover of *E. posidoniae* (cm²_{colony}.shoot⁻¹), the relationship between the colony mass (mgDM.shoot⁻¹) and the colony surface (cm²_{colony}) was established. Twenty cm² of *E. posidoniae* were scraped from a pool of shoots sampled in April 2005 and average grammage (gDM.cm⁻²_{colony}) was determined after drying at 60°C during 48 hours. This grammage was equal to 1.84 mgDM.cm⁻²_{colony}. We have made the assumption that grammage was constant throughout the year.

Stable Isotopes

Colonies of *E. posidoniae* were ground using a mortar and pestle to obtain a homogeneous powder. Acidification can affect the isotopic ratio of nitrogen and of sulphur, so for this reason N and S stable isotope compositions were determined prior to acidification (PINNEGAR & POLUNIN, 1999; CONNOLLY & SCHLACHER, 2013). However, because colonies are lightly calcified and because the carbon stable isotope ratios of carbonate do not reflect the animal diet, samples for determining C stable isotope compositions were acidified in a closed glass receptacle using vapours of fuming HCl (37%, P.A., Merck). Measurements were conducted using an Isoprime 100 mass spectrometer (Isoprime, United Kingdom) coupled to a Vario

Microcube elemental analyser (Elementar, Germany). Stable isotope ratios were expressed in δ notation (in ‰) according to the following:

$$\delta X = \frac{(R_{\text{sample}} - R_{\text{standard}})}{R_{\text{standard}}} \times 1000$$

where X is ^{13}C or ^{15}N or and R is the corresponding ratio $^{13}\text{C}/^{12}\text{C}$, $^{15}\text{N}/^{14}\text{N}$ or $^{34}\text{S}/^{32}\text{S}$ for samples or standards. Carbon, nitrogen and sulphur isotopic ratios are expressed relative to the international standards vPDB (Vienna Peedee Belemnite), to atmospheric air, and to vCDT (Vienna Cañon Diablo Troilite), respectively. Certified reference materials were IAEA-N1 (ammonium sulphate) ($\delta^{15}\text{N} = +0.4 \pm 0.2\text{‰}$), IAEA C-6 (sucrose) ($\delta^{13}\text{C} = -10.8 \pm 0.2\text{‰}$) and IAEA S1 (silver sulphide) ($\delta^{34}\text{S} = -0.3\text{‰}$). Routine measurements were precise to within 0.2‰ for both $\delta^{13}\text{C}$ and $\delta^{15}\text{N}$, and 0.3‰ for $\delta^{34}\text{S}$.

For potential food sources of *E. posidoniae*, we have taken data published relating to the Calvi Bay for carbon and nitrogen but have measured our own $\delta^{34}\text{S}$ for leaves of *P. oceanica* and suspended organic matter (SPOM).

Calculation of filtration rates

Based on literature data and our study, we have calculated the hourly filtered water volume and the associated potential daily amount of phytoplanktonic biomass filtered by our population of *E. posidoniae* according to following equations:

$$\text{Filtered volume} = \text{Filtration rate} \times E. \textit{posidoniae} \text{ biomass}$$

$$\text{Filtered volume} = \text{Filtration rate} \times E. \textit{posidoniae} \text{ biomass}$$

$$\text{Filtered biomass} = \text{Plankton biomass} \times \text{Filtered volume} \times \% \text{ Retention}$$

Water volume filtered by *E. posidoniae* is expressed in $\text{ml} \cdot \text{h}^{-1} \cdot \text{m}^{-2}_{\text{seafloor}}$, *E. posidoniae* biomass in $\text{gDM} \cdot \text{m}^{-2}_{\text{seafloor}}$ and filtration rate in $\text{ml} \cdot \text{h}^{-1} \cdot \text{gDM}^{-1}$.

Filtration rates were measured using *Electra bellula*, an Australian epiphytic species of the seagrass *Amphibolis* spp. and macroalgae (LISBJERG & PETERSEN, 2000). Biomass of filtered material is expressed in $\mu\text{gN} \cdot \text{m}^{-2}_{\text{seafloor}} \cdot \text{d}^{-1}$ or $\mu\text{gC} \cdot \text{m}^{-2}_{\text{seafloor}} \cdot \text{d}^{-1}$. Planktonic biomass nitrogen and carbon were measured in the Calvi Bay between 1997 and 1999 (LEPOINT et al., 2004) and averaged according to the following periods: “wintering” (January, December), blooming (February, March, April), post-blooming (May, July, August), fall (September- October). Retention efficiency was fixed to 25% (i.e. 25% of the particles passing through the filter are effectively retained by the filter), which is a minimum for this type of bryozoan (LISBJERG & PETERSEN, 2000). We did not take into account any variability of this retention efficiency, for example in relation to particle size.

Because conditions concerning normality were met (D’Agostino & Pearson omnibus normality test), isotopic data were analysed using a one-way ANOVA test with sampling dates as independent factors. Tukey’s Multiple Comparison test was used to assess pairwise differences when ANOVA revealed statistically significant effects. All test results were considered as significant when p was ≤ 0.05 . Statistical calculations were performed using GraphPad Prism 5 software.

RESULTS

Dry mass of leaves of *P. oceanica* showed a classical seasonal evolution, with minimal values during the winter (e.g. November 2002), maximum values during the summer (e.g. June) and a drastic decrease as a consequence of the autumnal leaf fall (Fig. 2). Total epiphytic dry mass also displayed seasonal trends, with maximal values reached in May (Fig. 2). Total epiphytic dry mass constituted between $1.13 \pm 0.88\%$ in November 2002 and $25.98 \pm 5.29\%$ of the total aboveground biomass in April 2003. Dry mass of *E. posidoniae* was very low in winter samples, increased in early spring, reached a maximal point in April and decreased

drastically between June and July (i.e. before leaf abscission) (Fig. 2). The remaining epiphytic biomass, which was mainly represented by epiphytic algae, was also minimal in winter samples, increased slightly later than that of *E. posidoniae*, was maximal in July and drastically decreased between July and September (Fig. 2). *E. posidoniae* represented between 0.5 ± 0.3 % of the total epiphytic dry mass in November 2002 and 47.2 ± 5.3 % in March 2003, which corresponded respectively to 0.01 and 10 % of the total aboveground dry mass.

The total number of colonies per shoot was minimal in winter and maximal in spring (i.e. March to May) samples, varying between 0 and 229 colonies per shoot (Fig. 3). If this number is expressed in terms of the shoot density at 10 m depth, this represented between 0 and 103,000 colonies of *E. posidoniae* per m^2_{seafloor} .

The total number of ancestrulae was very low (Fig. 3). They were almost absent from September to December, showed low abundance in January and February, peaked in March and decreased drastically in June.

Ancestrulae were mainly (60 to 100%) found on the internal face (i.e. the concave face). This positioning was conserved in developed colonies and averaged $80 \pm 20\%$.

Using colony grammage ($1.84 \text{ mgDM} \cdot \text{cm}^{-2}_{\text{colony}}$) and colony dry mass (mgDM), we have calculated the average surface shoot area covered by *E. posidoniae*. This varied between 0 in December 2003 and 90 cm^2 at the end of April 2004. Using these data and the surface of leaves calculated from our biometric data (i.e. leaf length and width), the proportion of leaf covered by *E. posidoniae* colonies was calculated (Fig. 4). It was minimal in December (0.01 %) and maximal in late April ($9.5 \pm 2.5\%$). It decreased from June till autumn, when it reached less than 2.5%. The covered surface was mainly the inner leaf face.

The measured $\delta^{34}\text{S}$ values ranged from 13.9 to 18.2‰ (16.6 ± 1.9 ; mean \pm SD) for SPOM and from 14.2 to 18.8‰ (17.03 ± 1.4 ; mean \pm SD) for leaves of *P. oceanica*. These $\delta^{34}\text{S}$ values did not differ significantly between the two food sources. $\delta^{13}\text{C}$, $\delta^{15}\text{N}$, $\delta^{34}\text{S}$ values of individual colonies of *E. posidoniae* ranged between -21.6 and -17.3‰

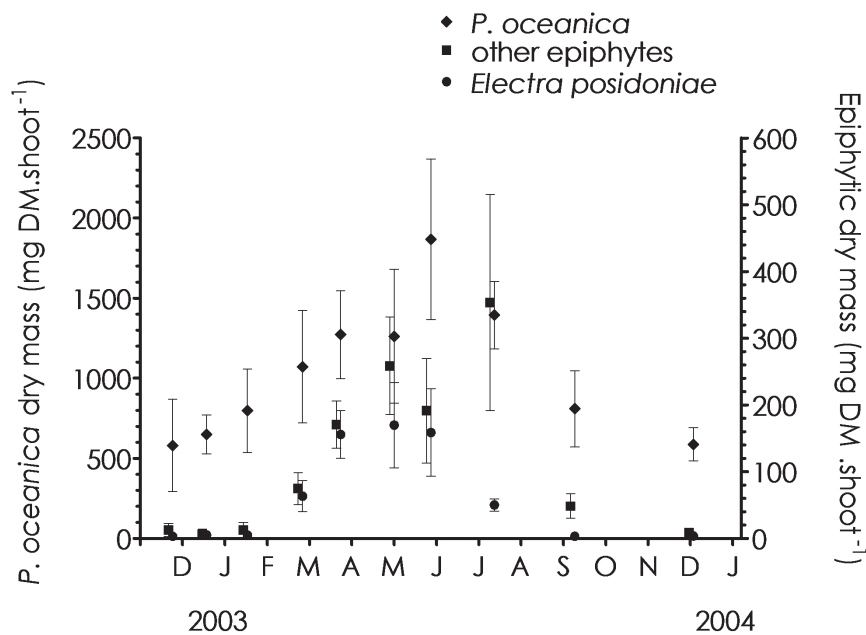


Fig. 2. – Dry mass (mean \pm S.D.) of leaves of *Posidonia oceanica*, of their epiphytic bryozoa *Electra posidoniae*, and of their other epiphytes, collected at a depth of 10 m in Revellata Bay between November 2003 and November 2004.

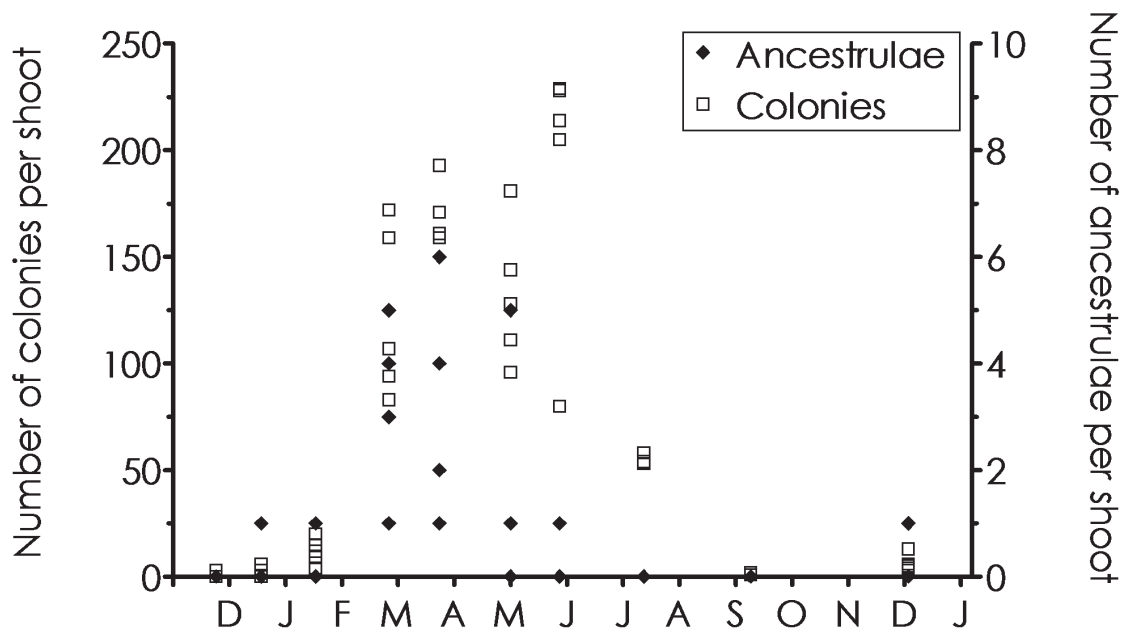


Fig. 3. – Total number of colonies of *Electra posidoniae* and of their ancestrulae, settled on leaves of *Posidonia oceanica* sampled at a depth of 10 m in Revellata Bay between November 2003 and November 2004.

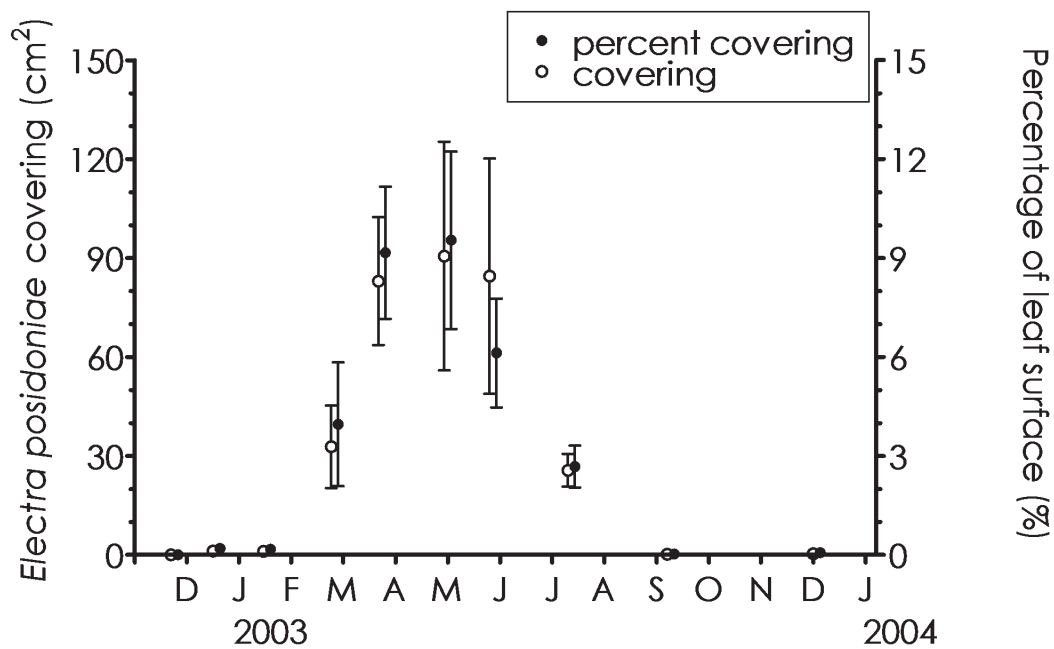


Fig. 4. – Averaged values (\pm S.D.) of actual and percentage of leaf surface area of *Posidonia oceanica* covered by *Electra posidoniae* on leaves of *P. oceanica* sampled at a depth of 10 m in Revellata Bay between November 2003 and November 2004.

TABLE 1

Summary of ANOVA results.

Sources of variation		$\delta^{13}\text{C}$ (‰)			$\delta^{15}\text{N}$ (‰)			$\delta^{34}\text{S}$ (‰)	
	MS	F	p	MS	F	p	MS	F	p
Dates	4.73	$F_{4,20}=7.56$	<0.001	4.12	$F_{4,20}=34.50$	<0.001	0.57	$F_{4,20}=0.49$	NS

($-19.9 \pm 1.2\text{‰}$; mean \pm SD), between -0.5 and 2.7‰ ($1.6 \pm 0.9\text{‰}$; mean \pm SD), and between 15.5 and 19.8‰ ($17.7 \pm 1.1\text{‰}$; mean \pm SD), respectively (Fig. 5). One way ANOVA results showed a significant variability according to sampling date for $\delta^{13}\text{C}$, $\delta^{15}\text{N}$ but not for $\delta^{34}\text{S}$ (Table 1). Tukey's Multiple Comparison Test showed that for both delta values there were significant differences between early spring samples (February, March, April) and late spring or summer samples (May, June, July), with a tendency for both delta values to increase over time. The amount of material was not sufficient to perform individual colony isotopic measurements for fall and winter samples.

Using our quantitative data and literature, we have calculated (Table 2) that, during phytoplankton blooms (February-April), a population of *E. posidoniae* at a depth of 10 m may filter up to 36 L of water per day and per m^2 of seafloor, corresponding to a transfer of 0.3 and 1.3 mg DM of nitrogen and carbon, respectively.

DISCUSSION

Our results show the important contribution of *E. posidoniae* to the epiphytic biomass of *P. oceanica*. It is an early colonizer of the leaf surface, developing before the characteristic photophilous algae, and therefore it contributes mostly to spring epiphyte biomass. Epiphytic accrual on *P. oceanica* is progressive and involves a succession of organisms from a bacterial biofilm to a complex multi-layered epiphytic community

(NOVAK, 1984; MAZZELLA & RUSSO, 1989; CEBRIAN et al., 1999). *E. posidoniae* develops before photophilous macroalgae and faster than calcareous algae (LEPOINT et al., 2007). This successional pattern is common at the NW Mediterranean basin scale (VAN DER BEN, 1971; MAZZELLA & RUSSO, 1989; DALLA VIA et al., 1998; CEBRIAN et al., 1999; PRADO et al., 2008; JACQUEMART & DEMOULIN, 2008) and implies that common environmental factors govern the epiphytic temporal settlement.

There is an important gap between leaf fall (September) and recolonization of leaves of *P. oceanica* (from January but mainly at the end of winter) by larvae of *E. posidoniae*. For many epiphytic bryozoans, other habitats (i.e. rhizomes, rocks and stones) may have overwintering populations that contribute to supplying larvae in spring for leaf colonization (COCITO et al., 2012, LEPOINT et al., 2014). This is not the case for *E. posidoniae* as this species is strictly only found on leaves of *P. oceanica* (GAUTIER, 1961; MATRICARDI et al., 1991). Connectivity between populations growing at different depths in the meadow and affected by differences in the phenology of the host plant (e.g. temporal difference of leaf growth and fall between deeper and shallower beds) may be important to ensure the supply of recruits between different meadow areas. Nevertheless, a time gap exists between leaf fall and recolonization peak in March. Therefore it is probably crucial that this species (similarly to other *Electra* species) has planktonotrophic larvae able to survive a longer time in the water column in comparison to most

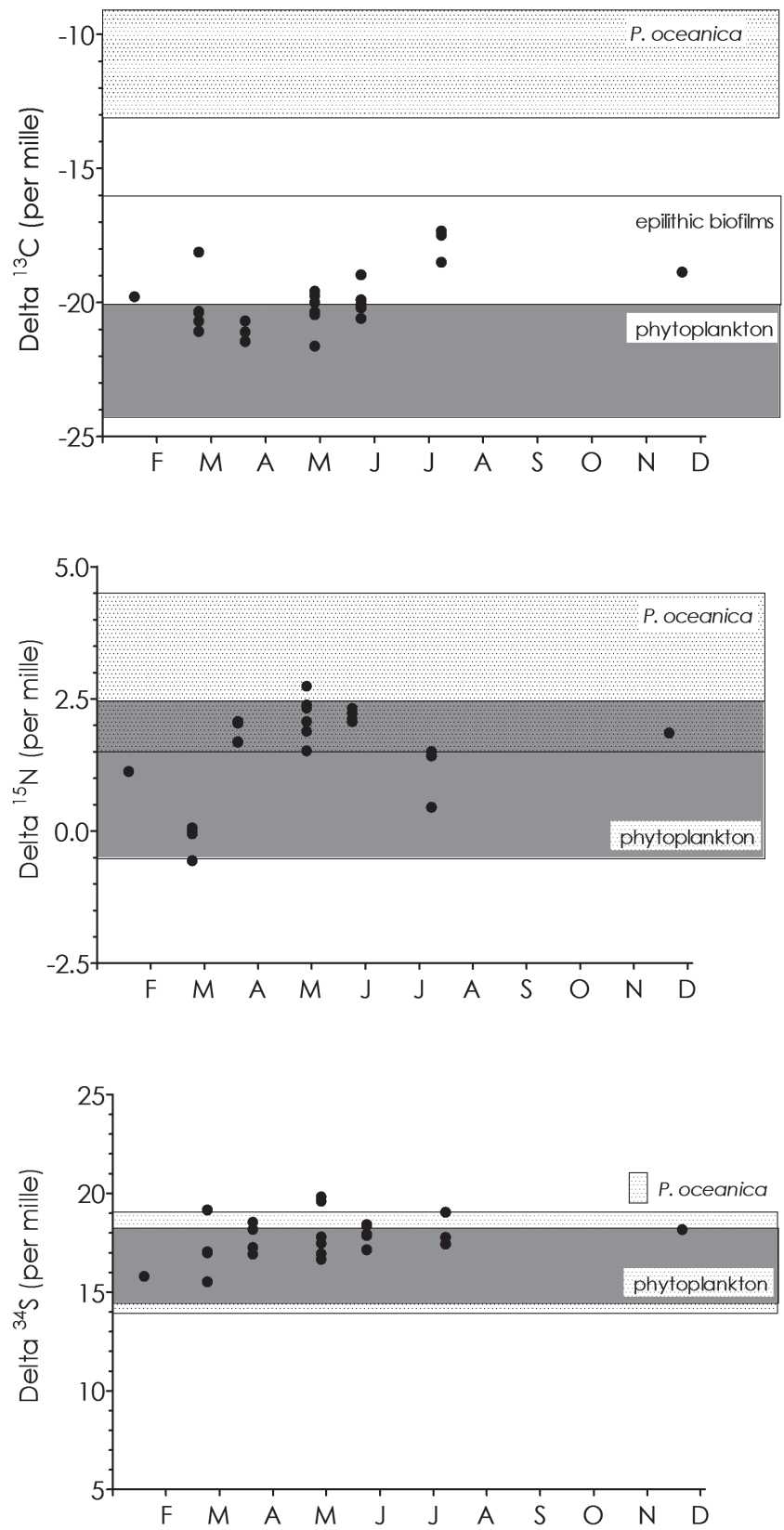


Fig. 5. – $\delta^{13}\text{C}$, $\delta^{15}\text{N}$ and $\delta^{34}\text{S}$ values (mean \pm s.d.) of colonies of *Electra posidoniae* settled on leaves of *Posidonia oceanica* collected at a depth of 10 m in the Revellata Bay between February 2003 and December 2004. Range for phytoplankton and for *P. oceanica* from LEPOINT et al. (2000) and LEPOINT et al. (2003). Range for biofilm grown on artificial substrates from VERMEULEN (2012).

TABLE 2

Surface covering, biomass, filtered volume and daily planktonic biomass filtered by *Electra posidoniae* Gautier in a *Posidonia oceanica* meadow (Revellata Bay, Corsica). Data used for calculation come from a: this study; b: (Lepoint et al., 2004); c: (Lisbjerg & Petersen, 2000). See Material and Method for details.

Dates	<i>E. posidoniae</i> covering ^a		Planktonic biomass ^b		<i>E. posidoniae</i> biomass ^a	Filtering rate ^c	Filtered volume	Filtered N biomass	Filtered C biomass
	cm ² shoot ⁻¹	cm ² m ⁻² _{seafloor}	µgN L ⁻¹	µgC L ⁻¹	gDM.m ⁻²				
January	1.1	507	13.2	71.4	0.9	20	19	1	8
February	32.8	14815.1	31.9	146.4	27.3	20	545	104	479
March	83	37515.3	31.9	146.4	69	20	1381	264	1213
April	90.6	40955.5	31.9	146.4	75.4	20	1507	288	1324
May	84.6	38218.1	22.7	89.5	70.3	20	1406	192	755
July	25.7	11600	22.7	89.5	21.3	20	427	58	229
September	0.2	99.4	19.8	73.8	0.2	20	4	<0.5	2
November	0.02	9.5	13.2	71.4	<0.1	20	<1	<0.1	<0.5
December	1.2	547	13.2	71.4	1	20	20	2	9

other bryozoan larvae (GAUTIER, 1961). The life span of such larvae is unknown but is estimated by GAUTIER (1961) to be a few weeks. Larvae of *E. posidoniae* are potentially major contributors to meroplankton (i.e. the larval planktonic stage of benthic animals) in the water column, considering the maximal colony density found at a depth of 10 m (i.e. more than 100,000 colonies per m square).

Leaf colonization by *E. posidoniae* is restricted both spatially and temporally. This restriction is partially due to the larval “choice” to specifically settle on the inner concave side of the leaf (MATRICARDI et al, 1998; this study). Reasons for such specific settlement are unclear (e.g. competition with macroalgae and/or feeding current organization) (MATRICARDI et al, 1998). Competition with macroalgae is often invoked to explain the spatio-temporal restriction of animal settlement and to explain their seasonal eviction from certain benthic habitats, as it is the

case for epiphytic communities (MAZZELLA & RUSSO, 1989; DALLA VIA et al., 1998; PRADO et al., 2008). In addition to competition, a colony of *E. posidoniae* may be overgrown by macroalgae. This has been observed on the apex of *P. oceanica* leaves where many photophilous brown macroalgae grow, particularly in late spring and summer (see fig. in MAZZELLA et al., 1992).

Nevertheless, middle parts of the leaves of *P. oceanica* are rarely or never colonised by photophilous macroalgae and show the maximum of colonisation by *E. posidoniae*. Therefore, the decreasing biomass of colonies of *E. posidoniae* almost to the point of disappearance before leaf abscission is not solely related to spatial competition or algae overgrowth. Trophic constraints could also explain this observed pattern. Indeed, the peak of colonisation by *Electra* and its biomass increase clearly match the phytoplanktonic dynamic, and particularly

the diatom bloom in the Revellata bay (LEPOINT et al., 2004). Many Mediterranean benthic suspensivores experience a drastic decrease in their activity or biomass in late spring and summer (i.e. aestivation) as a consequence of food shortage (COMA & RIBES, 2003). Diatoms, a major contributor to small suspensivore feeding, are abundant in the water column only during late winter and early spring (February to March, sometimes April). When their biomass decreases, phytoplanktonic communities become dominated by smaller organisms (2 - 20 μm), which are probably consumed less by large bryozoans (MCKINNEY & JACKSON 1989). Food shortage may occur in this system for benthic suspensivores such as gorgonian corals and is a major cause of mortality for many species (COMA & RIBES, 2003). Food shortage could thus be likely to affect survival of *E. posidoniae* after the phytoplanktonic bloom, even in the absence of competition with epiphytic macroalgae.

Nevertheless, alternative food sources exist in the seagrass meadow, for example re-suspended particles coming from dead seagrass material as well as detached epiphytic microalgae (i.e. tychoplankton). The latter are very abundant on seagrass leaves as epiphytes (NOVAK, 1984; MAZZELLA & RUSSO, 1989; DE STEFANO et al., 2000) and may detach because of leaf movements. There is no doubt, considering the isotopic data, that *E. posidoniae* relies heavily on phytoplanktonic biomass for feeding. However, phytoplankton is unlikely to represent their exclusive food source. Indeed, their $\delta^{13}\text{C}$ values were always in the upper part of the range of planktonic $\delta^{13}\text{C}$ values, and close to $\delta^{13}\text{C}$ values of epilithic biofilm. They were also higher than those of suspensivore organisms found in other habitats (e.g. rocky habitats) (LEPOINT et al., 2000). A significant contribution from alternative food source(s) displaying a higher $\delta^{13}\text{C}$ value cannot be excluded, particularly during the late spring and the summer, when phytoplanktonic biomass is low. Considering the isotopic composition ranges displayed by epiphytes and seagrasses, contribution by detached epiphytic diatoms to the diet of *E. posidoniae* is likely to be

more important than the contribution by detritic seagrass material. Contribution of seagrass material to the bryozoan diet was not clearly detected here; but, mathematically, a small contribution cannot be excluded. Additionally, a contribution by microbes associated with detritus and displaying the same isotopic composition to their substrate is also feasible. This is particularly possible in July when bryozoan $\delta^{13}\text{C}$ reaches its peak and moves closest to the seagrass isotopic composition. Detritic seagrass may constitute a variable part of the diet of grazers associated with seagrass litter accumulation (STURARO et al., 2010) or seagrass meadows (VIZZINI, 2009; MICHEL, 2011). Detritic particles found in the meadow ranged widely in terms of size, as dead leaves may be fragmented inside the meadow by water motion (i.e. hydrophysical fragmentation), by microbial degradation, and by detritivorous fauna producing large amounts of fecal pellets. This material may be re-suspended and thereby become available for bryozoan feeding. Due to the colony size we were not able to measure stable isotopic composition in fall and early winter samples when detritic seagrass particles are sometimes abundant in the water column (DAUBY et al., 1995).

In our study, data relating to the stable isotopes composition of nitrogen and sulphur did not prove particularly useful as they did not discriminate very well between the potential food sources. However, $\delta^{15}\text{N}$ values confirmed the low trophic level of *E. posidoniae* (i.e. close to primary producer isotopic compositions and lower than those of zooplankton, LEPOINT et al. 2000) and, therefore, the low contribution of zooplankton (i.e. primary consumers) as a potential food source.

It is well established that meadows of *P. oceanica* function as a trap for planktonic particles (GACIA et al., 2002). Suspensivore activity, including that of *E. posidoniae*, is another possible mode of transfer between the water column and benthic compartment, increasing the role of the meadow as a sink for water column primary production (LEMMENS

et al., 1996). Such coupling is significant in Australian seagrass meadows, although mainly attributed to macrobenthic suspensivores (LEMMENS et al., 1996). In March and April 2003 (i.e. during phytoplankton bloom), the calculated surface area of *E. posidoniae* reached 4 m² of colony per m² of seafloor (Table 2). Based on published measurements for bryozoan filtering capacities (LISBJERG & PETERSEN, 2000), and on phytoplanktonic biomasses measured in our study area (LEPOINT et al., 2004), phytoplanktonic biomass potentially trapped by the feeding activity of *E. posidoniae* and transferred from the water column to the benthic compartment was estimated (Table 2). Filtered volume and biomass transfer are a small fraction of the particles settling in the meadow (GACIA et al., 2002), but this fraction is concentrated in the epiphytic compartment and is enriched in nitrogen and phosphorus, two elements that often limit primary production and that may indirectly benefit *P. oceanica* and other epiphytes through the waste products of *E. posidoniae* (NH₄ for example) (BRACKEN, 2004).

In conclusion, it appears that *E. posidoniae* is a central species of the leaf epiphytic community on *P. oceanica*, dominating the epiphytic biomass in early spring. It contributes to the coupling between the water column and the seagrass meadow and is likely to significantly contribute to the planktonic larval community. Its spatio-temporal colonization pattern may be related to competition with other epiphytes, and probably to food shortages occurring in late spring and summer. It is mainly a phytoplankton feeder; although alternative food sources cannot be excluded (tychoplankton and detritus of *P. oceanica*).

Many questions relating to this epiphytic specialist remain unanswered, such as the driver of larval specific positioning, its reproductive strategy to fill the gap between leaf fall and leaf growing season, or the way it interacts with its vegetal host (adhesion, positive/negative interactions) or with other epiphytes.

ACKNOWLEDGEMENTS

Authors are grateful to STARESO for their support and for access to laboratory facilities. Many thanks to Loïc Michel for his critical corrections of this manuscript and to François Remy for SEM photography of *Electra posidoniae*. G.L. is presently Research Associate at Fonds National de la Recherche Scientifique (F.R.S.- F.N.R.S)(BELGIUM), and benefited from a postdoctoral fellowship from FRS - F.N.R.S during this study. This study was financed by a FRS - F.N.R.S contract (FRFC 2.45.69.03) and the Action de Recherche Concertée 10/533 (French-speaking Community of Belgium). This is the MARE paper number 269.

REFERENCES

- ALCOVERRO T, PEREZ M & ROMERO J (2004). Importance of within-shoot epiphyte distribution for the carbon budget of seagrasses: the example of *Posidonia oceanica*. *Botanica Marina*, 47: 307-312.
- BALATA D, PIAZZI L, NESTI U, BULLERI F & BERTOCCI I (2010). Effects of enhanced loads of nutrients on epiphytes on leaves and rhizomes of *Posidonia oceanica*. *Journal of Sea Research*, 63: 173-179.
- BOERO F, CHESSA L, CHIMENZ C & FRESI E (1985). The zonation of epiphytic hydroids on the leaves of some *Posidonia oceanica* (L.) Delile beds in the central Mediterranean. *Pubblicazione della Stazione Zoologica di Napoli I : Marine Ecology*, 6: 27-33.
- BOROWITZKA MA, LAVERY PS & VAN KEULEN M (2006). Epiphytes of seagrasses. In: LARKUM AWD, ORTH RJ, DUARTE CM (eds). *Seagrasses: Biology, Ecology and Conservation*, Springer, Berlin: 441-461.
- BRACKEN M (2004). Invertebrate-mediated nutrient loading increases growth of an intertidal macroalga. *Journal of Phycology*, 40: 1032-1041.
- CEBRIAN J & LARTIGUE J (2004). Patterns of herbivory and decomposition in aquatic and terrestrial ecosystems. *Ecological Monographs*, 74: 237-259.
- CEBRIAN J, ENRIQUEZ S, FORTES M, AGAWIN N, VERMAAT JE, DUARTE CM (1999). Epiphyte

- accrual on *Posidonia oceanica* (L.) Delile leaves: implications for light absorption. *Botanica Marina*, 42: 123-128.
- COCITO S, LOMBARDI C, CIUFFARDI F & GAMBI MC (2012). Colonization of Bryozoa on seagrass *Posidonia oceanica* 'mimics': Biodiversity and recruitment pattern over time. *Marine Biodiversity*, 42: 189-201.
- COMA R & RIBES M (2003). Seasonal energetic constraints in Mediterranean benthic suspension feeders: effects at different levels of ecological organization. *Oikos*, 101: 205-215.
- CONNOLLY RM & SCHLACHER TA (2013). Sample acidification significantly alters stable isotope ratios of sulfur in aquatic plants and animals. *Marine Ecology Progress Series*, 493: 1-8.
- DALLA VIA J, STURMBAUER C, SCHONWEGER G, SOTZ E, MATHEKOWITSCH S, STIFTER M, RIEGER R (1998). Light gradients and meadow structure in *Posidonia oceanica*: ecomorphological and functional correlates. *Marine Ecology Progress Series*, 163: 267-278.
- DAUBY P, BALE AJ, BLOOMER N, CANON C, LING RD, NORRO A, ROBERTSON JE, SIMON A, THÉATE J-M, WATSON AJ, FANKIGNOULLE M (1995). Particle fluxes over a Mediterranean seagrass bed: a one year case study. *Marine Ecology Progress Series*, 126: 233-246.
- DE STEFANO M, MARINO D & MAZZELLA L (2000). Marine taxa of i on leaves of *Posidonia oceanica*, including a new species and two new varieties. *European Journal of Phycology*, 35: 225-242.
- GACIA E, DUARTE CM & MIDDELBURG JJ (2002). Carbon and nutrient deposition in a Mediterranean seagrass (*Posidonia oceanica*) meadow. *Limnology and Oceanography*, 47: 23-32.
- GACIA E, COSTALAGO D, PRADO P, PIORNO D & TOMAS F (2009). Mesograzers in *Posidonia oceanica* meadows: an update of data on gastropod-epiphyte-seagrass interactions. *Botanica Marina*, 52: 439-447.
- GAUTIER YV (1961). Recherches écologiques sur les bryozoaires Chilostomes en Méditerranée occidentale. Thèse de Doctorat, Université de Marseille, Marseille.
- HAYWARD PJ (1975). Observations on the bryozoan epiphytes of *Posidonia oceanica* from the island of Chios (Aegean Sea). In: POUYET S (ed), *Bryozoa*, Presse de l'Université Claude Bernard, Lyon: 347-356.
- JACQUEMART J & DEMOULIN V (2008). Comparison of the epiphytic macroflora of *Posidonia oceanica* leaves in different meadows of the western Mediterranean. *Flora Mediterranea*, 18: 393-420.
- LEMMENS JWTJ, CLAPIN G, LAVERY PS & CARY J (1996). Filtering capacity of seagrass meadows and other habitats of Cockburn Sound, Western Australia. *Marine Ecology Progress Series*, 143: 187-200.
- LEPOINT G, HAVELANGE S, GOBERT S & BOUQUEGNEAU JM (1999). Fauna vs flora contribution to the leaf epiphytes biomass in a *Posidonia oceanica* seagrass bed (Revellata Bay, Corsica). *Hydrobiologia*, 394: 63-67.
- LEPOINT G, NYSSSEN F, GOBERT S, DAUBY P & BOUQUEGNEAU JM (2000). Relative impact of a seagrass bed and its adjacent epilithic algal community in consumer diets. *Marine Biology*, 136: 513-518.
- LEPOINT G, DAUBY P, FONTAINE M, BOUQUEGNEAU JM & GOBERT S (2003). Carbon and nitrogen isotopic ratios of the seagrass *Posidonia oceanica*: Depth-related variations. *Botanica Marina*, 46: 555-561.
- LEPOINT G, GOBERT S, DAUBY P & BOUQUEGNEAU JM (2004). Contributions of benthic and planktonic primary producers to nitrate and ammonium uptake fluxes in a nutrient-poor shallow coastal area (Corsica, NW Mediterranean). *Journal of Experimental Marine Biology and Ecology*, 302: 107-122.
- LEPOINT G, BALANCIER B & GOBERT S (2014). Seasonal and depth-related biodiversity of leaf epiphytic Cheilostome Bryozoa in a Mediterranean *Posidonia oceanica* meadow. *Cahiers de Biologie Marine*, 55: 57-67.
- LISBJERG D & PETERSEN JK (2000). Clearance capacity of *Electra bellula* (Bryozoa) in seagrass meadows of Western Australia. *Journal of Experimental Marine Biology and Ecology*, 244: 285-296.
- MABROUK L, HAMZA A, BEN BRAHIM M & BRADAI MN (2011). Temporal and depth distribution of microepiphytes on *Posidonia oceanica* (L.) Delile leaves in a meadow off Tunisia. *Marine Ecology*, 32: 148-161.
- MATEO MA, CEBRIAN J, DUNTON K & MUTCHLER T (2006). Carbon Flux in Seagrasses. In: LARKUM AWD, ORTH RJ, DUARTE CM (eds). *Seagrasses: Biology, Ecology and Conservation*, Springer, Berlin: 159-192.

- MATRICARDI G, MONTAGNA P & PISANO E (1991). Settlement and growth strategies of *Electra posidoniae* Gautier on *Posidonia oceanica* (L.) Delile. In: BIGEY FP (ed), Bryozoaires actuels et fossiles: Bryozoa living and fossil. Nantes (France): 255-262.
- MAZZELLA L, SCIPIONE MB & BUIA MC (1989). Spatio-temporal distribution of Algal and Animal communities in a *Posidonia oceanica* meadow. Pubblicazione della Stazione Zoologica di Napoli I : Marine Ecology, 10: 107-129.
- MAZZELLA L & RUSSO GF (1989). Grazing effect of two *Gibbula* species (Mollusca, Archaeogastropoda) on the epiphytic community of *Posidonia oceanica* leaves. Aquatic Botany, 35: 353-373.
- MAZZELLA L, BUIA MC, GAMBI MC, LORENTI M, RUSSO GF, SCIPIONE MB, ZUPO V (1992). Plant-animal trophic relationships in the *Posidonia oceanica* ecosystem of the Mediterranean Sea: a review. In: JOHN DM, HAWKINS SJ, PRICE JH (eds), Plant-Animal Interactions in the Marine Benthos, Clarendon Press, Oxford: 165-187.
- MCKINNEY FK & JACKSON JBC (1989). Bryozoan Evolution. Unwin Hyman, Boston.
- MICHEL L (2011). Multidisciplinary study of trophic diversity and functional role of amphipod crustaceans associated to *Posidonia oceanica* meadows. PhD Thesis, University of Liège.
- NOVAK R (1984). A Study in Ultra-Ecology: Microorganisms on the Seagrass *Posidonia oceanica* (L.) Delile. Pubblicazione della Stazione Zoologica di Napoli I : Marine Ecology 5: 143-190.
- NIKULINA EA, HANEL R & SCHAFER P (2007). Cryptic speciation and parapatry in the cosmopolitan bryozoan *Electra pilosa* - Impact of the Tethys closing on species evolution. Molecular Phylogenetics and Evolution, 45: 765-776.
- PERES J-M & PICARD J (1964). Nouveau manuel de bionomie benthique de la mer Méditerranée. Edition revue et augmentée. Publication de la Station Marine d'Endoume, Marseille.
- PINNEGAR JK & POLUNIN NVC (1999). Differential fractionation of $\delta^{13}\text{C}$ and $\delta^{15}\text{N}$ among fish tissues: implications for the study of trophic interactions. Functional Ecology, 13: 225-231.
- PRADO P, ALCOVERRO T & ROMERO J (2008). Seasonal response of *Posidonia oceanica* epiphyte assemblages to nutrient increase. Marine Ecology Progress Series, 359: 89-98.
- STURARO N, CAUT S, GOBERT S, BOUQUEGNEAU J-M & LEPOINT G (2010). Trophic diversity of idoteids (Crustacea, Isopoda) inhabiting the *Posidonia oceanica* litter. Marine Biology, 157: 237-247.
- TOMAS F, TURON X & ROMERO J (2005). Effects of herbivores on a *Posidonia oceanica* seagrass meadow: importance of epiphytes. Marine Ecology Progress Series, 301: 95-107.
- VAN DER BEN D (1971). Les épiphytes des feuilles de *Posidonia oceanica* Delile sur les côtes françaises de la Méditerranée. Mémoires de l'Institut Royal des Sciences Naturelles de Belgique, 168: 1-101.
- VERMEULEN S (2012). Spatial and temporal responses of marine gastropods and biofilms to urban wastewater pollution in a Mediterranean coastal area. PhD Thesis, University of Liège.
- VIZZINI S (2009). Analysis of the trophic role of Mediterranean seagrasses in marine coastal ecosystems: a review. Botanica Marina, 52: 383-393.

Received: January 30th, 2014

Accepted: May 26th, 2014

Branch editor: Tom Artois

ERRATUM

to: QURESHI NA & SAHER NU 2012. Burrow morphology of three species of fiddler crab (*Uca*) along the coast of Pakistan. *Belgian Journal of Zoology* 142 (2): 114-126.

Figure 2 of the paper by QURESHI & SAHER (2012) was not an original drawing by the authors, but was redrawn after figure 1 in LIM & DIONG (2003).

The correct legend on page 117 should read:

Fig. 2. – Burrow architecture parameters selected for analyses were BD: Burrow diameter (mm), TBL: Total burrow length (mm) and TBD: total burrow depth (mm) (redrawn after figure 1 in LIM & DIONG 2003).

The following reference should be added:

LIM SSL & DIONG CH 2003. Burrow-morphological characters of the fiddler crab, *Uca annulipes* (H. Milne Edwards, 1837) and ecological correlates in a lagoonal beach on Pulau Hantu, Singapore. *Crustaceana*, 76(9): 1055-1069.